2018

# Mechanisms of B-Myb oncogenicity in ovarian cancer

Audra N. Iness
*Virginia Commonwealth University*

# Mechanisms of B-Myb oncogenicity in ovarian cancer

A dissertation submitted in partial fulfillment of the requirements for the degree of Doctor of Philosophy at Virginia Commonwealth University.

by

Audra N. Iness
Bachelor of Science, Biology- Anatomy and Physiology, 2013
California State University Fresno, Smittcamp Family Honors College

Director: Larisa Litovchick, MD, PhD
Associate Professor, Internal Medicine

Virginia Commonwealth University
Richmond, Virginia
December 7, 2018

# Acknowledgement

Anyone with research lab experience knows that a strong support team in an essential part of every experiment. I want to express my gratitude to my family and lab mates for being by my side along the physician scientist training journey—celebrating the victories with me and encouraging me to push through challenges. I especially want to thank my mom for the numerous supportive phone calls and my fiancé for going with me to the many late-night and weekend lab visits.

I would also like to acknowledge my thesis committee and the VCU MD-PhD program for investing not only in my educational development, but also in my personal well-being. Thank you for all of your advice and guidance.

I extend my thanks to Dr. Gordon Archer who encouraged me to “ask for forgiveness rather than permission.” This insightful phrase became not only my driving principle during graduate school, but a mantra by which I approach all challenges in my life.

Finally, with utmost gratefulness, I tremendously appreciate all of the opportunities afforded to me by my mentor, Dr. Larisa Litovchick. I feel privileged to have had the liberty to explore my interests—an opportunity that many never have the pleasure of experiencing. It is a wonder to look back and notice my professional and personal growth. Under her leadership and expertise, I have become stronger, more independent, and prepared for the next step along my journey. Thank you.

Table of Contents

List of Figures

# Abstract

MECHANISMS OF B-MYB ONCOGENICITY IN OVARIAN CANCER

By Audra N. Iness

A dissertation submitted in partial fulfillment of the requirements for the degree of Doctor of Philosophy at Virginia Commonwealth University.

Virginia Commonwealth University, 2018

Director: Larisa Litovchick, MD, PhD, Associate Professor, Internal Medicine

High expression of B-Myb (encoded by *MYBL2*), an oncogenic transcription factor, is associated with cell cycle deregulation and poor prognosis in several cancers, including ovarian cancer. However, the mechanism by which B-Myb alters the cell cycle is not fully understood. In proliferating cells, B-Myb interacts with the MuvB core complex including LIN9, LIN37, LIN52, RBBP4, and LIN54, forming the MMB (Myb-MuvB) complex, and promotes transcription of genes required for mitosis. Alternatively, the MuvB core interacts with Rb-like protein p130 and E2F4-DP1 to form the DREAM complex that mediates global repression of cell cycle genes in G0/G1, including a subset of MMB target genes. Here, we show that overexpression of B-Myb disrupts the DREAM complex in human cells, and this activity depends on the intact MuvB-binding domain in B-Myb.

Furthermore, we found that B-Myb regulates the protein expression levels of the MuvB core subunit LIN52, a key adaptor for assembly of both the DREAM and MMB complexes, by a mechanism that requires the S28 phosphorylation site in LIN52. To validate our cellular findings, we determined the effect of B-Myb levels on DREAM target gene expression in HGSOC tissue samples and corresponding patient outcomes. Given that high expression of B-Myb correlates with global loss of repression of DREAM target genes in breast and ovarian cancer, our findings offer mechanistic insights for aggressiveness of cancers with *MYBL2* amplification and establish the rationale for targeting B-Myb to restore cell cycle control.

# Chapter 1: Introduction

Adapted from

Iness A.N. & Litovchick L. (2018). MuvB: A Key to Cell Cycle Control in Ovarian Cancer. *Front. Oncol*. 8:223. doi: 10.3389/fonc.2018.00223

## Cell cycle regulation and cancer

Cancer cells are characterized by uncontrolled proliferation, whereas the ability to enter quiescence or dormancy is important for cancer cell survival and disease recurrence. Therefore, understanding the mechanisms regulating cell cycle progression and exit is essential for improving patient outcomes (1). The MuvB complex of five proteins (LIN9, LIN37, LIN52, RBBP4, and LIN54), also known as LINC (LIN complex), is important for coordinated cell cycle gene expression. By participating in the formation of three distinct transcriptional regulatory complexes, including DREAM (DP, RB-like, E2F, and MuvB), MMB (Myb-MuvB) and FoxM1-MuvB, MuvB represents a unique regulator mediating either transcriptional activation (during S-G2 phases) or repression (during quiescence). With no known enzymatic activities in any of the MuvB-associated complexes, studies have focused on the therapeutic potential of protein kinases responsible for initiating DREAM assembly or downstream enzymatic targets of MMB (2-4). Furthermore, the mechanisms governing the formation and activity of each complex (DREAM, MMB, or FoxM1-MuvB) may have important consequences for therapeutic response. The MMB complex is associated with prognostic markers of aggressiveness in several cancers whereas the DREAM complex is tied to disease recurrence through its role in maintaining quiescence (5-7).

**MuvB regulates cell cycle gene activation and repression**

Understanding the processes governing cell cycle regulation is especially important in high grade serous ovarian cancer (HGSOC) because of high rates of treatment resistance and recurrence. Retinoblastoma (Rb) family proteins, including pRb (retinoblastoma protein encoded by the *RB1* tumor suppressor gene), p107 (*RBL1*) and p130 (*RBL2*), are essential for entry into quiescence in mammalian cells (8, 9). pRb, p107 and p130 are also known as “pocket proteins” because they bind E2F transcription factors that regulate cell cycle dependent genes using a conserved “pocket” domain (10). While the tumor suppressor role of pRb is well established, the roles of p107 and p130 in cancer are not fully understood. However, Rb-like proteins (but not pRb) can recruit the evolutionarily conserved DNA binding protein complex MuvB to regulate gene expression. Recent studies reveal that through interaction with MuvB, p130 and p107 could play a unique and significant role in determining cancer aggressiveness and response to therapy.

Structurally related MuvB complexes including proteins encoded by the *LIN9*, *LIN37*, *LIN52*, *LIN54* and *RBBP4* genes, or their orthologs, have been shown to regulate gene expression in different organisms including *C. elegans*, *Drosophila* and *Homo sapiens* (11-14). In mammalian cells, MuvB participates in both repressor and activator gene regulatory complexes by alternating its binding partners at different points in the cell cycle. In G0/G1, MuvB is a component of the DREAM complex, which functions to repress gene expression for entering and maintaining quiescence. DREAM consists of p130, E2F4, and DP1 bound to MuvB, and its assembly requires phosphorylation of the LIN52

subunit of MuvB by dual-specificity tyrosine phosphorylation-regulated kinase (DYRK1A) (13, 15). DREAM disassembly occurs during the G1/S transition when cyclin-dependent kinases CDK4 and CDK2 phosphorylate p130 and MuvB subunits (13, 16-18). MuvB then dissociates from p130 and E2F4, leading to transcription of early and late cell cycle genes, including B-Myb and FoxM1 transcription factors. B-Myb recruits MuvB during the S phase, forming the MMB complex that binds to promoters of late cell cycle genes (15, 18-20). Furthermore, upon proteasomal degradation of B-Myb in S/G2, MuvB mediates timely recruitment of FoxM1 transcription factor to promoters of genes required for mitosis (20, 21). Therefore, by sequential association with three different DNA-binding transcription factors (E2F4, B-Myb, and FoxM1), MuvB coordinates cell cycle gene expression from quiescence through mitosis (**Fig. 1**) (2, 22). This unique function of MuvB is central to maintaining cell cycle regulation and appropriate responses to environmental stimuli. The degree of MuvB participation in quiescence-related (DREAM) or proliferation-related (MMB or FoxM1-MuvB) complexes could be an important factor in cancer biology and therapeutic response.

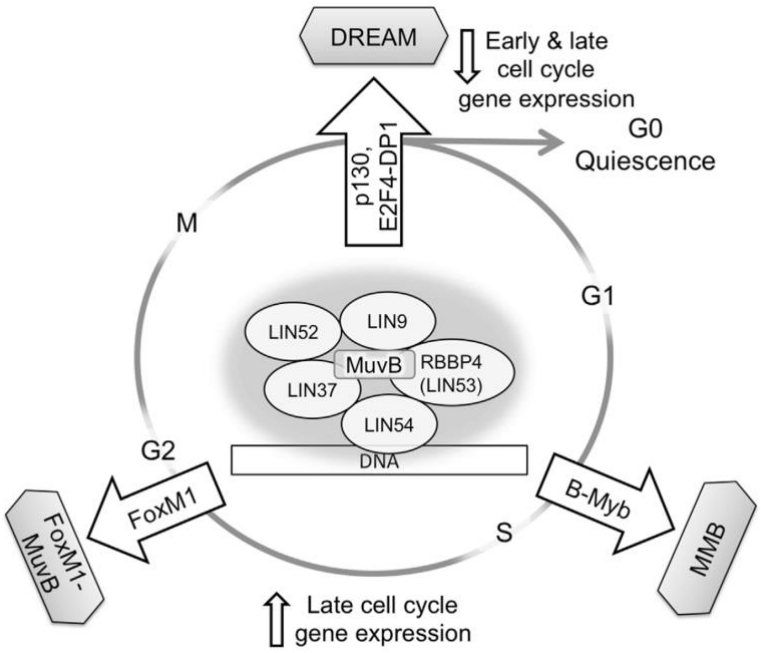


**Figure 1. MuvB contributes to gene regulation throughout the cell cycle**. MuvB binds p130/p107 and E2F4-DP1 in G0/G1 to form the DREAM complex and repress both early and late cell cycle genes. Upon cell cycle re-entry and during the S phase, MuvB binds B-Myb, forming MMB for expression of early cell cycle genes. The interaction between B-Myb and MuvB is important for recruiting FoxM1 for late cell cycle gene expression and subsequent mitosis.

High grade serous ovarian cancer is the most common of the epithelial malignancies in this disease site. Analysis of HGSOC data from The Cancer Genome Atlas (TCGA) reveals widespread variable genetic alterations of the factors involved in MuvB function (**Fig. 2**) (23). Interestingly, genes encoding different MuvB subunits appear to be targeted both by gene copy number losses (LIN52, LIN54) or gains (LIN9, LIN37). MuvB's involvement in complexes with different functions makes it challenging to parse out the contributions of individual proteins without understanding of their exact roles in the context of each complex. Unlike pRb, mutations targeting p130 or p107 in cancer are rare (24-26). However, perturbations in DREAM activity could occur through its altered

formation (e.g. aberrant activation of CDKs, inhibition of DYRK1A, or availability of MuvB components).

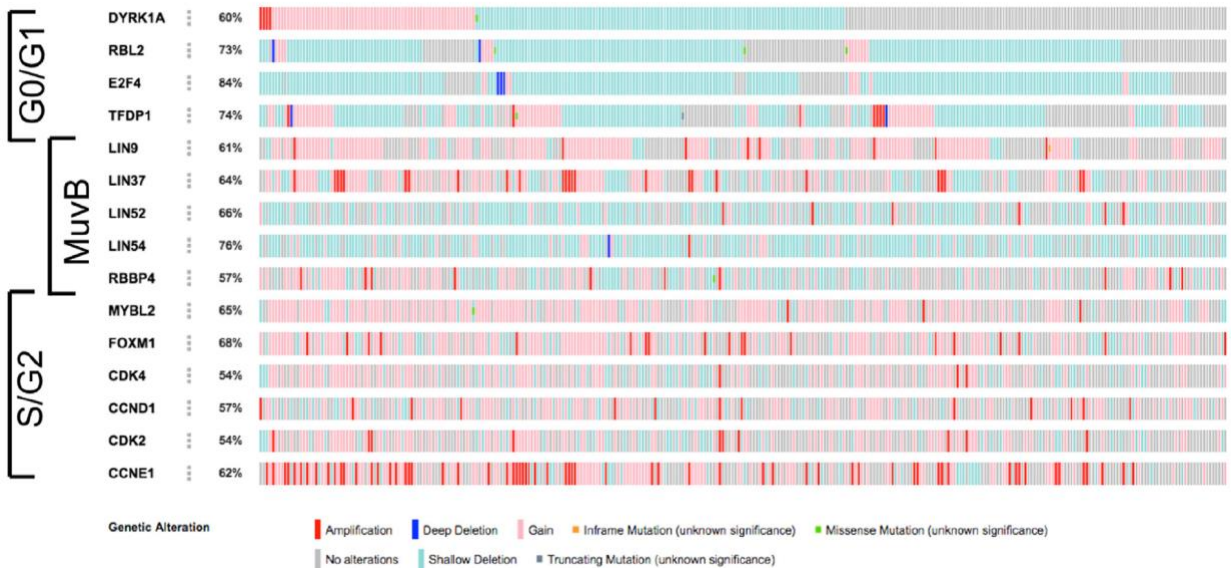


**Figure 2. Alterations in genes involved in MuvB complex function.** Figure shows summary of copy number alteration and mutation data from high-grade ovarian carcinoma samples (N = 316) visualized using cBio.org resource (23, 27). Note that the factors required for the G0/G1 function of the MuvB more frequently undergo genetic losses (blue color), whereas regions encoding genes associated with MuvB in S/G2 are frequently gained (pink) or amplified (red).

**Structural and functional studies of MuvB subunits reveal their unique roles**

Since the discovery of mammalian DREAM in 2007, the structure and specific functions of the MuvB subunits are now beginning to emerge (28). Histone-binding protein RBBP4 (alias RbAp48) has been extensively characterized for its involvement in various chromatin-modifying complexes (29-31). Although there is no direct evidence of interaction between DREAM and any chromatin co-repressor complexes, RBBP4 likely serves as an adaptor to recruit such complexes to DREAM-regulated promoters. A recent study of mouse fibroblasts devoid of MuvB subunit LIN37 found that although the remaining subunits were able to assemble a DREAM-like DNA-binding complex, its

repressor function was lost (32). Interestingly, the MMB-mediated transcription was not affected, suggesting that LIN37 specifically contributes to the repressor role of MuvB. The smallest (116 a.a.) MuvB subunit LIN52 plays a key role in DREAM formation by direct interaction with p130 or p107. This interaction requires phosphorylation of serine 28 in LIN52 by DYRK1A (15, 16). Importantly, a different region in LIN52 is also essential for MMB complex formation. Therefore, LIN52 phosphorylation status and availability could impact the function of both complexes (16). Studies in cell lines and mouse genetic models reveal the importance of another MuvB subunit, LIN9, for both cell proliferation and tumor suppression, emphasizing its structural role in both DREAM and MMB (16, 33-35). Recent work also implicated LIN9 in direct binding with FoxM1 for formation of the FoxM1-MuvB complex required for mitotic gene expression (36). Interestingly, while MuvB associates with DNA-binding transcription factors to achieve target gene specificity, it also possesses intrinsic DNA-binding activity through MuvB subunit LIN54 (37). LIN54 recognizes specific DNA sequences called cell cycle homology regions (CHR), and mutations disrupting the LIN54-DNA interface abolish the recruitment of MuvB to promoters harboring the CHR elements (21, 38). Many mitotic genes contain CHR elements required for their expression, consistent with the finding that loss of LIN54 results in cell cycle arrest and mitotic defects (21, 37, 39, 40). Together, these findings characterize the contributions of the individual subunits that can, in part, explain the multifunctional nature of the MuvB complex.

**MuvB function is influenced by major tumor suppressor pathways**

Discovery of mammalian MuvB complex further clarified the overlapping and unique roles of the Rb family members in cell cycle control. While pRb itself does not

interact with MuvB directly, formation of DREAM appears to be the major role of the other pocket proteins, p130 and p107 *in vivo* (13, 41). Previous studies demonstrated that inactivation of all three pocket proteins (pRb, p107 and p130) in mouse fibroblasts is necessary to block entry into quiescence (8, 42). Similarly, fibroblasts lacking MuvB subunit LIN37, or cells defective in MuvB-pocket protein interaction, are able to arrest in G0/G1 despite de-repression of DREAM target genes and aberrant formation of the proliferation-related MMB complex under the conditions of G0/G1 arrest (32, 41). However, depletion of pRb resulted in escape from G0/G1 arrest in LIN37 knockout cells (32). MuvB therefore becomes an essential regulator of the cell cycle and guardian of quiescence in the absence of functional pRb. Notably, copy number losses or mutations in the *RB1* gene (encoding pRb) are present in 67% of TCGA HGSOC samples.

In addition to cooperating with pRb for cell cycle exit, MuvB is functionally linked with p53. Activation of p53 in response to environmental stimuli, such as DNA damage, results in replacement of MMB with DREAM through a p21-dependent pathway (43-45). This switch is required for global cell cycle gene repression. Frequent mutations of the *TP53* gene in cancer (notably in 96% of HGSOC tumors) could lead to de-repression of oncogenic DREAM target genes, such as *Survivin* (*BIRC5*), *CDC25C*, and *PLK1* (23, 44, 46, 47). Therefore, deregulation of the p53-p21-MuvB pathway could have important implications for clinical outcomes in cancer. Indeed, in p53-mutant breast cancer cells, MuvB failed to dissociate from B-Myb (MMB complex) and bind p130/E2F4 upon DNA damage to form DREAM (48). Similarly, doxorubicin treatment of HCT116 colon carcinoma cells led to an increase in the population of G2/M cells and mRNA levels of late cell cycle genes when p53 was inhibited (44, 47). Basal MMB was also more

abundant in p53-mutant hepatocellular carcinoma (HCC) cells versus those with wild-type p53. Whereas DREAM assembly was increased with doxorubicin treatment in p53 wild-type cells, MMB complex formation was paradoxically increased upon treatment of p53 null cells (49). Importantly, MMB formation was essential for survival of p53 null HCC cells after doxorubicin-induced DNA damage, suggesting that inactivation of DREAM and aberrant formation of MMB contributes to chemoresistance of cancers with functional loss of p53, including HGSOC.

Oncogenic human papilloma viruses, such as HPV16 and HPV18, are known to inactivate pRb and p53 pathways through actions of viral proteins E7 and E6, respectively (50, 51). The structure of the LIN52-p107 complex revealed that E7 protein disrupts the DREAM complex by competing with MuvB subunit LIN52 for direct binding to p107/p130 (16). Indeed, LIN52 binds to a cleft in p130 or p107 bound by the LxCxExL motif present in HPV E7 and other oncogenic viral proteins, suggesting that displacement of the MuvB from DREAM could be essential for viral genome replication. In cancer cells expressing oncogenic HPV E7, MuvB is predominantly recruited to the MMB complex and contributes to proliferation of these cells (52-54). Interestingly, expression of E7 can impair the p53-dependent cell cycle checkpoint, independently of E6-mediated p53 degradation, by blocking p53-induced downregulation of DREAM target genes (55, 56). These findings demonstrate the importance of the p53-p21-MuvB pathway for maintaining the checkpoint function of p53, regulation of gene expression, and cell cycle arrest that is often altered in cancer (57).

**MuvB involvement in cancer**

The significance of MuvB subunit expression in human cancers has not been extensively studied, and MuvB is mostly linked to prognosis through association with B-Myb. Both amplification of the 20q13 *MYBL2* locus (encoding B-Myb) and over-expression of MMB target genes are associated with aberrant cell proliferation, cell cycle deregulation, and poor prognosis in many cancers including breast, liver, and ovarian (49, 58, 59). In biochemical studies of HCC tumor-derived tissues, high LIN9-B-Myb (MMB) and low LIN9-p130 (DREAM) complex formation was associated with poor overall survival, despite no significant difference in LIN9 levels (49). These findings were independently corroborated in a bioinformatics study of HCC data from TCGA showing a significant correlation between elevated expression of *MYBL2*, *LIN9*, *LIN52*, or *FOXM1* and poor overall survival (60).

A recent study using a *K-Ras*$^{G12D}$*;p53*$^{null}$ mouse model of lung cancer revealed an important role for MMB in tumorigenesis whereby a conditional deletion of *B-Myb* or *Lin9* significantly suppressed tumor formation (3). This study also demonstrated that MMB target gene *KIF23 (MKLP1)* was required for lung tumor formation and represents a potentially druggable MMB target. Investigation of MuvB, B-Myb, and FOXM1 targets in breast cancer cells yielded further ties to MMB-regulated kinesins whereby inhibition of two targets (KIF23 and PRC1) significantly reduced MDA-MB-231 cell proliferation. Analysis of the TCGA breast cancer data revealed correlations between high expression of mitotic kinesins and poor outcomes, suggesting that these MMB-regulated genes could serve as a prognostic signature or therapeutic targets (61). Furthermore, several MMB

downstream targets are included in a chromosomal instability signature, used to predict clinical outcomes in multiple cancer types (62, 63).

Whereas high MMB levels are associated with a poor prognosis in many cancers, DREAM could contribute to cancer recurrence by promoting cancer cell survival under stressful conditions. In gastrointestinal stromal tumors (GIST), the DREAM complex has been implicated in imatinib mesylate resistance by promoting entry into quiescence (1, 7). Depletion of LIN52, or simultaneous knock-down of both E2F4 and LIN54, significantly enhanced imatinib-induced GIST cell apoptosis as compared with drug treatment alone. Pharmacological inhibition of DYRK1A also significantly increased imatinib-induced GIST apoptosis. Therefore, modulating DREAM formation through DYRK1A kinase activity is a potential therapeutic angle.

**MuvB in ovarian cancer**

The cell cycle effects of DREAM and MMB are of particular interest in the context of HGSOC (64). HGSOC is the most lethal of the gynecologic malignancies that is typically diagnosed at an advanced stage, with a median survival rate <5 years (65, 66). The majority of patients treated with surgery and platinum-based chemotherapy have a complete response to therapy, while 25% patients have primary platinum resistance associated with decreased survival (67). While long disease-free intervals are common, they typically shorten over time, and patients become platinum-resistant (68). HGSOC tumors are characterized by loss-of-function p53 mutations, making it plausible that the inability to assemble DREAM and enter quiescence could contribute to the initial high treatment sensitivity of HGSOC. It is important to investigate the status of key cell cycle

regulators, including DREAM and MMB, in HGSOC with primary and acquired platinum resistance.

Ovarian cancer recurrence has been linked to formation of cellular aggregates (spheroids) comprised of quiescent cells and disseminated through peritoneal fluid. The DREAM complex is assembled upon spheroid formation and plays an active role in maintaining quiescence (69). Inactivation of DREAM by depleting DYRK1A or LIN52 in the ascites-derived HGSOC primary cell lines resulted in reduced spheroid cell viability upon carboplatin treatment. DREAM inactivation led to enhanced cell death. Similarly, DYRK1A inhibition with small molecule drug INDY led to MMB complex formation, compromised DREAM-mediated cell cycle gene repression, and enhanced cell death in HGSOC primary cultures in response to carboplatin treatment (69, 70). This result provides rationale for investigating the therapeutic potential of targeting DREAM in combination with cytotoxic chemotherapy. Pharmacological inhibition of DYRK1A is currently under consideration for the treatment of conditions in which it is overexpressed (Down syndrome and Alzheimer disease) as well as Down syndrome-associated pediatric leukemia (71, 72). Several specific and efficient DYRK1A inhibitors have been reported but further studies are needed to identify candidates suitable for clinical use. The plant-derived alkaloid drug harmine is an effective inhibitor of DYRK1A, but its clinical utility is limited by its potent monoamine oxidase A inhibitory activity (1, 72, 73). A recent report describes a clinically safe and potent new DYRK1A inhibitor CX-4549 that is active against several DYRK1A substrates in cell and animal-based assays (74). Its ability to block DREAM assembly and entry into quiescence has not yet been evaluated.

Pharmacologically targeting DYRK1A could be challenging because this ubiquitously expressed kinase is involved in a variety of processes in different cell types. Some cancers express high levels of DYRK1B, a close homologue present mostly in skeletal muscle. Like DYRK1A, DYRK1B also phosphorylates S28 in LIN52 and stabilizes DREAM (15). DYRK1B inhibition was thus proposed as a way to circumvent the untoward effects of DYRK1A pharmacological inhibitors (4, 75). Several studies suggest that tumor cells expressing DYRK1B more heavily rely on its activity and that DYRK1B depletion compromises the ability to maintain quiescence (76-79). Notably, DYRK1B protein expression is detected in 75% of resected ovarian tumors and up to 10% of ovarian cancers have *DYRK1B* gene amplification (23, 78, 80). Treatment of the ovarian cancer cells overexpressing DYRK1B with RO5454948 (inhibitor of both DYRK1 kinases) resulted in cell cycle re-entry and apoptosis whereas the normal ovarian epithelial cells remained viable (79). However, the only known drug with some selectivity against DYRK1B (5-fold higher potency than for DYRK1A *in vitro*), AZ191, has not been evaluated *in vivo* (81).

**Conclusion**

Overall, the dual role of MuvB in both cellular quiescence and proliferation highlights the intricacy of cell cycle control as well as the importance of cooperation between tumor suppressor pathways. While MMB function is tied to aggressive disease and poor prognosis in cancer, there is robust evidence implicating DREAM function in chemotherapy resistance and cancer cell survival. Therefore, a shift in the utilization of MuvB, for either DREAM or MMB formation, could represent a strategy by which cancer cells exploit the cell cycle. Manipulating MuvB could provide substantial regulatory control

over the cell cycle, as supported by evidence that both DREAM (via blocking DYRK1 kinases), or MMB (via druggable downstream targets), could be targeted for cancer therapy. Given the ongoing development of clinically-viable drugs, the next challenge will be to determine optimal conditions for applying these treatments. Further structure-function studies of the DREAM and MMB, as well as their regulatory signaling pathways, will inform treatment strategies for targeting specific states of MuvB--either inhibiting cell proliferation or entry into quiescence. Although MuvB has been explored at the cellular level, studies with patient samples and clinical data are needed to validate *in vitro* findings and develop the personalized treatments required to modulate the cell cycle key, MuvB.

## Chapter 2: The cell cycle regulatory DREAM complex is disrupted by high expression of oncogenic B-Myb

Adapted from

Iness, A.N., Felthousen, J., Ananthapadmanabhan, V., Sesay, F., Saini, S., Guiley, K.Z., . . . Litovchick, L. (2018). The cell cycle regulatory DREAM complex is disrupted by high expression of oncogenic B-Myb. *Oncogene.* LID - 10.1038/s41388-018-0490-y [doi]. (1476-5594 (Electronic)).

Guiley, K.Z., Iness, A.N., Saini, S., Tripathi, S., Lipsick, J. S., Litovchick, L., & Rubin, S.M. (2018). Structural mechanism of Myb–MuvB assembly. *Proceedings of the National Academy of Sciences*.

### Introduction

Since its discovery in 1988, several studies have established *MYBL2* (encoding B-Myb) as a clinically important oncogene (59, 82). Indeed, *MYBL2* is part of the Onco*type* DX® screening panel and validated DCIS (Ductal Carcinoma *in situ*) Score™, used to predict the risk of local recurrence in patients with breast cancer (83, 84). However, the specific cellular mechanisms of B-Myb's oncogenic activities are not fully understood.

Previous studies characterized B-Myb as a transcription factor involved in cell cycle regulation and expressed in proliferating cells (85). The essential role of B-Myb for cell proliferation is evidenced by failure of inner cell mass formation and embryonic death of *MYBL2* knock-out mice (86). Oncogenic functions of B-Myb have been attributed to its transcriptional activity, resulting in deregulated cell cycle gene expression (3, 6, 87). Studies in *Drosophila* and human cells revealed that B-Myb regulates transcription of developmental and cell cycle genes as part of an evolutionarily conserved multi-subunit protein complex, which shares common subunits with DNA-binding complexes formed by retinoblastoma (RB) family members (2, 28). In *Drosophila*, Myb functions as part of the

dREAM (RB, E2F, and Myb) complex that includes five proteins homologous to the products of the *C. elegans* multi-vulva class B (MuvB) genes: LIN9, LIN37, LIN52, LIN53/RBBP4 and LIN54 (88, 89). In the mammalian cell cycle, the orthologous DREAM (DP, RB-like, E2F, and MuvB) complex does not include Myb, and promotes cell cycle exit by repressing more than 800 cell cycle genes (including *MYBL2*) in quiescent cells (**Fig. 3**) (13, 14, 18). Interestingly, although pRb does not interact with the MuvB core, which only accommodates RB-like p130 or p107 (13, 16), this tumor suppressor functionally cooperates with DREAM in establishing and maintaining quiescence (32). DREAM is assembled in G0/G1 and depends on DYRK1A (dual-specificity tyrosine-phosphorylation regulated kinase 1A) phosphorylation of LIN52 (MuvB subunit) at serine 28 (S28) for bringing together p130 and the MuvB core (90).

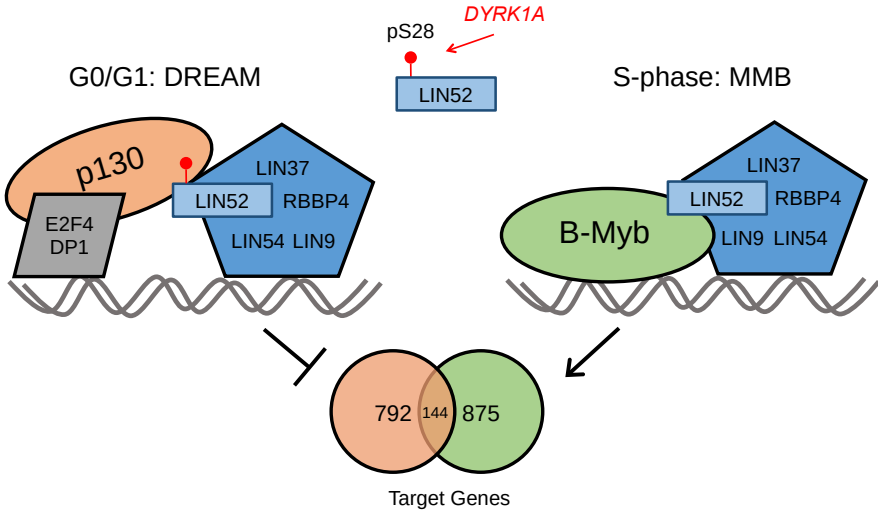


**Figure. 3. Schema of the DREAM (repressor) and MMB (activator) complexes.** These complexes use a common MuvB core (pentagons) to regulate both unique and shared target genes (Venn diagram)

Upon cell cycle progression, p130 is phosphorylated by cyclin-dependent kinases (CDKs) and dissociates from MuvB (16). In the S phase, MuvB binds B-Myb, forming the MMB (Myb-MuvB) complex that cooperates with FOXM1 transcription factor to activate G2/M

gene expression (20, 91). Importantly, LIN52 is required for MuvB to bind B-Myb, making LIN52 an essential component of both the DREAM and MMB complexes (16). Unlike DREAM, LIN52 binding to B-Myb is independent of S28 phosphorylation. Interestingly, the *Drosophila* dREAM complex includes the Myb and RB proteins together with MuvB, whereas the mammalian DREAM and MMB complexes exist in a cell cycle-dependent, mutually exclusive manner (12, 13, 18, 88). An *in vitro* study with reconstituted human complexes demonstrated that both B-Myb and p130 could simultaneously bind to MuvB, suggesting that their mutually exclusive binding *in vivo* is not due to structural constraints (16).

Studies of DREAM disruption by genome editing show that DREAM-deficient cells have abnormal binding of B-Myb to MuvB and loss of DREAM target gene repression under the conditions of G0/G1 cell cycle arrest (32, 41). Since B-Myb overexpression also deregulates the cell cycle (92, 93), we investigated whether B-Myb, when over-expressed, could play a causal role in disrupting DREAM. Our data shown here support the regulation of DREAM by B-Myb as a potential mechanism for the cell cycle defects observed in cancers with high B-Myb levels. Furthermore, we demonstrate that increased expression of B-Myb disrupts DREAM by compromising recruitment of LIN52 to the complex, and describe the regulation of LIN52 expression by B-Myb. These findings implicate global cell cycle deregulation by disrupting the DREAM repressor function as a means by which B-Myb exerts its oncogenic effects and promotes cancer progression.

## Results

### B-Myb inhibits DREAM assembly in non-transformed human fibroblasts

B-Myb overexpression is associated with a proliferative phenotype, which could be due to loss of DREAM function. Therefore, we assessed the effect of B-Myb gain of function on DREAM formation by expressing HA-B-Myb in non-transformed human fibroblasts immortalized with hTERT (BJ-hTERT) (90, 94). We first measured the proliferation rate of cells expressing HA-B-Myb compared to control cells expressing HA-GFP, using an ATP-dependent metabolic assay (95). As expected, BJ-hTERT cells expressing HA-B-Myb exhibited a significantly greater proliferation rate than controls (**Fig. 4A**). We then determined the effect of high B-Myb levels on DREAM assembly. While both the LIN37-p130 complexes (specific to DREAM) and LIN37-B-Myb complexes (corresponding to MMB) were present in the asynchronously cycling control cells, B-Myb overexpression resulted in almost no detectable p130 co-precipitating with LIN37. To clarify the effect of B-Myb on DREAM, we serum starved these cells to induce DREAM formation. As expected, DREAM formation increased in serum-starved control BJ-hTERT cells. Although B-Myb overexpressing cells formed p130/LIN37 complexes, DREAM levels were significantly diminished with HA-B-Myb expression (**Fig. 4B-D**). This result suggests that even in the presence of high B-Myb, DREAM disassembly remains partially dependent on environmental factors. Similar findings were obtained under alternative growth arrest conditions with palbociclib (CDK4/6 inhibitor) treatment (**Fig. 4E**, **F**). Therefore, although we previously showed that p130 and B-Myb could simultaneously bind to MuvB (16), here we observed that overexpression of B-Myb in non-transformed cells results in MMB formation under conditions that normally favor DREAM assembly.

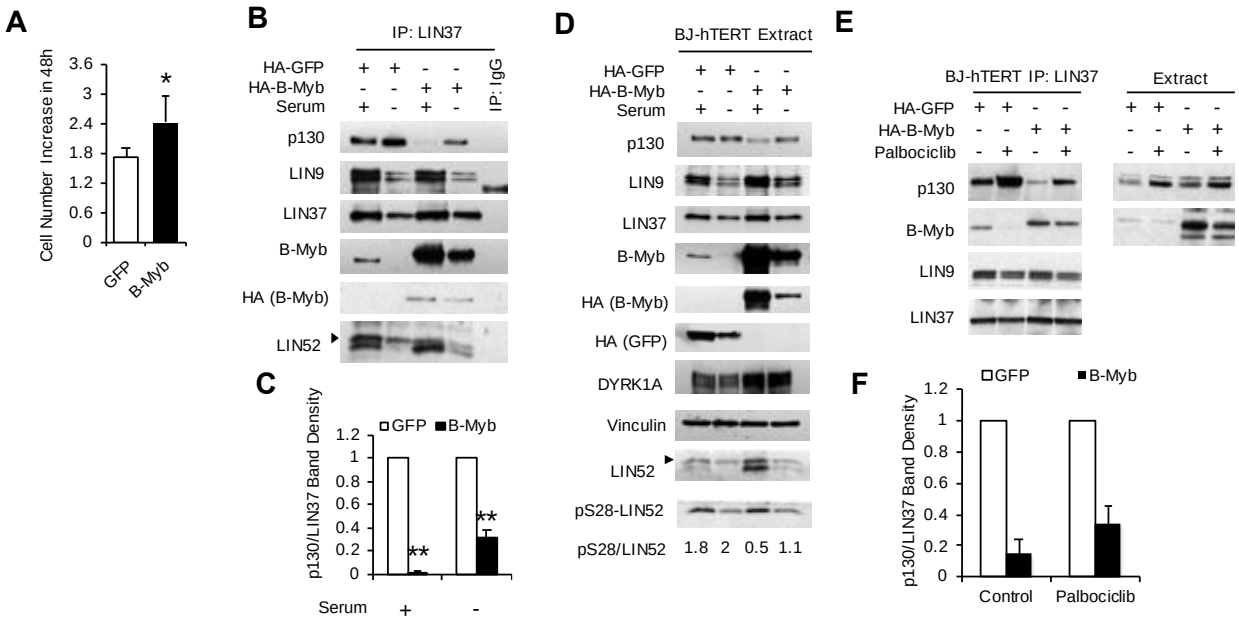


**Figure 4. B-Myb overexpression interferes with DREAM assembly in BJ-hTERT cells under the conditions of growth arrest. (A)** Increased proliferation of BJ-hTERT cell line expressing HA-B-Myb compared to HA-GFP (control). Graph shows average increase (N=3) of cell density on day 5 relative to day 3 after plating, to account for differences in plating efficiency between the cell lines (* - $p<0.05$). **(B)** IP/WB analysis of DREAM and MMB complexes in BJ-hTERT fibroblasts stably expressing HA-GFP (control) or HA-B-Myb. Where indicated, cells were incubated without serum for 48h to promote DREAM complex formation. **(C)** Quantification of **1B**. Relative abundance of p130 to LIN37 in B-Myb overexpressing cells was compared to that in the HA-GFP control cells (taken as 1). Graph shows average ± stdev of four independent experiments (** - $p<0.01$). **(D)** WB analysis of extract from 1B showing alterations in LIN9 level and LIN52 phosphorylation state. pS28/LIN52 ratio shows changes in pS28-LIN52 band density relative to the total LIN52 (both forms combined). The solid black arrow indicates pS28-LIN52 band here and throughout the remaining figures. Vinculin blot is shown to confirm equal loading. **(E)** IP/WB analysis of DREAM and MMB formation in BJ-hTERT stable cell lines expressing HA-B-Myb compared to HA-GFP control cells. Cells were incubated with 10μM palbociclib to induce G0/G1 arrest, or vehicle, for 24h before harvesting. **(F)** Quantification of **1E** analyzed as described previously in **1C**.

## B-Myb requires binding to MuvB for DREAM disassembly

To test the importance of MuvB binding for B-Myb-mediated DREAM disruption, we compared cell lines stably expressing either wild-type HA-B-Myb or a MuvB-binding deficient (MBD) mutant Q674A/M677A-B-Myb(96). As shown in **Fig. 5A, B**, expression of the HA-MBD mutant B-Myb negated the ability of B-Myb to disrupt DREAM formation

in both BJ-hTERT (**Fig. 5A**) and T98G cells (**Fig. 5B**), as indicated by comparable levels of p130-LIN37 complexes between parental and HA-MBD-expressing cells. Additionally, we validated the MuvB-binding deficient mutant B-Myb in HeLa cells (**Fig. 5C**). Since HeLa cells contain a known DREAM inhibitor, Human Papilloma Virus (HPV) viral oncoprotein E7, they serve as a model for further studying B-Myb-MuvB interactions (52). Here, we again noted disruption of B-Myb binding to MuvB, as revealed by the lack of HA-tagged protein co-precipitation with MuvB component LIN37.

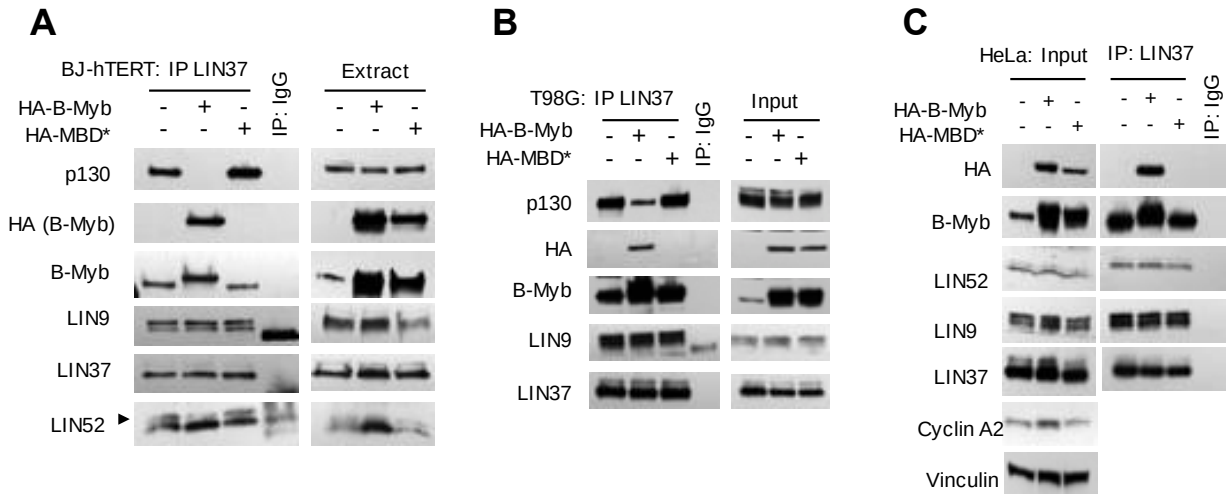


**Figure 5. Disruption of B-Myb-MuvB binding across three sets of cell lines. (A)** IP/WB analysis for DREAM/MMB assembly in BJ-hTERT cells stably expressing HA-GFP (control), HA-tagged WT or MuvB-binding deficient mutant (MBD) B-Myb. **(B)** Same as in **5A** except in T98G parental cells. **(C)** Validation of disrupted B-Myb-MuvB binding in HeLa cells that innately lack DREAM formation.

Additionally, expression of HA-MBD B-Myb significantly inhibited cell growth, as compared with cells expressing HA-B-Myb WT protein. However, there was no significant difference between growth of the parental control cells and either HA-B-Myb WT or MBD mutant cell lines (**Fig. 6A**). Chromatin immunoprecipitation (ChIP) of HA indicated loss of HA-MBD mutant binding to the *CCNB1* promoter (encoding cyclin B1), a known CHR-containing and MuvB-targeted promoter (**Fig. 6B**) (38). Collectively, these data indicate

that B-Myb binding to MuvB is required for DREAM disruption. Lack of promoter binding by the HA-MBD mutant further reinforces the conclusion that B-Myb exerts its effects through contact with MuvB.

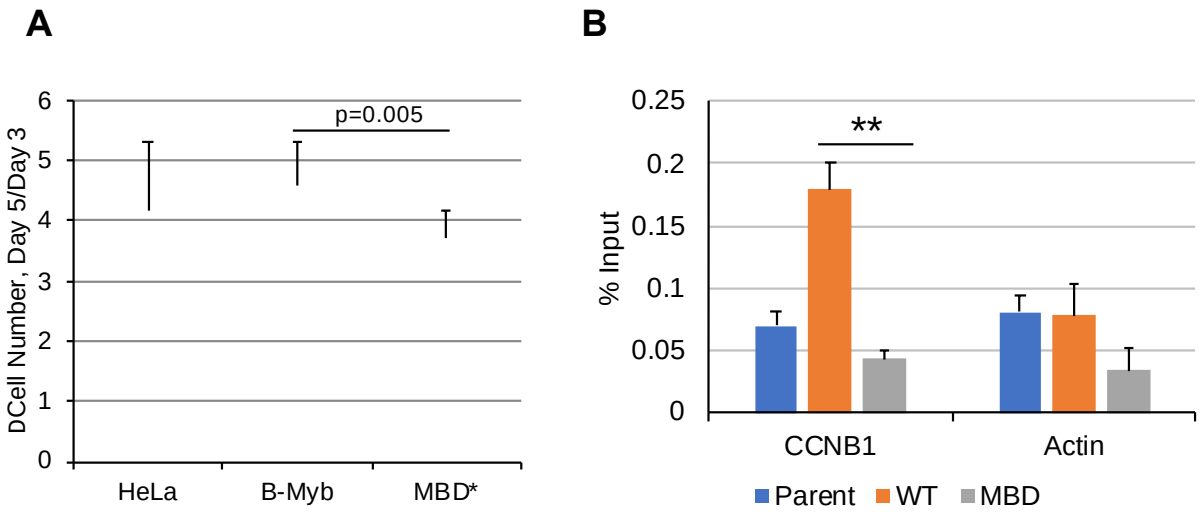


**Figure 6. Functional characterization of HA-MBD HeLa cells. (A)** HeLa cells stably expressing HA-tagged wild-type or MBD mutant (Q674A/M677A) B-Myb were counted at 3 and 5 days after plating. Graph shows average ± stdev of four independent experiments. **(B)** ChIP of HA in HeLa cells expressing HA-B-Myb WT or MBD mutant. Parental cells are a control. Data represent 2 biological replicates and 1 technical replicate). Graph shows average ± stdev (** - $p<0.01$)

**Regulation of MuvB by high B-Myb expression**

Though MuvB binding is necessary for B-Myb to disrupt DREAM, B-Myb overexpression did not affect the interaction between LIN37 and MuvB proteins LIN9 and LIN52 (**Fig. 4B, 5**). However, we noted an increased abundance of LIN9 and LIN52 proteins in the non-starved B-Myb overexpressing BJ-hTERT cells compared to control (**Fig. 4B, D**). This could be attributable to transcriptional regulation, as DREAM binds to *LIN9* and *LIN52* promoters (43). In line with DREAM-mediated repression, RT-qPCR analysis confirmed downregulation of LIN9 and LIN52 mRNA with serum starvation. In non-starved cells, HA-B-Myb was significantly associated with increased *LIN9* and *LIN52*

expression, a trend also observed with both genes in the serum starved state (**Fig. 7A, B**). Given a modest 1.5-fold increase of *LIN52* mRNA levels in the presence of HA-B-Myb, we measured LIN52 protein stability in BJ-hTERT cells using cycloheximide (CHX) chase assays and found that it was more abundant after 10h of CHX treatment in the HA-B-Myb-expressing cells as compared with control (**Fig. 7C**). Since LIN52 is a MuvB component essential for formation of both DREAM and MMB, we further investigated the effect of B-Myb overexpression on LIN52.

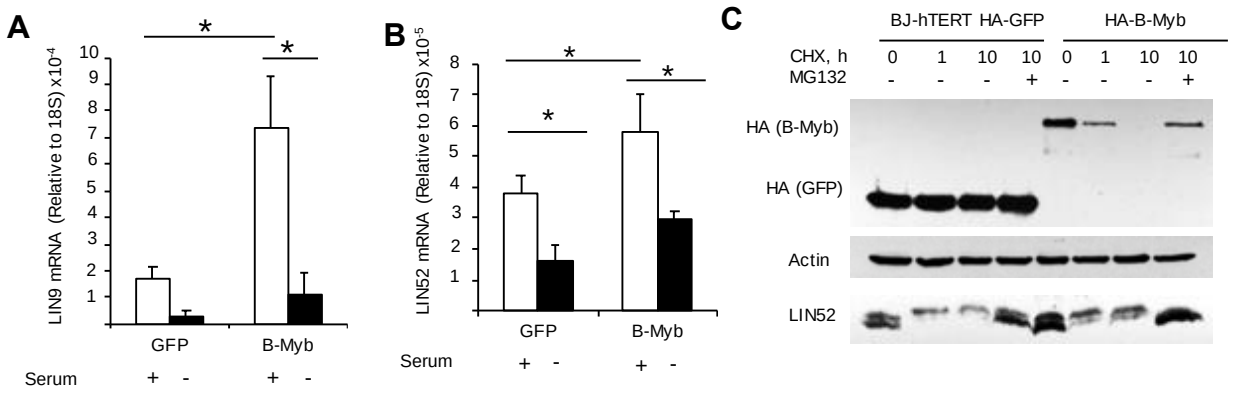


**Figure 7. B-Myb influences MuvB expression. (A)** RT-qPCR analysis of LIN9 and LIN52 mRNA expression in BJ-hTERT cell lines expressing GFP or HA-B-Myb. Cells were grown in the presence of serum, or serum-starved for 48 hours before analysis. Graph shows average ± stdev (N=3). Student's t-test p-values * - <0.05, ** - <0.01. **(B)** WB analysis of cycloheximide (CHX) chase assay of endogenous LIN52 in BJ-hTERT cells reveals increased expression and stability of LIN52 in HA-B-Myb-overexpressing cells compared to GFP (control).

**High B-Myb levels influence LIN52 regulation**

In addition to increased expression, we noted alterations in the relative abundance of S28-phosphorylated and un-phosphorylated LIN52 in the presence of HA-B-Myb (**Fig. 4D**). We have previously shown that slower migrating form of LIN52 appears when this protein is phosphorylated at S28 by DYRK1A kinase (15). Using a phospho-specific antibody, we confirmed that relative abundance of S28-phosphorylated LIN52 was decreased in the presence of HA-B-Myb in BJ-hTERT cells though it was not associated

with changes in DYRK1A level or kinase activity (**Fig. 8A**), suggesting that B-Myb could inhibit DREAM assembly by interfering with the key phosphorylation event required for MuvB binding to p130 (43).

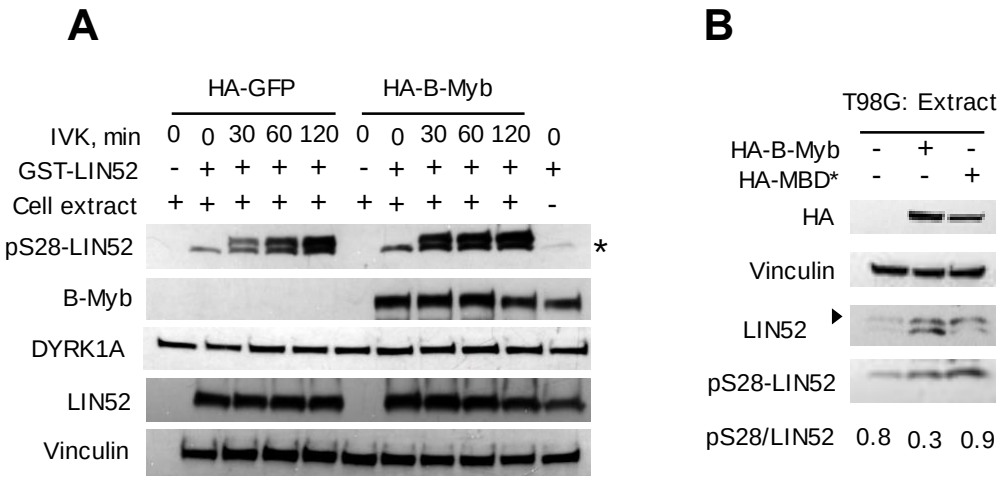


**Figure 8. B-Myb alters the relative abundance of pS28-LIN52 through a DYRK1A-independent mechanism. (A)** *In vitro* kinase assay using recombinant GST-LIN52 as a substrate shows no difference in DYRK1A kinase activity in the control and HA-B-Myb expressing BJ-hTERT cells. Purified GST-LIN52 was incubated with cell extracts and ATP, resolved on SDS-PAGE and analyzed using phosphoS28-specific antibody. See also Figure 13A confirming the specificity of the assay. (B) WB using extracts from T98G cells in **5B** showing changes in LIN52 protein and relative abundance of pS28-LIN52.

To further validate and characterize the effect of B-Myb on DREAM assembly, we used T98G glioblastoma cells because they have been studied extensively in cell cycle research, including initial characterization of DREAM and MMB (13). Although this cancer cell line lacks *MYBL2* amplification, T98G cells express readily detectable levels of B-Myb (unlike BJ-hTERT), making them amenable to both loss and gain of function studies of B-Myb (13, 90, 92, 97). Similar to BJ-hTERT cells (**Fig. 5A**), expression of wild-type B-Myb, but not the MBD mutant resulted in decreased DREAM assembly (**Fig. 5B**). Consistent with this result, we observed that the endogenous LIN52 protein was more abundant and relatively less phosphorylated in the presence of HA-B-Myb than in parental T98G cells,

or the cells expressing MBD HA-B-Myb (**Fig. 8B**). These findings reinforced the important role of B-Myb-MuvB binding not only for DREAM disruption, but also for influencing LIN52 protein, and led us to further investigate regulation of LIN52 as a novel mechanism by which B-Myb impacts cell cycle gene expression.

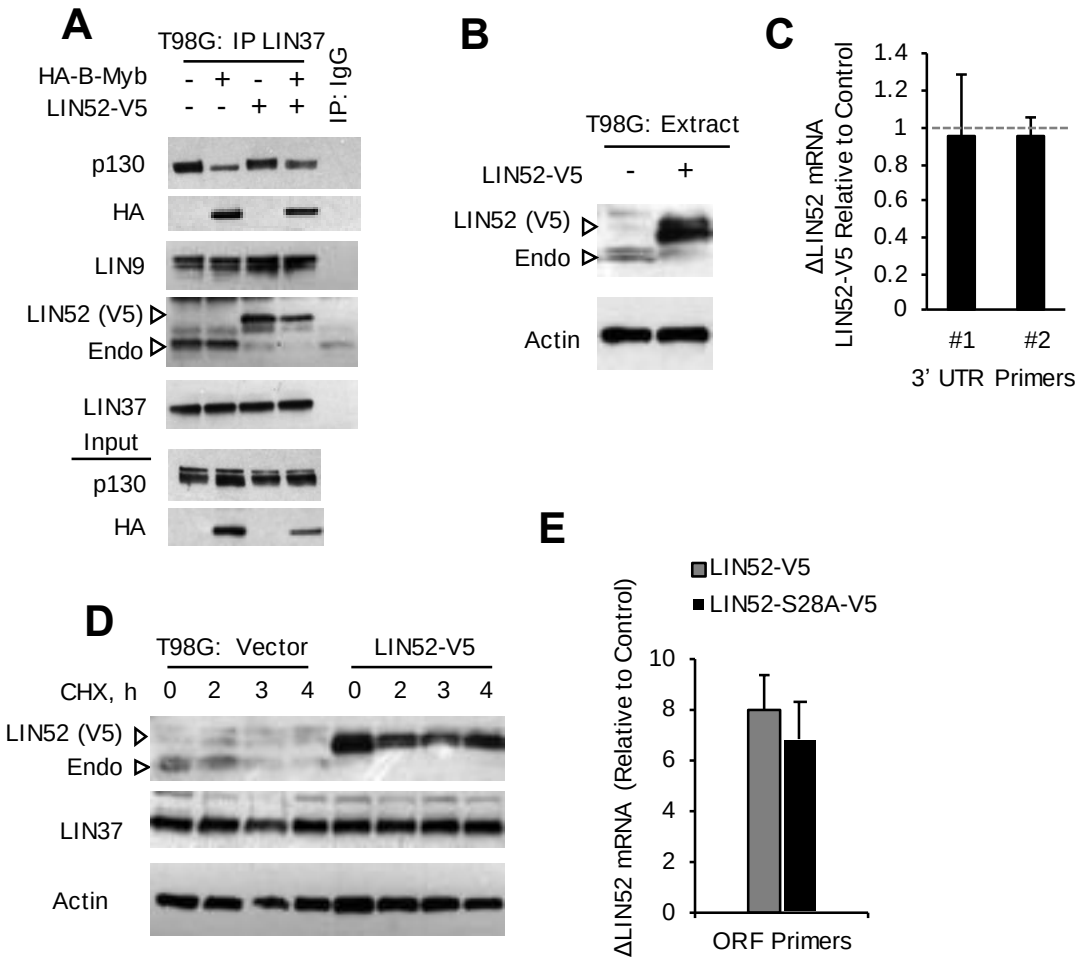


**Figure 9. Effects of B-Myb and LIN52 overexpression in T98G cells reveal regulation at the protein level. (A)** IP/WB analysis of T98G cells stably expressing LIN52-V5, HA-B-Myb, or both, compared with control parental cells. Open arrow indicates position of the indicated proteins here and throughout the following figures. **(B)** WB analysis shows downregulation of endogenous LIN52 in T98G cells stably expressing LIN52-V5. **(C)** RT-qPCR analysis with primers specific to endogenous LIN52 mRNA reveals no significant changes in the presence of ectopic LIN52. Graph shows average ± stdev (N=3, $p>0.05$).

**(D)** WB analysis of cycloheximide (CHX) chase experiment using T98G stable cell lines expressing empty vector or LIN52-V5. **(E)** RT-qPCR analysis shows similar expression of the wild-type and S28A-mutant LIN52 mRNA detected using primers specific to the open reading frame (ORF). Graph shows average ± stdev of three independent experiments (Student's t-test $p>0.05$).

**LIN52 expression is controlled at the protein level**

Since B-Myb disrupts DREAM and also increases LIN52 protein abundance, we tested whether DREAM assembly is influenced by ectopic overexpression of LIN52 alone. However, analysis of T98G cells stably expressing LIN52-V5, HA-B-Myb, or both, showed no substantial impact of ectopically expressed LIN52 on DREAM assembly (**Fig. 9A**). Furthermore, LIN52-V5 appeared to replace endogenous LIN52 from LIN37 complexes, likely because of decreased endogenous LIN52 expression in the presence of LIN52-V5 (**Fig. 9B**). RT-qPCR analysis with primers specific for endogenous LIN52 mRNA revealed no significant changes in the presence of LIN52-V5, indicating that LIN52 downregulation occurs at the protein level (**Fig. 9C**). This prompted us to assess the stability of both endogenous and ectopically expressed LIN52 using CHX chase assays. We noted that both endogenous and ectopically expressed LIN52 proteins were both markedly depleted after 3h of CHX treatment (**Fig. 9D**), suggesting that LIN52 was less stable in T98G cells than in BJ-hTERT (**Fig. 7C**). We were not able to estimate the turnover rate of endogenous LIN52 in LIN52-V5-expressing cells because of its low expression. Of note, we did not observe significant degradation of MuvB protein LIN37 under these conditions.

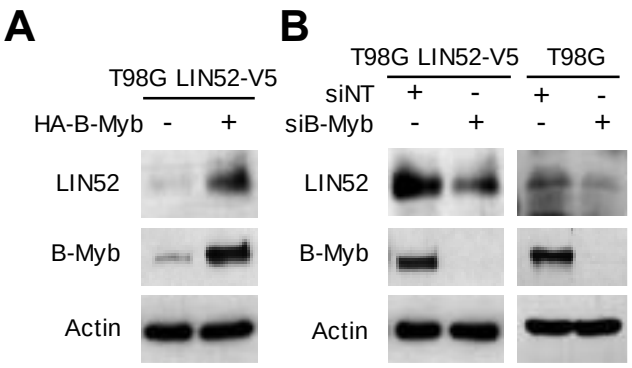


**Figure 10. LIN52 protein level is associated with changes in B-Myb expression. (A)** WB analysis of T98G cells stably expressing LIN52-V5 alone, or together with HA-B-Myb shows that B-Myb overexpression causes upregulation of the ectopically expressed LIN52. **(B)** Same as **10A**, only after transient knockdown of B-Myb using siRNA. siNT, non-targeting siRNA control. Blots show both ectopic and endogenous LIN52.

To further validate our finding that B-Myb regulates LIN52 protein expression, we altered B-Myb levels in T98G cells stably expressing LIN52-V5. As in case of endogenous LIN52, overexpression of B-Myb resulted in increased expression of the LIN52-V5 protein in T98G cells (**Fig. 10A**). Furthermore, siRNA knockdown of B-Myb led to downregulation of LIN52-V5 as well as the endogenous LIN52 protein (**Fig. 10B**). Together, our data presented above show that B-Myb is able to disrupt DREAM assembly when highly expressed, and support the role of B-Myb in regulation of LIN52 expression at the protein level.

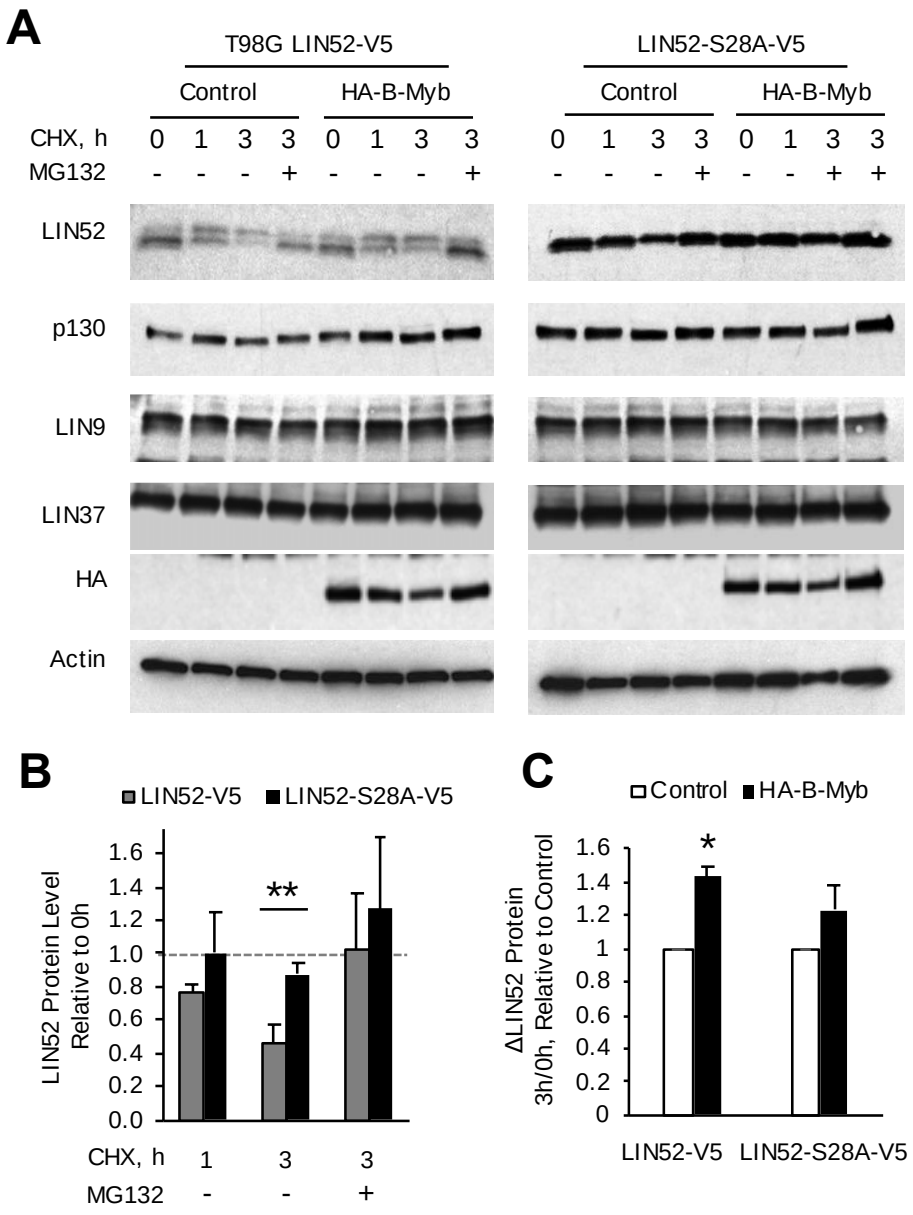


**Figure 11. B-Myb overexpression in T98G cells stabilizes LIN52 but not S28A-LIN52 mutant. (A)** Representative immunoblots show CHX chase assays using T98G cells stably expressing LIN52-V5 or LIN52-S28A-V5 proteins alone, or together with HA-B-Myb. **(B, C)** Quantitative analysis of LIN52-V5 and LIN52-S28A-V5 CHX chase assays shown in **11A**. In panel **B**, graph represents average ± stdev (N=5) of LIN52 LIN52-S28A band density in control cells without B-Myb overexpression. LIN52 band density was first normalized to actin and then plotted relative to 0h (** - $p<0.01$). In panel **C**, graph shows the average change in LIN52 band density at 3h compared to 0h, in the presence of HA-B-Myb relative to that in the control cells. Note that LIN52-V5 stability in the presence of HA-B-Myb is significantly greater than in cells expressing LIN52-V5 alone (N=3, * - $p<0.05$) whereas LIN52-S28A-V5 is not significantly affected by HA-B-Myb.

**Regulation of LIN52 stability by B-Myb requires intact S28 residue**

We then examined the relative effects of B-Myb expression and S28 phosphorylation on LIN52 protein stability in a series of quantitative CHX assays by comparing the effect of B-Myb on wild-type LIN52 and non-phosphorylatable S28A-LIN52 mutant using established T98G cell lines (90). The S28A mutation abolishes the DYRK1A-phosphorylation site essential for DREAM formation without interfering with the MMB complex assembly (16). Using CHX assays, we determined that the half-life of wild type LIN52-V5 in T98G cells was approximately 3h **(Fig. 11A, B).** Using MG132 together with CHX blocked the degradation of LIN52-V5 in this assay, suggesting that LIN52 degradation involves the proteasome. As expected, expression of HA-B-Myb in these cells resulted in significant stabilization of ectopically expressed LIN52-V5 by approximately 40% **(Fig. 11A, C).** Interestingly, the LIN52-S28A mutant remained significantly more abundant at the 3h time point than wild-type LIN52-V5 (**Fig. 11B**). Furthermore, whereas the stability of wild-type LIN52-V5 was significantly impacted by the presence of HA-B-Myb, stability of the S28A mutant LIN52 remained unchanged (**Fig. 11A, C**). Despite this finding, we noted that there is an apparent persistence of the upper LIN52 band over the time course of CHX treatment, suggesting that a subset of phosphorylated LIN52 may be protected from degradation. We also monitored levels of LIN9, LIN37 and p130 in the same CHX chase experiments, and stability of these proteins did not show the same dependency on B-Myb as LIN52 (**Fig. 11A**). Together, these data show that stability of LIN52 is regulated by B-Myb and requires an intact S28 residue.

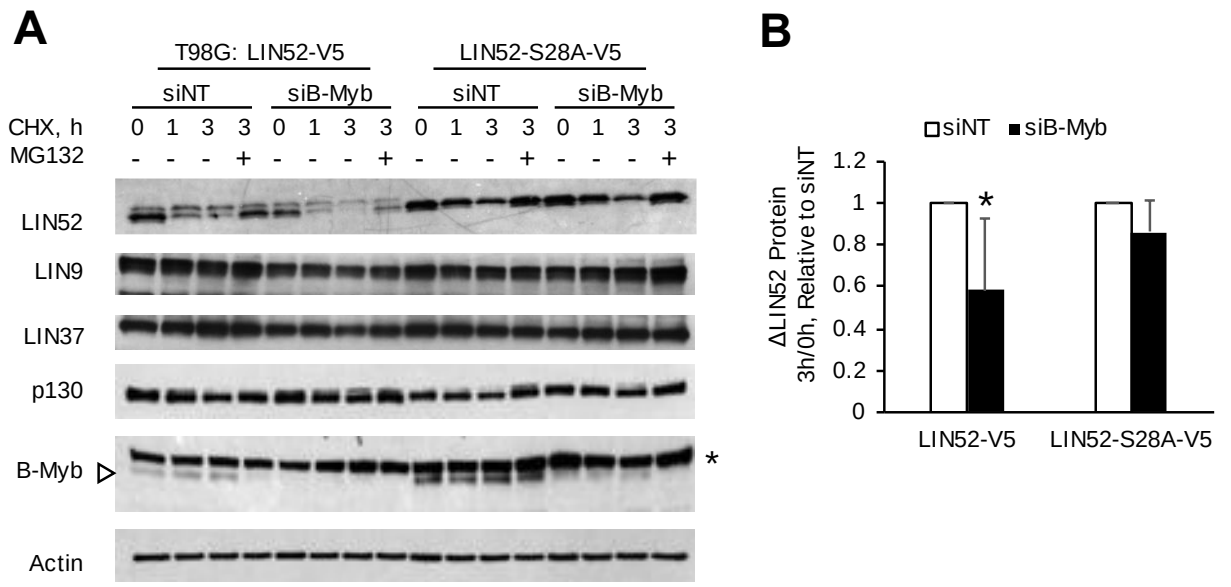


**Figure 12. Depletion of B-Myb in T98G cells increases turnover of LIN52 but not the S28A-LIN52 mutant. (A)** Representative immunoblots show that RNAi knockdown of B-Myb decreases stability of wild type LIN52, but not LIN52-S28A-V5. T98G cells stably expressing LIN52 proteins were transfected with siNT (non-targeting) or B-Myb-specific siRNA, and used for CHX chase assays after 36 hours. Note the relative stability of LIN9 and LIN37 compared with that of LIN52. Asterisk indicates non-specific band. **(B)** Graph shows average change in LIN52 band density at 3h compared to 0h, in siB-Myb transfected cells relative to that in siNT cells. Note that LIN52-V5 stability in the presence of siB-Myb is significantly lower than in siNT-transfected cells (N=3, * - $p<0.05$) whereas LIN52-S28A-V5 is not significantly affected

These conclusions were additionally supported when LIN52 stability was analyzed under the conditions of B-Myb knock-down. Indeed, LIN52-V5 protein decayed more rapidly after CHX treatment in T98G cells with RNAi-mediated B-Myb knock-down compared to cells transfected with non-targeting (NT) control siRNA (**Fig. 12A, B**). Here, we again found that B-Myb exhibits no significant effect on LIN52-S28A-V5 protein stability. Since B-Myb is still able to bind to LIN52-S28A-V5 (90), these results suggest that phosphorylation at the S28 plays a role in regulating LIN52 levels.

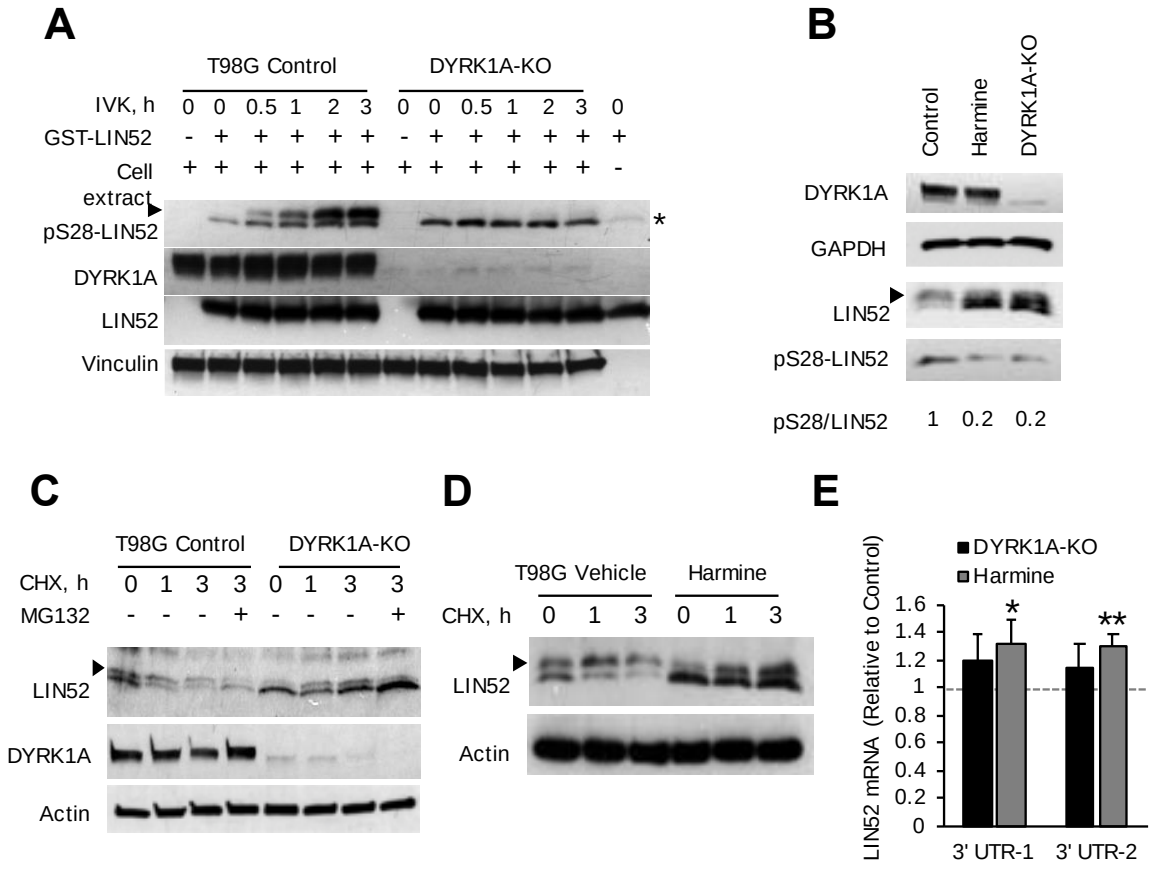


**Figure 13. Phosphorylation of LIN52 by DYRK1A at S28 regulates its stability. (A)** In vitro kinase assay showing LIN52 phosphorylation at S28 by DYRK1A kinase in control T98G cells, but not in the DYRK1A-KO cells. GST-LIN52 was incubated with cell extracts in the presence of ATP as indicated. Presence of LIN52 phosphorylation at S28 as well as the total GST-LIN52 and DYRK1A, was assessed by WB. Asterisk denotes non-specific band. **(B)** WB analysis of the endogenous LIN52 and pS28-LIN52 in control T98G cells, DYRK1A knockout (KO) cells, or cells after harmine inhibition of DYRK1A kinase activity. **(C, D)** CHX chase assays show that endogenous LIN52 protein is more stable in DYRK1A-KO cells or in harmine-treated cells, as compared to control. (E) RT-qPCR analysis reveals a modest increase in LIN52 mRNA expression when DYRK1A is inhibited, as compared to control cells. Graph shows average ± stdev (N=3, * and ** correspond to p-value <0.05 and <0.01, respectively).

**DYRK1A regulates LIN52 stability**

Given that LIN52 phosphorylation at S28 is mediated by DYRK1A (90), we wanted to determine the role of DYRK1A in regulating LIN52 levels. We used the CRISPR/Cas9 genome editing approach (98) to generate T98G cells devoid of DYRK1A protein (DYRK1A-KO). To validate the specificity of DYRK1A as S28-LIN52 kinase, we performed an *in vitro* kinase assay with extracts from T98G parental and DYRK1A KO cells using WB detection of pS28-LIN52 as readout. As shown in **Fig. 13A**, S28-LIN52 kinase activity was greatly diminished in T98G DYRK1A KO cells compared to control. LIN52 was expressed at higher steady-state levels and appeared in a predominantly un-phosphorylated form in DYRK1A-KO cells or in T98G cells treated with a DYRK1A kinase inhibitor, harmine (99) (**Fig. 13B**). Phosphospecific WB confirmed a substantial reduction in S28-phosphorylated LIN52 with either harmine treatment or DYRK1A KO. The remaining pS28-LIN52 in DYRK1A-inhibited cells could be due to phosphorylation by alternative LIN52 kinases, such as CDKs (100). Additionally, DYRK1B, a homologue of DYRK1A that is less abundant in T98G cells, could partly compensate for the lack of DYRK1A in KO cells (15).

We then performed CHX chase experiments and showed that the stability of endogenous LIN52 is enhanced when DYRK1A is absent or inhibited by harmine (**Fig. 13C, D)**. RT-qPCR analysis revealed a modest increase in LIN52 mRNA expression when DYRK1A is knocked out or inhibited (**Fig. 13E**), suggesting that LIN52 is also regulated by DYRK1A at the level of transcription. Taken together, our data demonstrate that LIN52 is regulated at the protein level, and that DYRK1A-dependent phosphorylation is involved in the control of LIN52 stability.

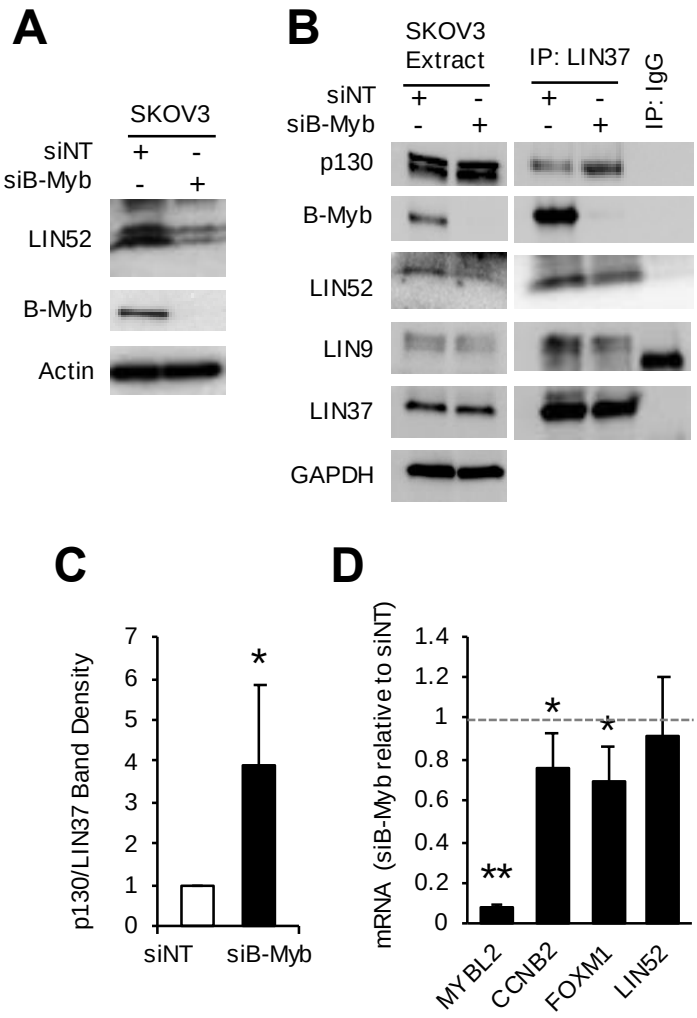


**Figure 14. Effect of B-Myb on the DREAM complex function in cancer cells. (A)** WB analysis of the extracts from siRNA-transfected SKOV3 cells shows decreased expression of LIN52 in B-Myb-depleted cells compared to control. **(B)** IP/WB analysis shows increased binding of p130 to LIN37 (indicative of DREAM formation) in SKOV3 cells transfected with B-Myb-specific siRNA compared to control cells. **(D)** Quantification of **14B**. Relative abundance of p130 to LIN37 in siB-Myb transfected cells was compared to that in the siNT treated control cells (taken as 1). Graph shows average ± stdev of three independent experiments (* - $p<0.05$). **(D)** RT-qPCR analysis shows decreased expression of *FOXM1* (DREAM target) and *CCNB2* (DREAM and MMB target) genes upon B-Myb knockdown in SKOV3 cells. Graph shows average ± stdev of three independent experiments (* - $p<0.05$).

**Model of B-Myb-mediated DREAM disruption in cancer**

Finally, we sought to apply our model of B-Myb-mediated DREAM disruption to clinically relevant cancer models, such as SKOV3 serous ovarian carcinoma cells known to harbor *MYBL2* gene amplification (101). As shown in **Fig. 14A**, B-Myb knock-down resulted in downregulation of LIN52, as we observed previously in T98G cells expressing LIN52-V5 (**Fig. 10B**). Asynchronously growing SKOV3 cells contain low steady state levels of DREAM, and a robust increase of DREAM formation was detected after RNAi-mediated knock-down of B-Myb (**Fig. 14B, C**). RT-qPCR analysis shown in **Figure 14D** confirms the knockdown of *MYBL2*, as well as a decreased expression of a known MMB-target gene *CCNB2* (43). Importantly, this analysis also revealed decreased expression of a representative DREAM-only target gene (*FOXM1*), in agreement with the observed increase of the DREAM formation (**Fig. 14C**). LIN52 mRNA levels were not significantly influenced by depletion of B-Myb, further supporting the conclusion that B-Myb regulates LIN52 predominantly at the protein level.

Overall, our data support a model by which B-Myb accumulation during cell cycle progression or due to overexpression in cancer interferes with LIN52 phosphorylation at S28 by DYRK1A kinase that is required for the DREAM assembly. This leads to increased LIN52 abundance and stability, while also disrupting DREAM assembly, so that more MMB complex is formed, ultimately resulting in compromised repression of DREAM-target genes (**Fig. 15**).

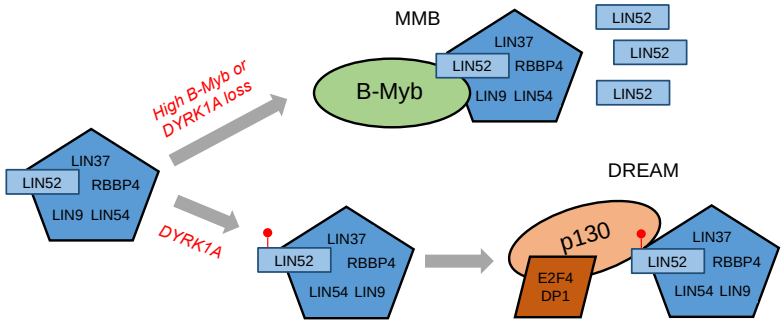


**Figure 15. Model of opposing regulation of DREAM by B-Myb and DYRK1A.** High expression of B-Myb or inhibition of DYRK1A can interfere with DREAM assembly by promoting accumulation of unphosphorylated LIN52, resulting in deregulation of cell cycle expression in cancer.

## Discussion

The DREAM and MMB complexes share the common MuvB core and appear to assemble in a mutually exclusive manner during mammalian cell cycle progression (2, 28). Several studies demonstrated that the DREAM and MMB complexes exist during different stages of the cell cycle with minimal overlap during the G1-S transition (13, 18, 20, 90). It was also shown that release of the MuvB core from DREAM requires cyclin-CDK phosphorylation of DREAM components and that chemical inhibition of either CDK4 or CDK2 stabilizes the DREAM under the conditions of cell cycle re-entry (16, 17). However, since B-Myb was not expressed in CDK-inhibited cells, it was unclear whether B-Myb could play an active role in DREAM disassembly. Here we show that DREAM is disrupted in human cells when B-Myb is highly expressed and is able to bind to MuvB core. Given our previous observation and studies in *Drosophila* that both RB-like protein and B-Myb can simultaneously associate with MuvB, we do not propose that p130 and B-Myb compete for LIN52 binding (12, 16). Alternatively, we suggest that B-Myb promotes DREAM disassembly by inhibiting LIN52 phosphorylation. LIN52 is then stabilized for

formation of additional MMB complexes that, in turn, are required to facilitate transcription of the duplicated genome after DNA replication is complete in late S-G2 phases. In this model, CDKs and B-Myb could cooperate to establish a positive feedback loop to disrupt the DREAM and relieve the E2F-mediated repression of cell cycle genes.

We found that levels of LIN52 and LIN9 in the cell are tightly controlled and regulated by B-Myb, both directly by transcription of mRNA and, in case of LIN52, also at the post-transcriptional level. Regulation of LIN52 by B-Myb is especially interesting given its role as the key MuvB component required for assembly of both DREAM and MMB. We observe that LIN52 is tightly regulated at the protein level and ectopic LIN52 expression results in increased turnover of the protein by both proteasome-dependent and independent mechanisms. We have previously demonstrated that the phosphorylated S28 residue plays a key role in direct binding of LIN52 to p130, required for DREAM assembly (16, 90). Our observation that overexpression of B-Myb in human cells promotes accumulation of un-phosphorylated LIN52 could partly explain the increased stability of LIN52 protein in the presence of highly expressed B-Myb. In support of this mechanism, unlike the wild-type LIN52, changes in B-Myb level do not impact the stability of LIN52-S28A. It remains to be established how B-Myb can interfere with LIN52 phosphorylation and degradation. B-Myb could stabilize LIN52 by regulating expression of proteins that degrade or stabilize LIN52, or by recruiting a phosphatase that will remove the LIN52 phospho-S28 mark. It is also possible that steric hindrance by B-Myb could block DYRK1A's access to the S28 site in LIN52. In our study, inhibition of S28A LIN52 phosphorylation consistently resulted in accumulation of total LIN52 protein. However, given the continued presence of the slower migrating form of LIN52 in CHX chase assays,

phosphorylation state does not completely account for LIN52 protein regulation. Therefore, further studies are needed to investigate these mechanisms.

This study also provides important insights into subunit interactions within the MuvB complex. Here, LIN52 appears to have shorter half-life than LIN9 or LIN37, possibly because of its special regulatory role. Indeed, LIN52 is required for both DREAM and MMB formation and makes direct contact with both p130/p107 and B-Myb (16, 96). Therefore, changes in LIN52 levels will influence the overall functional integrity of MuvB core. This is supported by diminished co-immunoprecipitation of MuvB complex components when LIN52 is depleted by shRNA (90). However, other studies have shown that LIN37 and LIN54 are also downregulated when LIN9 is depleted, suggesting a possibility that some of MuvB subunits need to co-fold together during translation (14). A recent study found that in LIN37 knockout cells, the remaining MuvB subunits were normally expressed and formed a complex capable of binding to either p130, or B-Myb, and while the MMB function remained intact, the DREAM repressor function was compromised (32). It is also intriguing to note that B-Myb was unable to contact the *CCNB1* promoter or disrupt DREAM assembly independent of MuvB binding. This supports the importance of B-Myb's regulation of MuvB (particularly LIN52) for its impact on cell cycle gene expression. Together, these findings suggest that the abundance of MuvB core could be important for its biological functions, for example to ensure the specificity of binding to the promoter sites, and needs to be tightly regulated. In the future, it will be interesting to investigate the consequences of failure to maintain the proper levels of MuvB core subunits in the cell as well as the independent function of MuvB, which remains largely unknown.

B-Myb is overexpressed in many types of cancer and is recognized as a poor prognostic factor, but the known role of B-Myb as a transcription factor required for mitotic progression does not fully explain its established association with a more aggressive cancer phenotype. Our finding that B-Myb disrupts the DREAM complex in cells could explain why high expression of B-Myb leads to cell cycle deregulation in human cancers. Since *MYBL2* itself is a DREAM target gene, this might create a positive feedback loop in which increased B-Myb expression perpetuates DREAM disruption and further loss of transcriptional regulation. Several of the MMB downstream targets upregulated in late S-G2 phases of the cell cycle, such as Aurora kinase A, Polo-like kinase B and others have been proposed for developing anti-cancer therapies (3). Better understanding of the mechanisms that bring about high expression of these genes in cancer will be important to inform the future pre-clinical and clinical studies and to optimize patient stratification. Overall, we have shown a novel model describing some of the molecular processes underlying deregulated cell cycle gene expression in cancers with B-Myb amplification or overexpression. These findings argue that B-Myb is not only a negative prognostic factor through increased MMB formation and activation of the mitotic gene expression program, but also through decreased DREAM assembly and loss of repression of more than 800 cell cycle-regulated genes. Further studies with tumor samples are needed to validate our model in patients and evaluate methods of targeting B-Myb to restore cell cycle control.

# Chapter 3: Clinical pathologic expression of cell cycle regulatory complexes in high grade serous ovarian carcinoma.

## Introduction

Cell cycle regulation is a key factor influencing treatment response and outcomes of HGSOC patients. The DREAM complex has been shown to mediate recurrence by maintaining cells in a dormant state and, in turn, treatment resistance (69). One of the main determinants of progression free survival in HGSOC patients is response to therapy (66). However, survival rates do not directly relate to therapeutic response. Low grade lesions are generally associated with longer progression free survival than high grade lesions, but also are known to exhibit more chemoresistance. The proposed explanation for this observation is that the slower proliferation rate of low grade carcinomas limits the opportunity for platinum intercalation induced DNA damage, yet the less aggressive nature of these lesions is generally equated with longer progression free survival (102).

Additionally, HGSOC patients could benefit from development of a predictive biomarker—an indicator of treatment response. Current standard of care for HGSOC patients involves aggressive surgery and subsequent chemotherapy (platinum-taxane). About 25% of patients have platinum-resistant disease that recurs within 6 months of finishing chemotherapy (103). A predictive biomarker would allow physicians to tailor therapies to either reduce toxicity for patients with platinum-sensitive disease or inform the use of alternative or more aggressive treatment of predicted platinum resistant disease. Currently, no such widely-accepted biomarkers exist (104). Given that B-Myb expression levels are often increased in HGSOC, and its prominent cell cycle effects, it

is worthwhile to investigate B-Myb's potential as a predictive marker. Also, since the DREAM complex has been tied to cellular dormancy and resistance to platinum-based chemotherapy, then perhaps B-Myb levels influence treatment response through DREAM disruption and increased MMB formation **(Fig. 16)**.

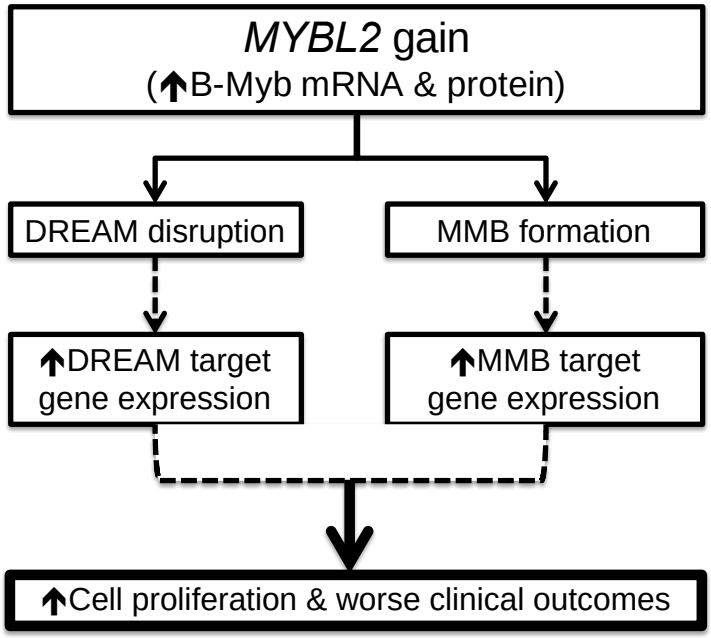


**Figure 16. Working model of B-Myb-driven cell cycle deregulation and cellular proliferation.** B-Myb is highly expressed in HGSOC and sequesters MuvB, leading to increased MMB formation and disrupted DREAM assembly. In turn, expression of both DREAM and MMB target genes are increased. Compromised cell cycle gene regulation leads to increased cell proliferation and worse patient outcomes.

**Modeling B-Myb-mediated DREAM disruption with The Cancer Genome Atlas**

To further investigate the functional relationship between B-Myb level and regulation of cell cycle dependent transcription, we analyzed gene expression data from The Cancer Genome Atlas (TCGA). We first looked at the *MYBL2* gene expression across all cancers and the corresponding normal tissue samples, when available. As previously reported, the *MYBL2* gene was overexpressed in multiple cancer types (**Fig. 17A**). For further analysis of transcriptome changes associated with high *MYBL2*

expression, we chose to focus on high grade serous ovarian carcinoma (HGSOC), since *MYBL2* gene copy number gain is present in 55% of the TCGA HGSOC samples and associated with a poor prognosis (**Fig. 17B**) (23). Similar analyses were conducted in parallel for breast cancer, for which the significance of B-Myb overexpression is well-documented (5, 59, 105, 106). We first validated that *MYBL2* genomic amplification correlated with increased B-Myb mRNA expression (**Fig. 18A**) as well as with significant up-regulation of cell cycle regulated genes (**Fig. 18B, C**) then proceeded to characterize the most differentially expressed genes between tumor samples with high and low *MYBL2* expression levels.

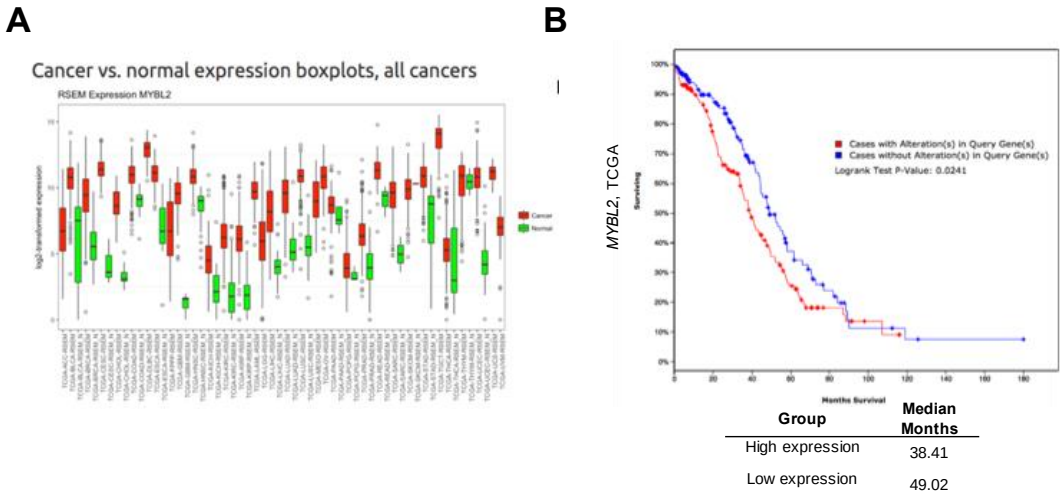


**Figure 17. B-Myb is highly expressed in many cancers and is associated with poor overall survival in HGSOC. (A)** Analysis of *MYBL2* (encoding B-Myb) expression across all cancers shows widespread upregulation. **(B)** Kaplan-Meier survival analysis from HGSOC TCGA data set.

As expected, we found that most differentially expressed genes in both cancer types were highly enriched in functional gene ontology categories representing cell cycle processes. Furthermore, both MMB and DREAM target genes were overrepresented among the most differentially expressed genes in the high-*MYBL2* samples (**Fig. 19A,**

**B**), and high B-Myb levels were associated with increased MMB and DREAM target gene expression. Remarkably, the top 50 upregulated genes associated with high *MYBL2* in breast cancer analysis, and top 49 genes in HGSOC, have been previously annotated as DREAM target genes identified in global location studies (**Fig. 20A, B**) (13, 43). Since MMB does not regulate some of these genes directly, this finding supports the model whereby B-Myb-mediated DREAM disruption plays a role in deregulation of cell cycle gene expression program in cancers with high B-Myb expression.

**A**

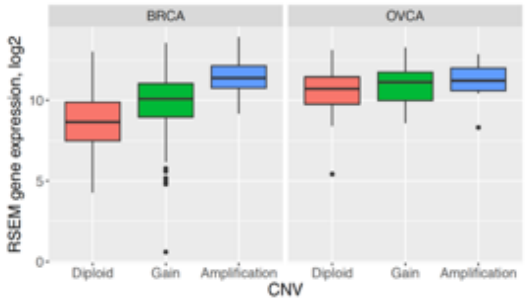


| t-test: | BRCA | OVCA |
|---|---|---|
| Diploid v. Gain | $8.74e^{-27}$ | $4.45e^{-02}$ |
| Diploid v. Amplification | $1.15e^{-12}$ | $5.11e^{-01}$ |
| Gain v. Amplification | $2.79e^{-7}$ | $8.99e^{-01}$ |

**B**

| *Gene Set Name (top 10)* | *# Genes in Gene Set (K)* | *# Genes in Overlap (k)* | *k/K* | *p-value* | *FDR q-value* |
|---|---|---|---|---|---|
| Cell Cycle | 1316 | 90 | 0.0684 | 9.92E-100 | 4.40E-96 |
| Cell Cycle Process | 1081 | 85 | 0.0786 | 1.60E-98 | 3.54E-95 |
| Mitotic Cell cycle | 766 | 77 | 0.1005 | 1.78E-96 | 2.64E-93 |
| Organelle Fission | 496 | 59 | 0.119 | 1.24E-76 | 1.38E-73 |
| Mitotic Nuclear Division | 361 | 51 | 0.1413 | 1.02E-69 | 9.04E-67 |
| Cell Division | 460 | 50 | 0.1087 | 2.56E-62 | 1.89E-59 |
| Chromosome Segregation | 272 | 42 | 0.1544 | 9.24E-59 | 5.86E-56 |
| Sister Chromatid Segregation | 176 | 37 | 0.2102 | 4.94E-57 | 2.74E-54 |
| Chromosome Segregation | 1009 | 57 | 0.0565 | 4.34E-55 | 2.14E-52 |
| Nuclear Chromosome Segregation | 228 | 38 | 0.1667 | 2.07E-54 | 9.16E-52 |

**C**

| *Gene Set Name (top 10)* | *# Genes in Gene Set (K)* | *# Genes in Overlap (k)* | *k/K* | *p-value* | *FDR q-value* |
|---|---|---|---|---|---|
| Chromosome Organization | 1009 | 76 | 0.0753 | 4.24E-25 | 1.88E-21 |
| Negative Regulation of Nitrogen Compound Regulatory Processes | 1517 | 91 | 0.06 | 6.98E-23 | 1.55E-19 |
| Regulation of Transcription from RNA Polymerase II Promoter | 1784 | 99 | 0.0555 | 2.21E-22 | 3.00E-19 |
| Cell Cycle | 1316 | 83 | 0.0631 | 2.71E-22 | 3.00E-19 |
| Neurogenesis | 1402 | 85 | 0.0606 | 1.04E-21 | 8.69E-19 |
| Regulation of Organelle Organization | 1178 | 77 | 0.0654 | 1.17E-21 | 8.69E-19 |
| Phosphate-Containing Compound Metabolic Process | 1977 | 103 | 0.0521 | 2.98E-21 | 1.89E-18 |
| Embryo Development | 894 | 65 | 0.0727 | 8.58E-21 | 4.76E-18 |
| Cell Development | 1426 | 84 | 0.0589 | 1.12E-20 | 5.18E-18 |
| Chromatin Modification | 539 | 50 | 0.0928 | 1.17E-20 | 5.18E-18 |

**Figure 18. *MYBL2* gain or amplification impacts cell cycle processes. (A)** Correlation between the copy number gains of *MYBL2* (B-Myb) and its high expression in breast and ovarian cancers. Table shows resulting p-values from the indicated pair-wise comparison t-tests. **(B)** Gene Ontology analysis of the genes significantly upregulated in breast cancer samples with *MYBL2* (B-Myb) amplification shows enrichment of cell cycle-related categories. Ten most significantly enriched Biological Process (BP) categories are shown. Genes significantly up-regulated in TCGA breast invasive carcinoma samples (107) with amplification of *MYBL2* gene (25% of total tumors) were downloaded from cBioportal.org (N=243), and filtered to remove genes located on 20q as possibly co-amplified with *MYBL2*. The remaining 171 genes were then analyzed using MSigDB gene ontology

annotation software to identify significantly enriched biological process categories (108, 109). **(C)** Same analysis as **18B** except with TCGA HGSOC samples (23). *MYBL2* gene was underwent gains or amplifications in 55% of all tumors. Of the initial data from cBioportal.org (N=1106), the remaining 916 genes (after correcting for potential q20 co-amplification) were then analyzed (108, 109).

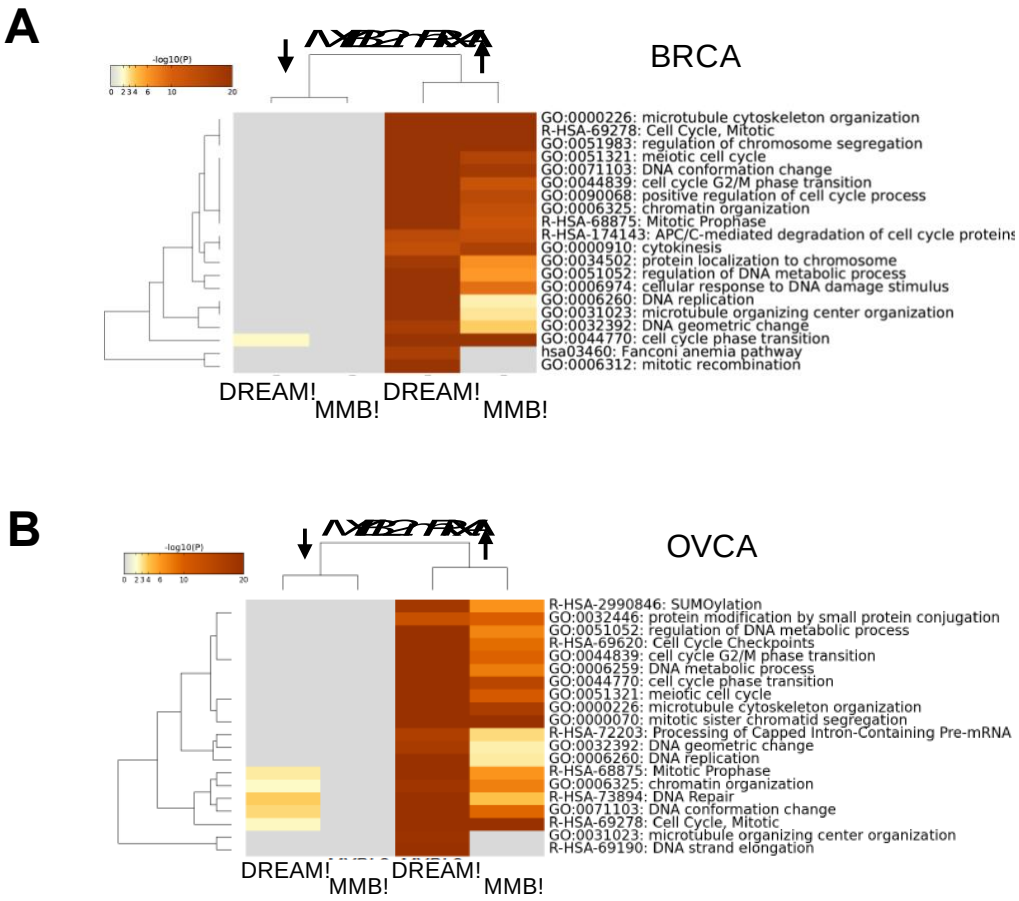


**Figure 19. Differential gene expression analysis in the presence of high or low B-Myb. (A, B)** Heatmaps of functional enrichment results of *MYBL2* up and downregulated gene sets overlapping DREAM or MMB target genes in breast **(A)** and ovarian **(B)** cancers. The gray, yellow and red gradient indicates non-significant, less significant and more significant enrichment of functional terms of the corresponding gene sets, respectively. In both cancers, DREAM target genes were significantly upregulated when *MYBL2* expression is high, are significantly enriched in cell cycle and DNA replication-related processes. Note that the MMB-target genes show less significant enrichment in those processes. The down-regulated DREAM- and MMB-target genes do not show significant functional enrichment.

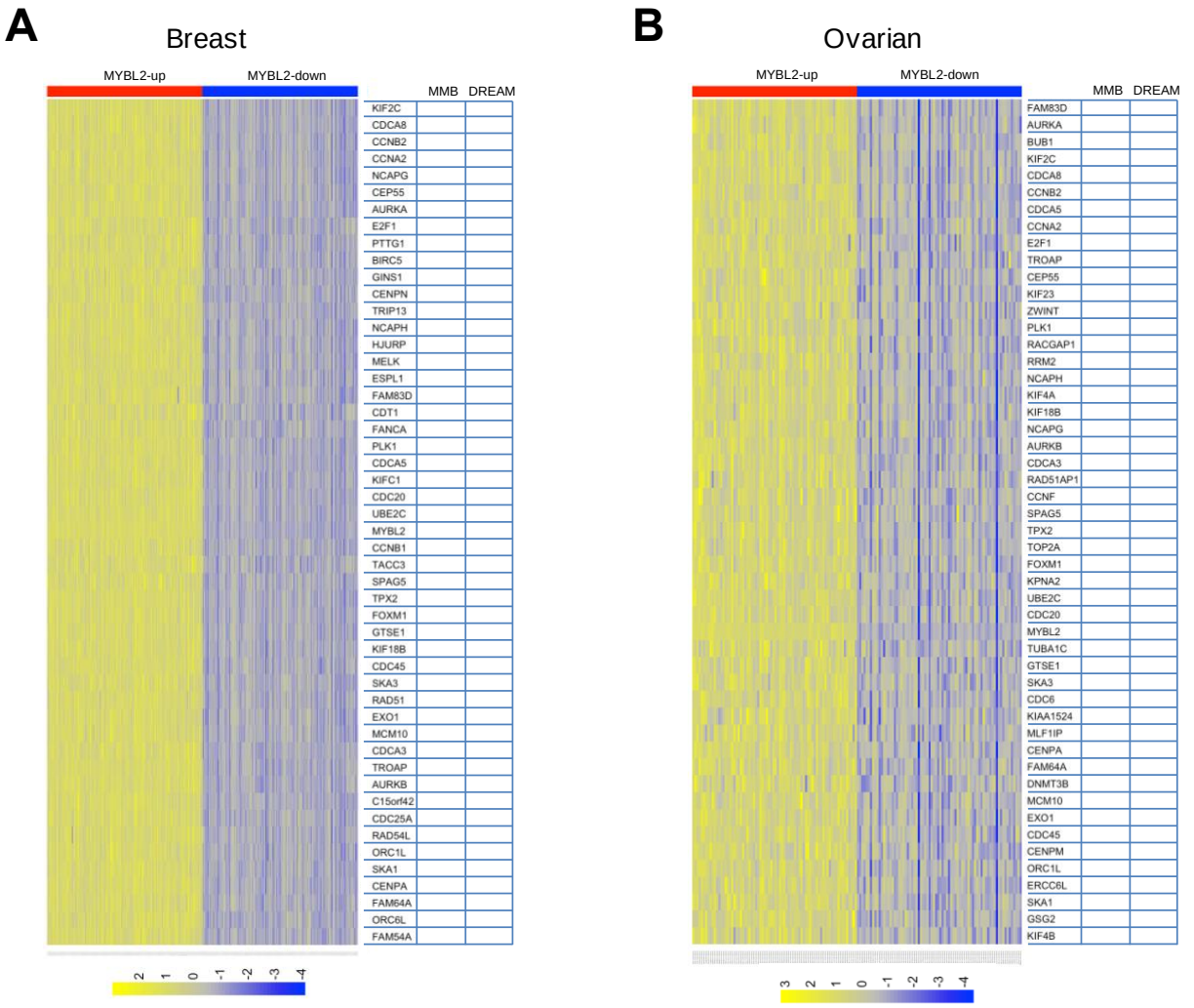


**Figure 20. DREAM and MMB targets are represented among the top 50 most differentially expressed genes in the presence of high or low B-Myb. (A, B)** DREAM and MMB target genes are significantly upregulated in breast and ovarian cancers with high B-Myb expression (Fisher's exact test p-values $1.2^{-102}$ and 0.0065, respectively). Top 50 up-regulated genes in TCGA gene expression dataset of breast and ovarian cancer tumors with high expression of B-Myb are shown ($\chi^2$ with Yates correction $p<0.001$). Genes were annotated as DREAM or MMB targets using http://www.targetgenereg.org (43).

## Characterization of HGSOC clinical specimens

We have shown that high B-Myb expression disrupts DREAM formation in human cell lines, resulting in increased proliferation. Additionally, our analysis of TCGA data supported our cellular model and showed that *MYBL2* undergoes gene copy number gain

in the majority of HGSOC tumor samples. We next sought to validate these findings with clinical specimens and to investigate the role of DREAM- and MMB-regulated gene expression in HGSOC patient outcomes. To this end, we assessed *MYBL2* and DREAM target gene expression by RT-qPCR, relating them to each other as well as clinicopathologic measures.

**A**

| Variable | Category | Proportion | % |
|---|---|---|---|
| Age (years) | <65 | 39/52 | 75 |
| | ≥65 | 13/52 | 25 |
| Stage | 2 | 2/52 | 4 |
| | 3 | 41/52 | 79 |
| | 4 | 9/52 | 17 |
| Optimal Debulking | Yes | 22/45 | 49 |
| | No | 23/45 | 51 |
| Adjuvant Chemotherapy Regimen | None | 5/45 | 11 |
| | Carboplatin+taxane | 39/45 | 87 |
| | Single agent carboplatin | 1/45 | 2 |
| BRCA Status | No identified mutation | 9/12 | 75 |
| | BRCA1 mutation | 0/12 | 0 |
| | BRCA2 mutation | 1/12 | 8 |
| | Other pathogenic mutation | 2/12 | 17 |
| Recurrence | No | 7/34 | 21 |
| | Yes | 27/34 | 79 |
| Platinum Sensitivity | No (≤6 months between chemotherapy completion and recurrence) | 12 | 36 |
| | Yes (>6 months between chemotherapy completion and recurrence) | 21 | 64 |

**B**

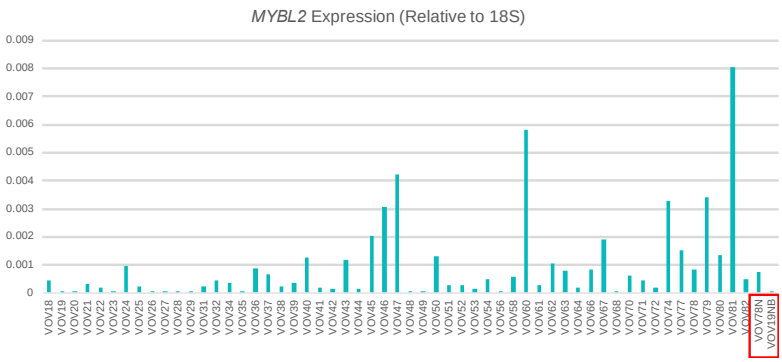


**Figure 21. Characterization of HGSOC tumor samples. (A)** Clinicopathologic characteristics of HGSOC lesions. **(B)** RT-qPCR gene expression analysis for *MYBL2*. Data are normalized to 18S ribosomal RNA as a housekeeping gene control. The red box outlines sections of normal-like tissue.

This retrospective investigation utilized tissue bank surgical pathology and cytology samples taken from 57 HGSOC lesions collected between November, 2000 and April, 2017. Only samples for which there were available matched clinical data were analyzed (N=52). Demographic information, follow-up, treatment, and outcomes data were obtained by chart review by an investigator blinded to the primary research question and laboratory findings (**Fig. 21A**). Samples from patients lost to clinical follow up were also excluded. Our HGSOC patient population, though relatively small, is clinically representative of the national population with stage of diagnosis (86% stages 3 and 4 versus 85% nationally) and percent recurrence (79% versus 80-85% nationally for stages

3 and 4) (23). Whereas 8% of our study population possessed *BRCA1/2* mutations, rates of approximately 13% have been reported in other studies (110). Finally, our population was, on average, slightly younger than the national average (58 years versus 63 nationally) (66). We also characterized the relative degree of *MYBL2* expression across our study population. TCGA analysis showed genetic alterations resulting in aberrantly high expression of *MYBL2* in approximately 55% of HGSOC cases. In our study population, 51% of samples had *MYBL2* expression levels greater than that of two adjacent normal-like tissue samples (**Fig. 21B**).

**Testing the B-Myb-mediated DREAM disruption model using gene expression analysis**

After assessing the representativeness of our study population, we proceeded to test our working model of DREAM disruption by high B-Myb level using RT-qPCR analysis of HGSOC lesions. We used expression levels of DREAM-and MMB-controlled genes as a functional readout for the status of these opposing transcriptional regulators. *MYBL2* and DREAM target gene expression were measured and correlated. Target genes of interest were selected based on criteria of high differential gene expression (**Fig. 20B**), established cell cycle role, and clinical interest (**Fig. 22A, B**). After selection, all primers for these genes were validated before proceeding with RT-qPCR. A panel of housekeeping control genes (18S, actin, GAPDH) were tested to determine which yields the most consistent results across tumor samples (111). This lead us to proceed with 18S ribosomal RNA as our housekeeping control. Additionally, since two independent sets of RNA were prepared per sample and multiple reactions were run for comparison, *MYBL2*

expression was used as an internal control. *MYBL2* expression was compared across batches of RNA to ensure consistent results across reactions (**Fig. 22C**).

Of the selected genes, *FOXM1* is of particular interest due to its reported robust upregulation and prognostic role in HGSOC (23, 112-114). RT-qPCR analysis of DREAM target genes (*AURKA*, *KIF23*, *CCNB2*, *LIN9, E2F1,* and *FOXM1*) revealed positive and significant correlations between *MYBL2* and all genes tested, with the exception of LIN9: *LIN9* ($\rho$=0.2599, p=0.0553), *AURKA* ($\rho$=0.4114, p<0.01), *KIF23* ($\rho$=0.4953, p<0.001), *CCNB2* ($\rho$=0.3278, p<0.05), *E2F1* ($\rho$=0.3926, p<0.01) and *FOXM1* ($\rho$=0.5033, p<0.001) (**Fig. 23**). Corresponding analyses of TCGA data produced similar results (**Fig. 24**). However, whereas *LIN9* and *MYBL2* expression were not correlative in our patient samples, *LIN9* did significantly correlate with *MYBL2* expression in the TCGA data. Additionally, all genes tested were upregulated in HGSOC TCGA data. Collectively, these data support our model, as evidenced by derepression of DREAM target genes and high expression of MMB target genes positively correlating with *MYBL2* expression. Our data corroborate previous TCGA analyses and suggest a possible *MYBL2* amplification gene

expression signature characterized by derepression of DREAM target promoters.

**A**

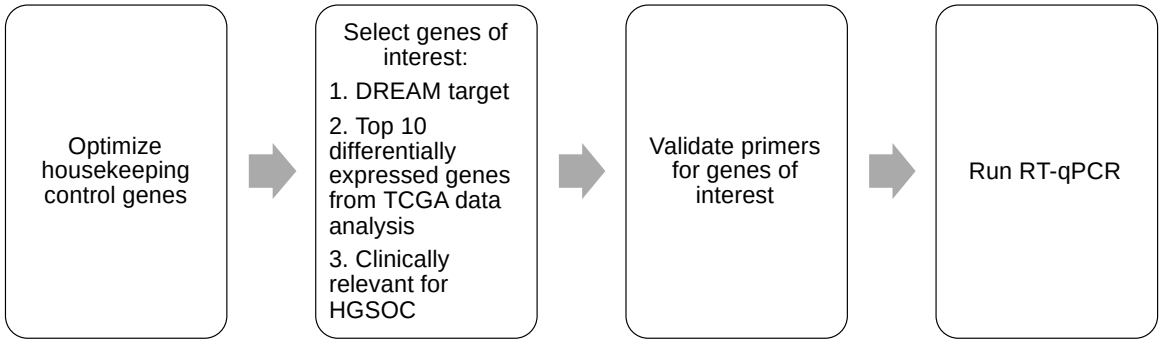


**B**

| Gene | Target | |
|---|---|---|
| | DREAM | MMB |
| *MYBL2* | √ | - |
| *AURKA* | √ | √ |
| *KIF23* | √ | √ |
| *CCNB2* | √ | √ |
| *LIN9* | √ | √ |
| *E2F1* | √ | - |
| *FOXM1* | √ | - |

**C**

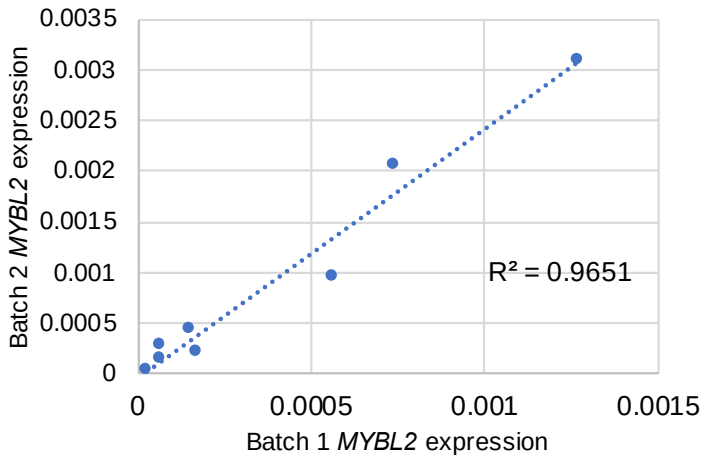


**Figure. 22 RT-qPCR methods for measuring DREAM status. (A)** Workflow for establishment of DREAM target gene RT-qPCR assay in HGSOC tumor samples. **(B)** Selected genes of interest and their corresponding transcriptional regulators. **(C)** Comparison in gene expression of *MYBL2* (relative to 18S) across two independent batches of eight RNA samples from the same tumors.

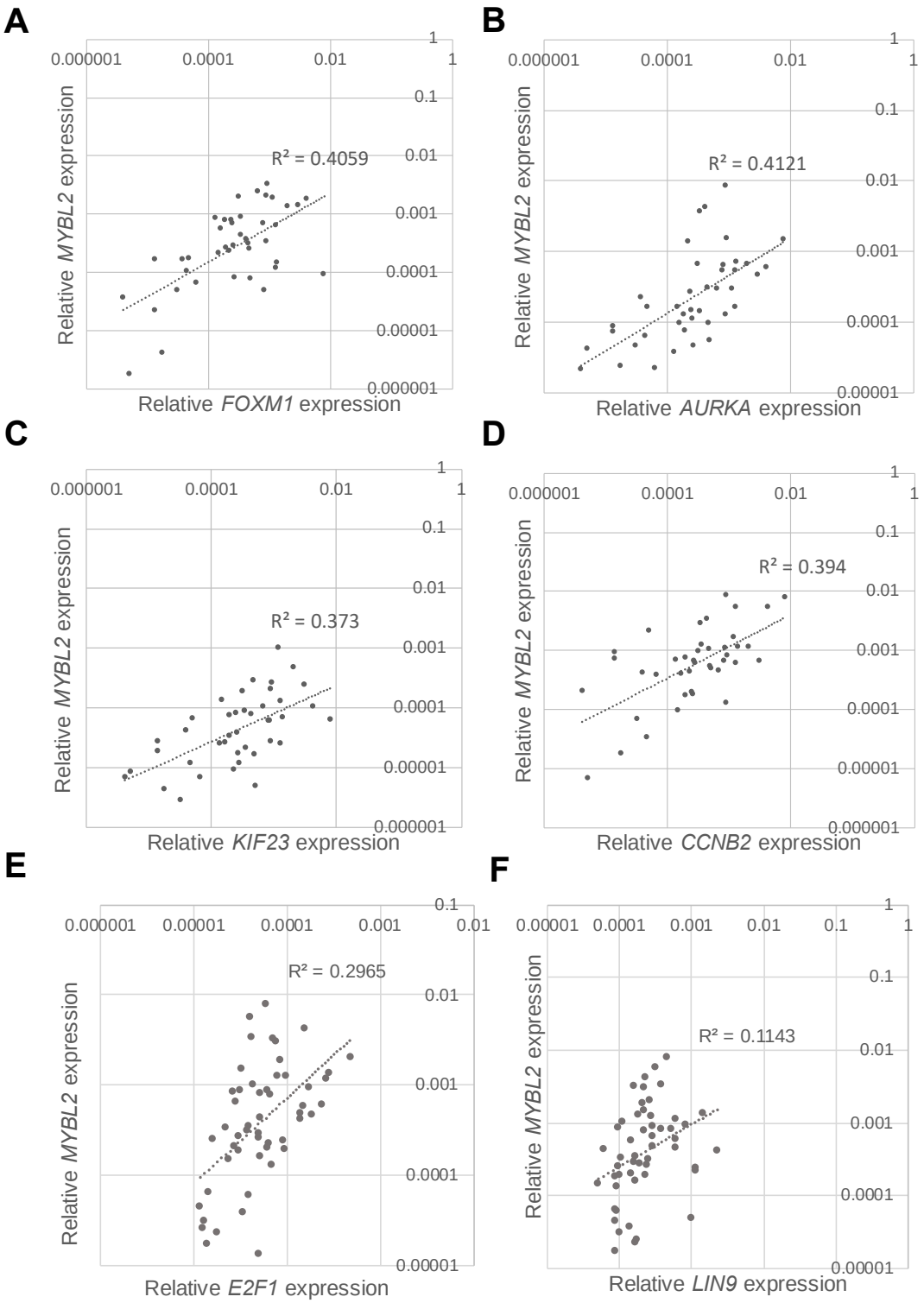


**Figure 23. *MYBL2* expression correlates with DREAM and MMB target gene expression. (A-F)** RT-qPCR analysis of human ovarian tumor surgical sections (N=54).

Expression of DREAM target genes is shown relative to that of *MYBL2*. Spearmann Rank Correlations were used for analysis.

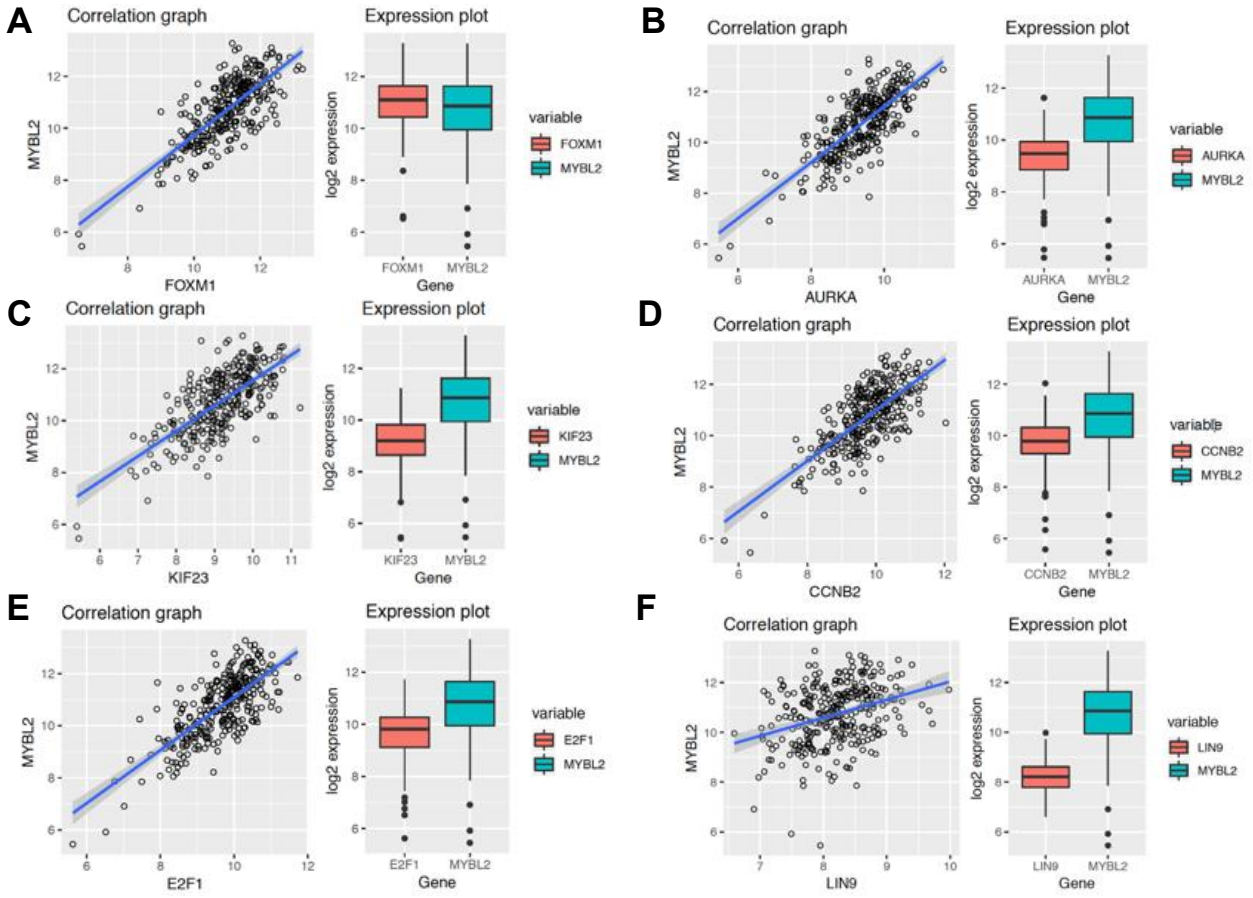


| Gene of interest v. *MYBL2* expression | Pearson correlation coefficient | p-value |
|---|---|---|
| ***FOXM1*** | 0.58464 | 2.5929E-58 |
| ***AURKA*** | 0.655 | 2.0862E-59 |
| ***KIF23*** | 0.541 | 9.193E-46 |
| ***CCNB2*** | 0.553 | 1.6334E-49 |
| ***E2F1*** | 0.571 | 4.0019E-53 |
| ***LIN9*** | 0.263 | 2.8341E-09 |

**Figure 24. *MYBL2* expression correlates with DREAM and MMB target gene expression in the TCGA data set. (A-F)** HGSOC TCGA gene expression data relating *MYBL2* expression to DREAM target genes of interest. Table shows results of Pearson correlations analysis.

**Clinical correlation analysis in patients with HGSOC**

To assess the clinical relevance of our RT-qPCR data, we next determined the relationship between gene expression and clinical classifications in the TCGA data set. The Cancer Genome Atlas Research Network reported four transcriptional subtypes of ovarian cancer based on mRNA expression patterns: immunoreactive, differentiated, proliferative, and mesenchymal (23). Recent studies have assigned histological classifications to these transcriptional profiles and are characterizing them clinically (115). We therefore began by evaluating the expression of our genes of interest across the four subtypes.

Intriguingly, all genes (with the exception of *AURKA*) were highly expressed in the proliferative subtype and more significantly expressed as compared with the mesenchymal subtype (**Fig. 25**). Though the Cancer Genome Atlas Research Network reported no significant differences in survival between the various subtypes, more studies are emerging to suggest the subtypes are prognostic indicators (23, 115). In a study of 312 HGSOC cases, OS was reportedly worst in the mesenchymal subtype (115). Another study found clinically significant benefits of PFS proliferative and mesenchymal subtypes in response to anti-VEGF therapy with bevacizumab, suggesting that these subtypes may also be utilized to guide personalized treatments (116). Therefore, we proceeded to evaluate the impact of our genes of interest on survival by ovarian cancer subtype.

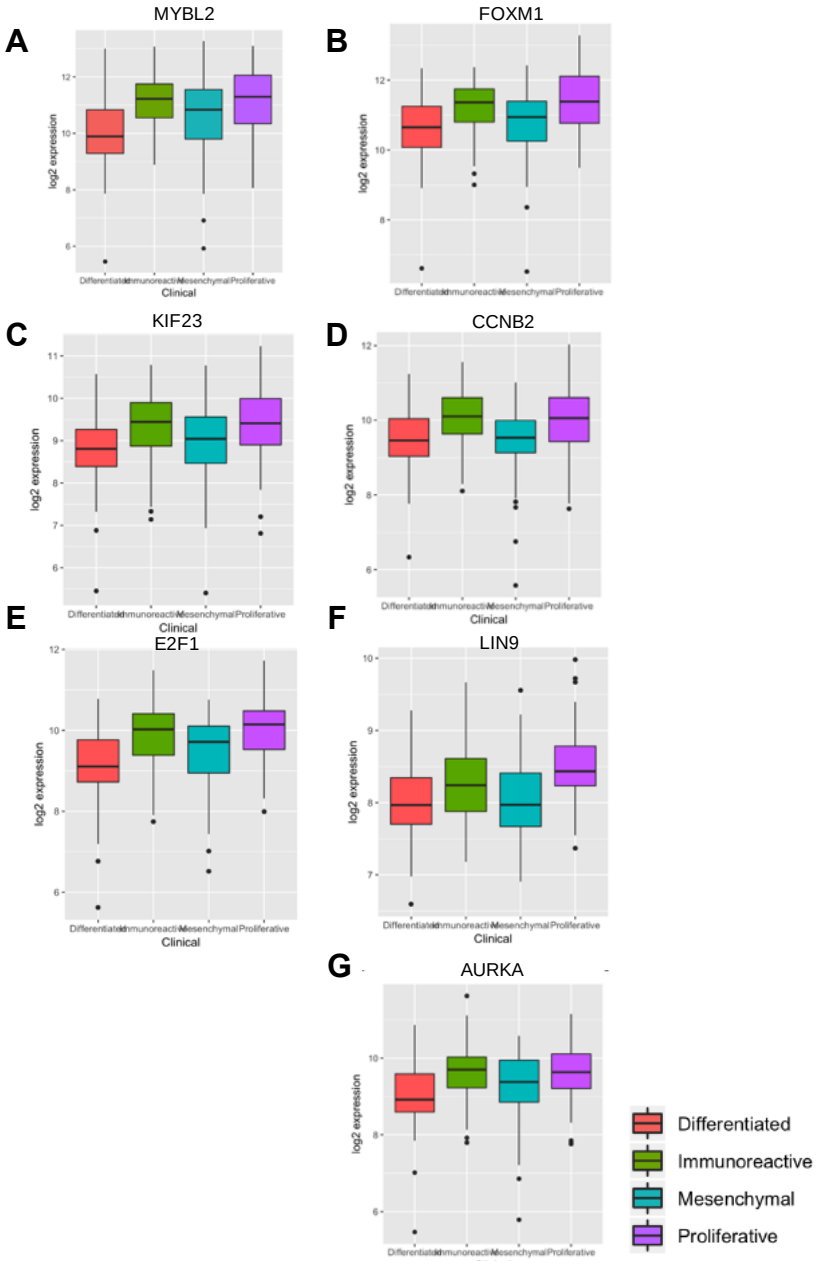


**Figure 25. Expression of genes of interest by transcriptional subtype. (A-G)** All genes of interest, aside from *AURKA*, are significantly highly expressed in the proliferative subtype as compared with the mesenchymal subtype of HGSOC (ANOVA with Tukey-HSD post-test, $p<0.01$).

Using Kaplan-Meier survival analysis and log rank tests, we found that high expression of *FOXM1* was associated with significantly decreased overall survival in the proliferative subtype (**Fig. 26A**) and the ovarian cancer data set collectively (HR 1.44;

95% CI, 1.04–1.99; p=0.027). This is in line with previous reports (23, 112, 114). High *MYBL2* expression was associated with decreased survival in the proliferative subtype as well, though not reaching significance (**Fig. 26B**). Like *FOXM1*, *MYBL2* expression was also indicative of a poor prognosis in the collective ovarian cancer data set, as shown previously in **Fig. 17B**. High *CCNB2* and low *LIN9* expression also significantly correlated with worse OS in ovarian cancer (HR 1.45; 95% CI, 1.05–2.01, p=0.023 and HR 0.7; 95% CI, 0.52–0.95, p=0.0019, respectively), but did not achieve significance in any of the four subtypes. *KIF23* and *E2F1* had no significant impact on OS in HGSOC cancer overall or any of the subtypes.

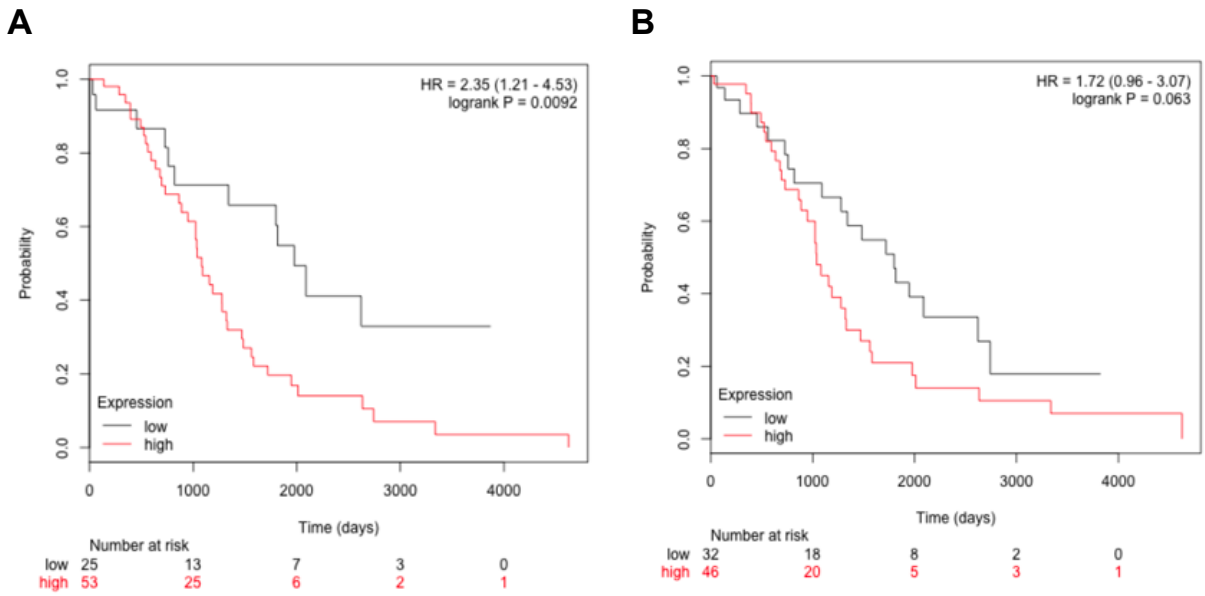


**Figure 26. Effect of *FOXM1* and *MYBL2* expression on survival in the proliferative subtype of HGSOC. (A, B)** High *FOXM1* (**26A**) or *MYBL2* (**26B**) expression significantly associates with decreased overall survival in HGSOC patients with the proliferative disease subtype. Data show Kaplan-Meier curves and Cox proportional hazard model.

Together, the data suggest that *MYBL2*, *FOXM1*, and *CCNB2* are indicative of a poor prognosis in ovarian cancer and may be especially relevant in the proliferative subtype of ovarian cancer.

Given our finding that many of the DREAM target genes are derepressed in the presence of high B-Myb and expression of these genes, in turn, is high in the proliferative subtype, we next explored the importance of B-Myb expression in the proliferative subtype. Using the TCGA HGSOC data set, we assessed the relationship between *MYBL2* expression and expression of the proliferative subtype markers, *MCM2* and *PCNA*. The correlations were positive and significant in both cases, suggesting that high B-Myb expression may be a contributor to the proliferative phenotype (**Fig. 27**). Additionally, both *PCNA* and *MCM2* are DREAM target genes. Overall, these results imply a mechanism by which high B-Myb expression drives DREAM disruption and, ultimately, cellular proliferation in this subtype of HGSOC.

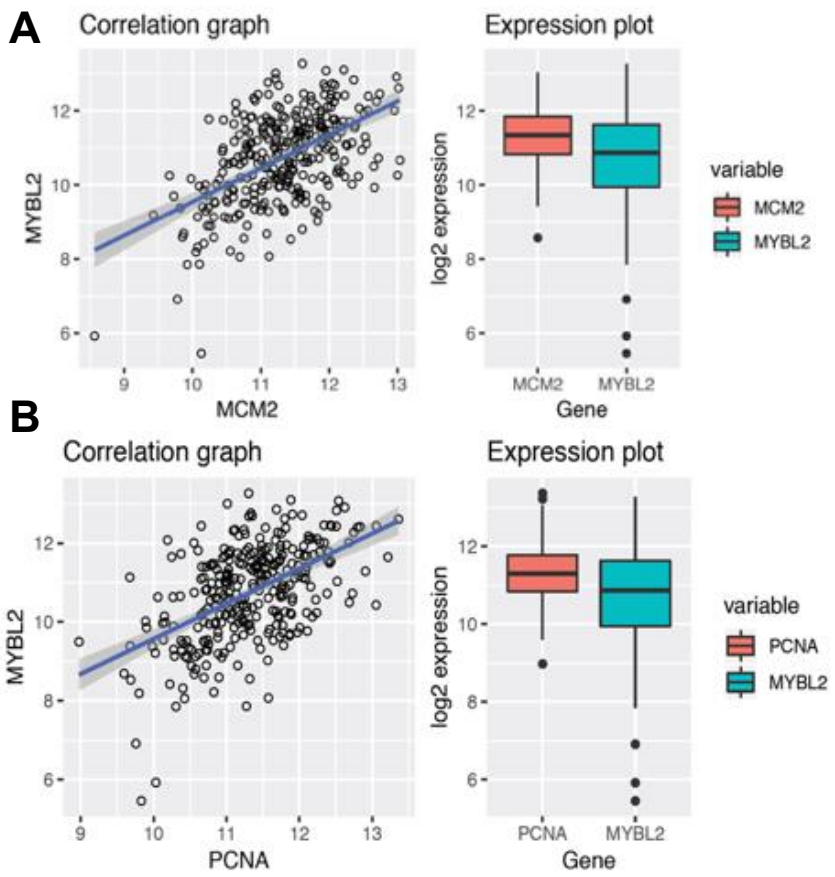


**Figure 27. *MYBL2* expression correlates with *MCM2* and *PCNA* expression in HGSOC proliferative subtype TCGA data.** (**A, B**) mRNA expression of HGSOC proliferative subtype markers significantly correlate with that of *MYBL2*. Pearson correlation analysis yielded ρ= 0.31356, p= 1.1902e-23 and ρ= 0.30555, p= 1.4144e-22 for *MCM2* and *PCNA*, respectively.

## Discussion

We have shown that increased expression of selected cell cycle genes correlates to increased formation of MMB, and reduced DREAM assembly in HGSOC tissue. High expression of *MYBL2* is also associated with deregulated cell cycle gene expression programs in HGSOC, suggesting that it may play an important role in the pathogenesis and clinical outcomes of patients. Larger scale studies would clarify the clinical prognostic value of the DREAM- and MMB-regulated gene expression. Additionally, it would be valuable to compare gene expression between HGSOC tumors and healthy control

fallopian tube cells. This would aid in better defining the “cutoff” point for “high” gene expression (111).

We found that *MYBL2*, *CCNB2*, *FOXM1, LIN9*, *KIF23,* and *E2F1* are all upregulated in the proliferative subtype (**Fig. 25**). The proliferative subtype is genetically defined by high expression of proliferation markers, *MCM2* and *PCNA* (23). Interestingly, both of these markers are DREAM target genes and significantly correlate with *MYBL2* expression (43). Their high expression, and co-expression with other DREAM targets (*MYBL2*, *CCNB2*, and *FOXM1*), is consistent with a phenotype of DREAM disruption. Additionally, another DREAM target, $p15^{PAF}$ (KIAA0101), was shown to be highly expressed in several cancers and a is possible contributor to a poor prognosis (117). This PCNA (proliferating cell nuclear antigen)-associated factor competes with p21-PCNA binding. PCNA is an important for successful DNA replication and repair. p21 functions to inhibit cell proliferation by binding to PCNA and disrupting replication machinery. Since $p15^{PAF}$ competes with p21 for PCNA binding, high $p15^{PAF}$ expression in cancer could be advantageous for tumor cell proliferation. However, co-transfection of $p15^{PAF}$ and p21 in Saos-2 and 293 cells did not significantly impact p21-mediated cell cycle arrest (117). On the contrary, knockdown of $p15^{PAF}$ in HeLa cells inhibited cell cycle progression and loss of Rb/E2F control lead to increased $p15^{PAF}$ expression, which contributed to S-phase progression (118).

Therefore, $p15^{PAF}$ could play a role in promoting cell cycle progression by its role in p21 inhibition. Additionally, one study recently identified $p15^{PAF}$ as a transcriptional target for FoxM1 in HGSOC (114). However, the specific regulation of $p15^{PAF}$ remains unclear, as it is not annotated as a FoxM1-MuvB target in another database (43).

Together, these points propose that the proliferative subtype might be the subtype with the most prominent DREAM disruption and, in turn, several mechanisms for perpetuating cellular proliferation (**Fig. 28**). It would be clinically valuable to further describe treatment responses in this subtype, especially since the DREAM complex has been implicated in recurrence (69).

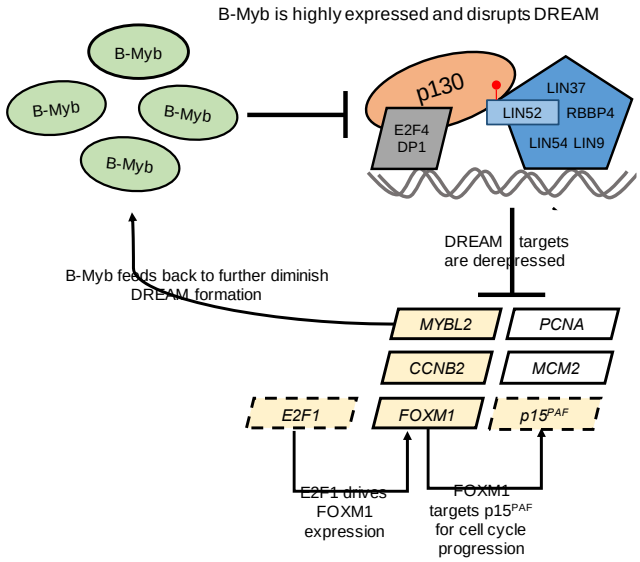


**Figure 28. Possible positive feedback loops driven by DREAM disruption in the proliferative subtype of HGSOC.** High B-Myb expression disrupts DREAM complex assembly which leads to increased expression of proliferative subtype markers, *PCNA* and *MCM2* (purple parallelograms). *MYBL2* expression is also increased, creating a positive feedback loop for further DREAM disruption. *E2F1*, another DREAM target, also contributes to *FOXM1* expression. High *FOXM1* expression may, in turn, increase $p15^{PAF}$ expression to alleviate inhibition of PCNA by p21.

Our findings overall suggest potential therapeutic angles for restoring cell cycle control in HGSOC. Though DREAM is implicated in harboring disease recurrence (69), inhibition of B-Myb and, in turn, restoration of DREAM assembly may be an appropriate tactic for the proliferative subtype of HGSOC as well as in cases of *FOXM1* (12% of cases) or *MYBL2* (55% of cases) genetic amplification (112). DREAM formation may curb the pathogenic mechanisms exacted by FoxM1, which is overexpressed in 84% of

HGSOC cases and was shown to be activated by E2F1 (23, 112). This strategy might have secondary effects of repressing DNA damage repair genes, sensitizing cells to PARP inhibitors, (119) and enhancing responses to paclitaxel and cisplatinum in platinum-resistant disease (120). DREAM repression of E2F1 might also reign in FoxM1 (112). Altogether, we propose a mechanism by which high *MYBL2* expression leads to DREAM disruption and worse outcomes of HGSOC patients. Targeting and inhibiting B-Myb may be a viable treatment option for certain patients.

# Chapter 4: Perspectives and future directions

## MuvB regulation

One remaining question from our work is the significance of alterations in LIN52 stability. We now understand that the half-life of LIN52 is much shorter than its MuvB counterparts, LIN9 and LIN37, and its phosphorylation at S28 influences its stability. It follows then that LIN52 perhaps plays an important role in stabilizing MuvB as a whole and, perhaps, p130 binding salvages MuvB from degradation. However, it is puzzling to rationalize that the same phosphorylation event that is essential for DREAM assembly also leads to decreased stability of a protein essential for DREAM formation. Our findings are also confounded by the fact that inhibition of S28 phosphorylation (whether by DYRK1A knock-down or S28A mutation) not only stabilizes LIN52, but also disrupts DREAM. It would be interesting to measure LIN52 stability in the presence of DREAM disruption by other means, such as with viral oncoproteins, to distinguish between the effects of phosphorylation and DREAM inhibition on LIN52 levels.

We have shown that B-Myb must contact the MuvB core in order to disrupt DREAM and it must be expressed at high levels to disrupt DREAM assembly. However, we did not explore the importance of B-Myb activity on DREAM formation. It would be interesting to determine the effect of C-terminal truncated of B-Myb on DREAM formation. The negative regulatory domain of this protein is deleted; therefore, B-Myb transcriptional activity is functionally amplified, but not at the genetic or protein levels. Perhaps it would have implications for HGSOC as well (121).

## Strategic modulation of cell cycle gene expression in high grade serous ovarian carcinoma

To place our studies into the context of the current clinical state of HGSOC treatment, we review the progress made toward new HGSOC therapies and propose novel mechanisms for taking advantage of the cancer cellular response to chemotherapy for maximal treatment benefit. Since chemotherapy induces gene expression changes and causes molecular derangement over time, we focus our discussion on cell cycle and DNA damage response gene transcriptional regulators: DREAM (DP, RB, E2F1, and MuvB), MMB (B-Myb-MuvB), and FOXM1-MuvB (122).

## Cell cycle regulation by MuvB-containing complexes

In healthy cells, the cell cycle is a well-coordinated sequential set of signaling events that involves two waves of gene expression: “early genes” in G1/S phases and “late genes” in G2/M (2). The DREAM complex is responsible for global repression of both early and late cell cycle genes in quiescence (G0/G1). It is formed when CDK4/6 activity is low and DYRK1A kinase phosphorylates LIN52 protein. This phosphorylation event brings together the binding of RB-like protein, p130, to a 5-protein complex, MuvB (containing LIN52, LIN9, LIN37, LIN54, and RBBP4) (13). Upon cell cycle re-entry, DREAM dissociates in a cyclin D-CDK4/6-dependent manner (90). MuvB then binds to B-Myb in the S phase to initiate the expression of late cell cycle genes. Maximal late cell cycle gene expression occurs when B-Myb recruits FoxM1 to MuvB (forming FoxM1-MuvB complex) in the G2/M phases (20). Therefore, by forming three distinct transcriptional regulatory protein complexes, MuvB ensures proper expression of cell cycle genes throughout all phases of the cycle (123).

Interestingly, several components of these regulatory complexes have been associated with HGSOC disease processes. DREAM has been implicated in HGSOC spheroid formation and treatment resistance in human cancer cells derived from ascitic fluid (69). B-Myb, member of the MMB complex, is often genetically amplified in HGSOC and was recently shown to disrupt DREAM complex assembly (124). Several studies have investigated the role of FoxM1 in HGSOC, especially since it was identified as the driver of the most commonly active HGSOC signaling pathway in analysis of The Cancer Genome Atlas (23). All of these complexes share the MuvB subunit in common. Additionally, they are all connected through their regulation of each other, either by controlling gene expression of complex components, or by influencing cell cycle-dependent processes. Therefore, understanding how MuvB-containing complexes are involved in response to chemotherapy could provide new avenues for treatment in HGSOC (**Fig. 29**).

| | | |
|---|---|---|
| **DREAM complex** | • Represses expression of early and late cell cycle genes<br>• Formed in G0/G1 and at the G1 DNA damage checkpoint (through the p53-p21-CHR pathway) (57)<br>• Associated with spheroid formation, dormancy, and drug resistance (69) | |
| **DNA damage** | • Homologous repair (HR) is an efficient process of DNA repair that, when performed successfully, contributes to cell survival.<br>• HR can only occur in G2/M phases after DNA is replicated.<br>• Error-prone non-homologous end joining (NHEJ) is a mechanism of DNA repair utilized in cell cycle phases in which DNA is not yet replicated.<br>• HR-deficient HGSOC are associated with treatment sensitivity (especially to poly ADP-ribose polymerase, PARP, inhibitors) and better clinical outcomes because the inability to use HR leads to replication stress and cell death.<br>• HR deficiency commonly occurs in the form of *BRCA*1/2 gene mutation or decreased expression. Resistance can occur through reversion mutations that restore functional BRCA1/2 proteins.<br>• HGSOC is p53 deficient meaning that these cells are reliant on the G2/M checkpoint in response to DNA damage.<br>• DREAM regulates expression of several genes in the DNA damage repair pathway. | |
| **MMB complex** | • Formed in the S phase for recruitment FoxM1 to MuvB and activation of late cell cycle genes<br>• Associated with proliferation and mitotic progression<br>• Formed by B-Myb binding to MuvB: B-Myb is highly expressed in HGSOC and associated with a poor prognosis (23)<br>• B-Myb expression is required for recovery from the G2/M DNA damage checkpoint (48). | |
| **Therapeutic goals** | **Concept** | **Therapeutic window** |
| | • Push cells into a state of replicative stress/mitotic crisis by damaging DNA and preventing its repair, leading to cell death<br>• Permanently halt cell cycle progression, leading to senescence | • HGSOC is often HR deficient whereas non-cancer cells are not.<br>• Cancer cell proliferation is greater than normal cell proliferation.<br>• Examples of cancer cell characteristics that open therapeutic windows: *BRCA1/2* mutantations, DREAM deficiency (DYRK1A loss, B-Myb amplification) |

**Figure 29. DREAM and MMB complex involvement in HGSOC treatment response**. Modulation of DREAM and MMB formation could alter cell cycle-dependent expression of DNA damage response gene programs as well as cell cycle progression overall. Pharmacologic control of DREAM or MMB could be potentially harnessed for treating HGSOC.

**DNA damage and repair**

Most chemotherapeutic agents used for treating HGSOC work by inducing DNA damage. Since HGSOC cells are often more proliferative than normal cells and exhibit defects in DNA repair pathways (such as *BRCA1/2* mutations), chemotherapy preferentially impacts the cancer cells over normal cells. Over time, the damage will accumulate to eventually result in cell death (23). Chemotherapeutic induction of DNA double strand breaks (DSBs) induces G1 cellular arrest through the ATM-CHK2 pathway involving p53. CHK2 inhibits cell division cycle 25 (CDC25A) phosphatase that alleviates the inhibitory phosphorylation of cyclin A-CDK2 and cyclin E-CDK2 complexes, blocking progression into the S phase (125). The ATR-CHK1 pathway is responsible for S and G2 arrest. ATR phosphorylates and activates CHK1 which goes on to activate Wee1 and inhibit CDC25A/C phosphatases. This overall leads to inhibited cell cycle progression through inactivation of cyclin dependent kinases, allowing time for proper DNA repair (126, 127). Importantly, the BRCA proteins (1 and 2), downstream mediators of these pathways, are essential for the process of homologous repair, and are often non-functional in HGSOC patients (23). This opens up another therapeutic window by using treatments that force cells into the error-prone non-homologous end joining (NHEJ) repair pathway leading to further DNA damage and cell death. Additionally, the DREAM complex is known to repress several genes encoding the DNA damage response and repair proteins: *CHK1*, *CHK2*, *BRCA1*, *BRCA2*, *RAD51*, *WEE1*, and *CDC25A/C* (43). The DREAM complex also assembles in a p53-p21-depdendent manner for repression of late cell cycle genes, halting progression through mitosis (57). Therefore, the status of

DREAM complex assembly could be significant in determining cancer cell response to chemotherapy.

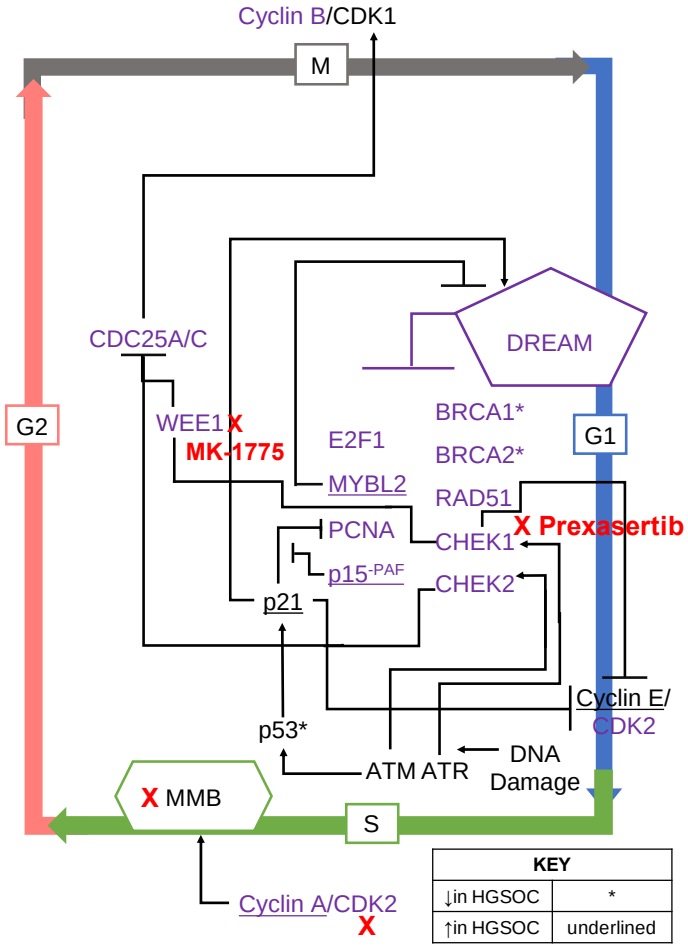


**Figure 30. Checkpoint and MMB inhibitors in HGSOC treatment.** Prexasertib is an ATP-competitive small molecule inhibitor of CHK1 and CHK2, blocking the G2 checkpoint and preventing cell cycle arrest in response to DNA damage. MK-1775 is a Wee1 small-molecule inhibitor that targets the CHK1-mediated pathway. Checkpoint inhibition might be more effective in cells with high cyclin E expression, driven by genetic amplification or DREAM disruption. Both checkpoint inhibitors are in clinical trials (phases II and I, respectively). B-Myb inhibition could compromise recovery from the G2 checkpoint and expression of late cell cycle genes, especially in patients harboring *MYBL2* amplification.

**Checkpoint inhibitors**

Since HGSOC is p53 null, G1 checkpoint regulation is lost, making the S and G2 checkpoints critical for preventing DNA damage-associated cell death. The synthetic

lethality associated with TP53 inactivation and checkpoint inhibition is well described (127). Inactivating the ATR–Chk1–Wee1 pathway is therefore a possible mechanism to by-pass the DNA-damage–induced G2 checkpoint arrest and lead to mitotic catastrophe and cell death (127). Two such clinical drugs include prexasertib and MK-1775. Prexasertib (LY2606368) is an ATP-competitive small-molecule inhibitor of Chk1 and Chk2 (128, 129). A phase II study of 28 patients found that prexasertib was clinically active in HGSOC patients with wild-type *BRCA1/2*. Of the 19 patients with platinum-refractory disease, 11 (58%) derived a clinical benefit from prexasertib treatment (129). MK-1775 is a Wee1 small-molecule inhibitor in phase I clinical studies. By abolishing the G2/M checkpoint, Wee1 inhibition enables cells to inappropriately enter mitosis, acquire further damage culminating in cell death. In a trial of 25 patients, two harboring *BRCA1/2* mutations (one with head and neck cancer and one with ovarian cancer) had partial responses to treatment with MK-1775 (125).

The positive outcomes of these early phase trials are reinforced mechanistically. Independent of treatment duration, p53-null cells arrest in G2, but ultimately adapt for mitotic progression. However, they fail to complete cytokinesis, become multinucleated, and undergo apoptosis. On the other hand, wild-type p53 cells reversibly arrest and repair the damage. This poses a good therapeutic window between HGSOC cells and normal cells. It also means that the p53 mutant status of HGSOC can be leveraged for treatment-induced cell death while minimizing the likelihood of toxicity (130).

Another point of consideration is cyclin E1 status. *CCNE1*, a DREAM target gene, is genetically amplified in approximately 20% of HGSOC cases and is associated with chemotherapy resistance and homologous recombination proficiency (127, 131).

However, cyclin E1 activates CDK2 and high expression of *CCNE1* leads to DNA damage, replication stress, and perhaps increased sensitivity to Chk1 (inhibits CDK2 to halt origins of replication) inhibition (127). Amplification of cyclin E could therefore make HGSOC tumors more susceptible for cell cycle checkpoint inhibition (131). In line with this rationale, of those with tumors over-expressing *CCNE1*, two thirds experienced benefits from prexasertib treatment (129).

**MMB inhibitors**

Recovery of p53 wild-type cells from reversible G1 or G2 cell cycle arrest involves p53-independent (Chk1 pathway) and dependent pathways as well as downregulation of DREAM cell cycle homology region (CHR)-containing targets, *CDC5C* and *CCNB1*. This argues that DREAM is involved in the DNA damage recovery process in some cancers through the p53-p21-CHR pathway. DREAM involvement is further supported by evidence of cells lacking p53 failing to downregulate target genes required for progression into mitosis. In p53 mutant cells, p130 does not replace B-Myb binding to MuvB. This leads to paradoxically increased G2/M gene expression following DNA damage. In p53 null cells, G2/M genes were more highly expressed compared with cells harboring wild-type p53. Interestingly, expression of PCNA, an “early” DREAM target gene, did not differ between p53 wild-type and mutant cells in response to DNA damage (48). Another “early” DREAM target gene dihydrofolate reductase (DHFR), expressed in G1/S, was also not strongly correlated with B-Myb expression or p53 status (48). These findings raise the question as to whether or not DREAM is still being assembled through a p53-p21-CHR-independent mechanism in response to DNA damage (57). Evidence also suggests DREAM formation is a part of G2/M arrest in response to DNA damage by mechanisms

independent of p53. A DNA sequencing study of 20 HGSOC cases (p53 deficient) analyzed before and after neoadjuvant chemotherapy revealed 86 genes that had significant changes in expression after treatment. These 86 genes represented signaling pathways involved in cell cycle regulation and DNA damage. Notably, expression of *E2F1*, *BRCA2*, *CCNB1*, and *CHEK1*—all of which are DREAM targets and most lacking a CHR element—was decreased by up to almost 5-fold after chemotherapy treatment and were among the top 10 most differentially expressed genes between pre- and post-treatment samples (122). On the contrary, another study of p53 null cells showed that cyclin B1, CDC2, and B-Myb might accumulate to a point of promoting cell cycle progression and eventual collapse in cytokinesis (48, 130). Given that these genes are early cell cycle genes that lack CHR elements, the mechanism whereby DREAM may influence them during DNA damage is unknown (43).

It is proposed that p53 null cells are dependent on B-Myb for G2 checkpoint escape and subsequent survival of DNA damage. Depletion of LIN9 or B-Myb, significantly reduced G2/M gene expression by doxorubicin in HCT116 p53 null cells, suggesting that the MMB complex formation is required for maximal expression of late cell cycle genes. Whereas no p53 wild-type cells entered mitosis after doxorubicin treatment, a fraction of HCT116 p53 null cells entered mitosis 48 and 72 hours after DNA damage. B-Myb or LIN9 depleted p53 deficient cells failed to enter mitosis, arguing that MMB complex formation may be necessary for cell cycle re-entry (132). Reduced B-Myb activity is also associated with chromosomal instability (133). Therefore, by blocking G2 checkpoint recovery, therapeutic B-Myb inhibitors may be clinically relevant in the context of p53 deficient cancers (48).

Recent studies have solved the partial crystal structure of B-Myb-MuvB binding, laying the foundation for development of small molecule inhibitors (96). Interestingly, whereas both DREAM and MMB require LIN52 for their assembly, p130 and B-Myb bind different regions of this protein (**Fig. 31**) (16, 134). This differential binding allows for the development of inhibitors specific for MMB assembly, leaving DREAM formation unaffected.

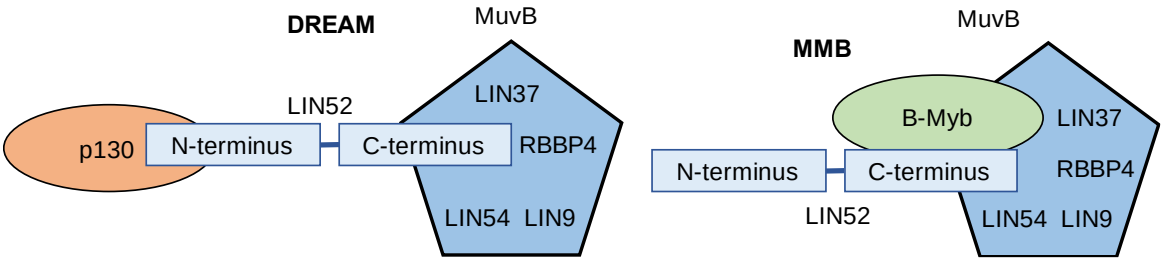


**Figure 31. p130 and B-Myb bind to different regions on LIN52.** Whereas p130 contacts the N-terminus of LIN52 for DREAM assembly, the C-terminus of LIN52 is required for MMB formation. This differential binding between DREAM and MMB formation allows for specificity of inhibitors for disrupting MMB.

Another potential target for B-Myb inactivation is by inhibiting cyclin A/CDK2, activator of B-Myb (6). It was recently shown that high B-Myb expression can lead to DREAM complex disruption (124). Since *MYBL2* is a DREAM target gene, this means that release from DREAM-mediated arrest is necessary for cell cycle re-entry and recovery from DNA damage (2). This also means that B-Myb-mediated DREAM disruption could potentiate a positive feedback loop: more B-Myb expression leads to further compromised DREAM assembly and de-repression of late cell cycle genes for checkpoint recovery and DNA damage repair (**Fig. 30**). Therefore, the approximately 55% of HGSOC cancers with 20q13 amplification or high B-Myb expression could be especially susceptible to MMB inhibition. Collectively, the reliance of HGSOC tumors on the G2 checkpoint, and B-Myb expression for checkpoint recovery, could make

checkpoint and MMB complex inhibitors viable therapeutic targets, especially in patients with high B-Myb expression.

**Homologous recombination repair**

TCGA analysis shows that 50% of HGSOC cases are deficient in homologous recombination (23). Patients harboring germline *BRCA1/2* mutations exhibit better responses to chemotherapy and, in turn, more favorable clinical outcomes (135). The specific mechanism for a more favorable prognosis is not known, though it is thought to be a product of more robust responses to platinum-based chemotherapy. The cell death associated with the use of poly ADP-ribose polymerase (PARP) inhibitors in BRCA-deficient cells is a form of 'synthetic lethality:' cells with intact HR repair will use PARP to restore single-stranded DNA breaks; whereas, in HR defective cells, PARP inhibition prevents DNA repair, resulting in double strand breaks, irreparable damage, and death (136). Specifically, since PARP is primarily involved in base excision repair, its inhibition is associated with the formation of single-strand breaks, stalled replication forks, and progression into major DSBs. In HR deficient cells, DNA can only be repaired through the error-prone non-homologous end joining (NHEJ) pathway (137). Upregulation of NHEJ ultimately leads to catastrophic damage and cell death and it is thought that downregulation of NHEJ might be a means by which tumors become resistant to PARP inhibition (138).

A recent study assessed the importance of *BRCA1/2* expression on ovarian cancer outcomes. Utilizing 12 non-neoplastic fallopian tubes as controls and 201 epithelial ovarian cancer lesions, this study related *BRCA1/2* expression to clinical characteristics. Ovarian cancers exhibited significantly higher expression (1.6- and 5-fold) of *BRCA1* and

*2*, respectively, as compared with normal fallopian tubes. Surprisingly, there were no correlations between *BRCA1/2* mutation status and any of the clinicopathologic characteristics studied. There was also no significant impact of promoter methylation status on patient outcomes. However, low *BRCA1* and *BRCA2* expression was associated with better overall survival (OS) only in HGSOC samples with wild-type *BRCA1*. Platinum sensitive disease was also characterized by lower *BRCA1/2* expression among *BRCA1* wild-type cases as compared with platinum refractory disease (135). Similarly, previous reports used siRNA knockdown of *BRCA1* in ovarian cancer cell lines to show that responsiveness to platinum agents was increased whereas efficacy of anti-microtubule therapies, such as taxanes, was abrogated. This same study found similar results in patients with low levels of *BRCA1* mRNA (139). Overall, *BRCA1/2* expression may be a predictive biomarker to gauge the sensitivity of cancers to platinum therapy and PARP inhibitors (135).

Indeed, response to platinum therapy has served as a surrogate predictor of HR status and maintenance therapy with PARP inhibition (136). However, there is currently no validated functional biomarker for the status of HR. Assays for HR deficiency are limited by their inability to differentiate tumors that are actively HR deficient from those with previously-acquired damage that have reverted back to being HR proficient (127). This is a common problem because one of the main mechanisms for HGSOC treatment resistance is restoration of BRCA1/2 activity. *BRCA1/2* can undergo revertant mutations and loss of methylation to re-express functional protein and, in turn, confer resistance to therapy (136). Increased activity of another DREAM target, RAD51, may also result in PARP inhibitor resistance, as it is an essential part of the HR repair mechanism (138).

There is also always the possibility that tumors might be sensitive to PARP inhibition despite platinum resistance (127). For example, whereas PARP inhibitors were initially indicated in cases of *BRCA*1/2 germline mutation, demonstrated clinical benefits lead the FDA to approve the use of niraparib as maintenance therapy for recurrent platinum sensitive ovarian cancer regardless of the BRCA1/2 status and olaparib use was also expanded for this indication (137, 140). Therefore, BRCA1/2 status alone cannot be a definitive predictive marker of treatment response and additional markers needed.

Combining platinum therapy or PARP inhibition with an HR inhibitor might sensitize cells to DNA damaging treatments. However, this combination my pose the risk of a low therapeutic window and the risk of enhanced toxicity (127, 137). Timing of combination therapy is also an important consideration. It is known that platinum therapy induces G1 arrest 24 hours after treatment whereas G2/M arrest occurs at 72 hours after treatment onset. Therefore, platinum therapy could potentially antagonize the effect of PARP inhibition by stalling the cells in G1. Arrest in G2/M also promotes resistance to PARP inhibition by preventing replication stress (137). Consecutive administration of the two drugs may produce different outcomes than concurrent administration. In support of this concept, a Phase I/Ib clinical trial showed that administration of carboplatin followed by combination therapy with olaparib had no effect on DNA adduct formation (141).

**LIN54-CHR inhibitors**

Given that DREAM regulates the expression of mediators of the DNA damage response pathways, and recent studies have shown the importance of their expression, DREAM formation may be an indicator of HR status and provide insights into treatment response. Whereas a large proportion of E2F motifs are found in early cell cycle genes,

CHR elements are required for the orderly progression of DREAM, MMB and FoxM1-MuvB complex binding to late cell cycle genes (21). Genes with CHR elements are annotated with processes related to mitosis, DNA metabolic process, response to DNA damage stimulus (21). They are present in 82% in the set of genes bound by DREAM, MMB, and FoxM1-MuvB. In contrast, E2F sites are enriched in DREAM-bound genes only (13). Cell cycle-dependent regulation of MuvB target genes was disrupted with CHR mutation (21). This could be a potential avenue for specifically targeting repression of early cell cycle genes, such as *BRCA1/2*, while preventing cell cycle arrest and, in turn, escape from DNA damaging drugs.

The mechanism of by which MuvB is targeted to CHR elements was revealed by the crystal structure of LIN54 bound to a CHR (38). This knowledge could be utilized for developing a LIN54-CHR inhibitor. By compromising MuvB contact with CHR elements, repression of late cell cycle genes would be alleviated while likely retaining repression of early cell cycle genes through contact with E2F sites. This means that a host of DNA repair genes (*BRCA1/2*, *RAD51*, *CHEK1/2*) would be repressed, likely rendering the cells HR deficient. This might be an especially good tactic for PARP-resistant cancers that are able to revert back to functional BRCA proteins. Similar to *BRCA* mutant tumors, repression of the HR pathway might also sensitize cells to PARP inhibitors. Therefore, LIN54-CHR inhibition might be an especially beneficial treatment option in patients with wild-type *BRCA*1/2. However, expression of late cycle genes could possibly promote inappropriate progression through mitosis in the face of unrepaired DNA damage, which could result in further accumulation of genomic alterations (**Fig. 32**). Alternatively, since *MYBL2* (an early cell cycle gene lacking a CHR element) would be repressed, the cells

may fail to recover from G2 arrest, similar to the effects of a MMB inhibitor. This could ultimately lead to clinical benefit of permanent arrest in senescence or cancer cell death.

| Early cell cycle (G1/S, no CHR) | | Late cell cycle (G2/M, contains CHR) | |
|---|---|---|---|
| **Gene↓** | **Potential consequence of LIN54-CHR inhibition** | **Gene↑** | **Potential consequence of LIN54-CHR inhibition** |
| ***MYBL2*** | • Lack of G2 DNA damage checkpoint recovery<br>• No recruitment of FoxM1 to MuvB<br>• Possibly delayed cell cycle progression and cell death | ***CDK2*** | • Progression into S phase<br>• Replication stress |
| ***BRCA1/2*** | • HR deficiency | ***CDC25A/C*** | • Aberrant cell cycle progression in the face of DNA damage |
| ***CHEK1/2*** | • Abolished DNA damage checkpoints | ***CCNB1*** | |
| ***RAD51*** | • HR deficiency | ***CDK6*** | |
| ***E2F1*** | • Decreased FoxM1 activation<br>• Decreased expression of pRb-dependent genes | ***FOXM1*** | • Potential drug resistance if resistance occurs through a MuvB-independent mechanism |
| ***CDK4*** | • Increased DREAM assembly<br>• Failure of cell cycle progression | | |
| ***WEE1*** | • Abolished DNA damage checkpoint | | |

**Figure 32. Possible gene expression and cellular consequences of LIN54-CHR inhibition.**

A LIN54-CHR inhibitor could be especially powerful when combined with a CDK4/6 inhibitor in cancers with high cyclin D expression. The high cyclin D expression creates a therapeutic window between cancer and normal cells, making cancer cells more susceptible to treatment with a CDK4/6 inhibitor, such as palbociclib. An open label phase II study of the palbociclib for recurrent ovarian cancer with intact pRb function and diminished p16 expression is ongoing (142). Another ongoing study is aimed at measuring the effects of combined palbociclib with platinum therapy in patients with metastatic cancer (143). Interestingly, cyclin D-CDK4/6 plays a role in DREAM

disassembly by phosphorylating p130 (90). Therefore, palbociclib could be used to stabilize DREAM through preventing p130 phosphorylation. A LIN54-CHR inhibitor could then be added to the treatment regimen for targeted de-repression of late cell cycle genes. Though *CDK4* is an early cell cycle gene containing an E2F site, *CDK6* contains a CHR and could be expressed for phosphorylation of p130. Palbociclib treatment would further protect retained repression of early cell cycle genes by guarding against any increase in CDK6 level. Collectively, this ensures that DNA damage repair genes are sufficiently repressed while late cell cycle gene are expressed. Therefore, the ability to differentially regulate cell cycle gene expression programs could possibly be fine-tuned with use of small molecule inhibitors.

Patients with high cyclin D1-expressing tumors might also benefit from anti-estrogen therapy. Cyclin D1, often upregulated in HGSOC, is capable of binding to and activating estrogen receptor $\alpha$ (ER$\alpha$) (144). High estrogen (E2) level is a risk factor for ovarian cancer (145) and, since ovarian tissue is hormonally responsive, estrogen antagonists (such as tamoxifen) and aromatase inhibitors have been of interest in ovarian cancer treatment. Studies using immunohistochemistry to determine expression of the estrogen ER$\alpha$ receptor found that it is strongly expressed in 30-60% of HGSOC cases. Some studies report positive ER$\alpha$ is associated with better OS and PFS; however, contradictory reports make the prognostic value of ER$\alpha$ expression remain a matter of debate (146). One such study utilized data from 894 ovarian cancer patients to assess for potential connections between ER status and either lymph node or peritoneal metastasis (145). There was no association between ER positivity and lymph node metastases. However, 86% of HGSOC peritoneal metastases were ER positive and there

was significantly higher ER positivity in peritoneal metastases of recurrent HGSOC than any other ovarian cancer subtype. Therefore, the association between ER positivity and better clinical outcomes in some studies may depend on the subtypes of ovarian cancer studied (145). Therefore, anti-estrogen therapy might be a rational treatment for HGSOC. Most of the clinical trials with estrogen antagonists, however, are small phase II trials or retrospective studies. Data thus far show that tamoxifen produces a response rate on the order of 10% whereas studies with letrozole, an aromatase inhibitor, produce responses in about 20% of patients (147, 148). Another retrospective study of 97 relapsed HGSOC patients treated with either tamoxifen (competitive estrogen inhibitor) or letrozole (aromatase inhibitor) found that the duration of response was significantly longer in those treated with letrozole as compared with those receiving tamoxifen therapy. Almost 60% of patients had a positive clinical response or stable disease for ≥3 months, suggesting that hormonal therapy provides a treatment option for stabilization of recurrent ovarian cancer (149).

Overall, more large-scale studies are needed to clarify the clinical utility of estrogen antagonists and aromatase inhibitors. Additionally, since no steps were taken to stratify patients based cyclin D level, it is unknown whether or not these treatments would produce more robust outcomes in certain subsets of patients. It would also be informative to determine the effects of palbociclib in combination with estrogen antagonists and aromatase inhibitors in patients with high cyclin D expression.

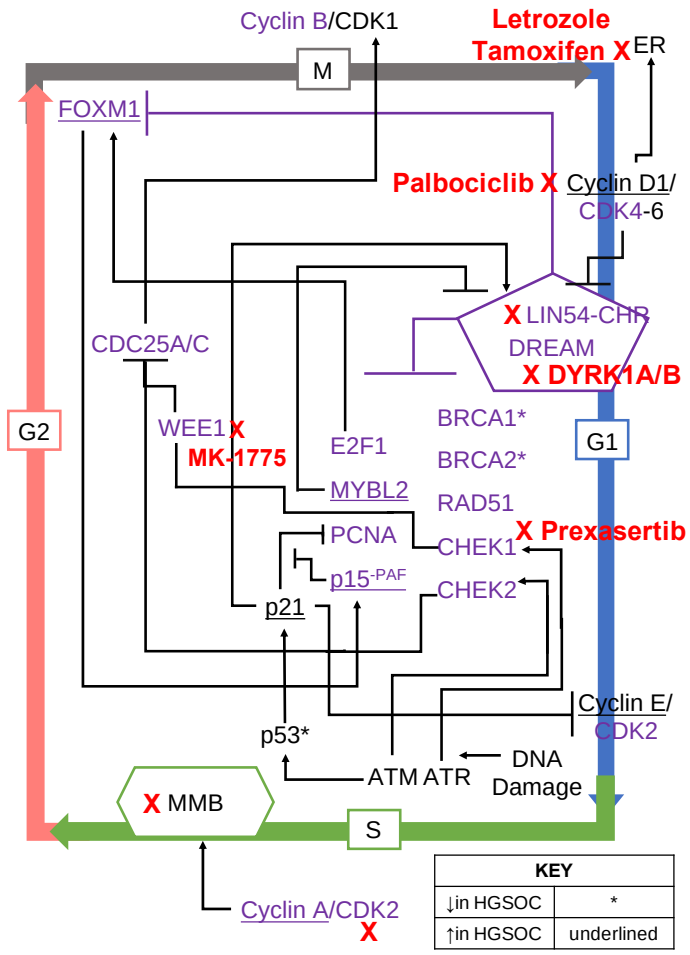


**Figure 33. FoxM1 signaling in HGSOC.** FoxM1 has been associated with treatment resistance and a poor prognosis in HGSOC. It is not yet certain whether or not these effects are mediated through interaction with MuvB in HGSOC. However, both MMB and LIN54-CHR inhibitors might curtail untoward effects of FoxM1 by blocking B-Myb-MuvB binding and *MYBL2* expression, respectively, ultimately eliminating FoxM1-MuvB formation.

**FoxM1 signaling in HGSOC**

An important consideration with these proposed treatment strategies is expression and activity of FoxM1, a CHR-containing late cell cycle gene. Since disruption of LIN54-CHR binding could contribute to de-repression of *FOXM1*, it is wise to weigh the potential consequences of its expression. FoxM1 a potential oncogenic transcription factor involved in invasion and angiogenesis (150). The FoxM1 transcription factor network is

activated in greater than 84% of HGSOC cases, mostly through genomic amplification of *FOXM1*, inhibition of p53 and pRb, and E2F1 activation (**Fig. 33**). These studies, however, did not assess DREAM status (112). FoxM1 upregulates the expression of genes involved in the HR DNA damage and repair pathway (119). Whereas FoxM1-MuvB activates these genes, DREAM represses them as well as the gene encoding FoxM1(43). In line with the p53-p21-CHR model of p53-mediated DREAM assembly, p53 was found to be a negative regulator of FoxM1. Likewise, DNA-damage resulted in upregulated FoxM1 in the absence of p53. This finding corroborates the idea of inappropriate MMB formation in response to DNA damage in the absence of p53. It was also proposed that DNA-damaging agents may not be as effective in the absence of p53 since FoxM1 is increased, protecting the cell against DNA-damage-induced apoptosis. Indeed, FoxM1 deficiency is associated with increased DNA breaks and knockdown of *FOXM1* sensitized cells to DNA damage (150, 151). Another study found that inhibition of FoxM1 with thiostrepton produced "BRCAness" and enhanced sensitivity to PARP inhibitors (119). FoxM1 is also highly expressed in ascitic metastatic cancer cells. Thiostrepton treatment decreased *FOXM1* mRNA expression as well as that of *CCNB1* and *CDC25B*. This ultimately led to cell death in cell lines and patient-derived ascites cancer cells. Combination treatment of patient-derived ascites cells *ex vivo* with thiostrepton, paclitaxel, and cisplatin revealed synergistic effects (120).

Despite all of these negative effects associated with high *FOXM1* expression, both LIN54-CHR and MMB inhibition may paradoxically thwart these damaging processes. B-Myb-MuvB binding is required for recruitment of FoxM1 to its promoters (2). *MYBL2* and *FOXM1* expression are upregulated in many p53 mutant cancers (48, 152). Like *MYBL2*,

*FOXM1* is also part of chromosomal instability signatures (CIN 70 and 25), characteristic of aneuploid tumors (62). B-Myb expression phases out at the end of the S phase while FoxM1-MuvB phosphorylation and activation dominates G2/M phase. The FoxM1-MuvB complex eventually dissociates as a result of APC/C-CDH1-mediated degradation in the M phase. Therefore, FoxM1 and B-Myb are interdependent. This is demonstrated by the depletion of B-Myb resulting in stalled replication forks and double-strand breaks being partly attributable to deregulation of *FOXM1* transcription (6). Decreased B-Myb level results in lower expression of G2/M phase-expressed genes and mitotic arrest. Similarly, FoxM1 depletion results in delayed mitotic entry as well as defective mitosis and cytokinesis (2). If B-Myb cannot bind to MuvB, then FoxM1 cannot be recruited to MuvB. If LIN54-CHR binding is disrupted, FoxM1 may be expressed, but B-Myb will not. In both cases, the MMB complex cannot form and FoxM1 cannot be recruited to its promoters. Additionally, *E2F1*, an activator of FoxM1, will remain repressed despite LIN54-CHR disruption (112). There some studies connecting the importance of FoxM1-MuvB to lung and breast cancer pathogenesis, but further studies are needed for HGSOC to define the molecular mechanisms by which FoxM1 exerts its unfavorable effects (3, 61).

**Discussion**

HGSOC has overall proven a challenging disease to treat. DNA damaging agents, such as carboplatin, remain the mainstay chemotherapy and more personalized therapies are needed. PARP inhibitors are also gaining traction; however, survival rates remain constant over the past several years. Given that susceptibility to DNA damage and initiation of the DNA damage response are cell cycle-dependent processes, an alternative

approach may be to complement DNA damaging agents with drugs having cell cycle modulatory properties.

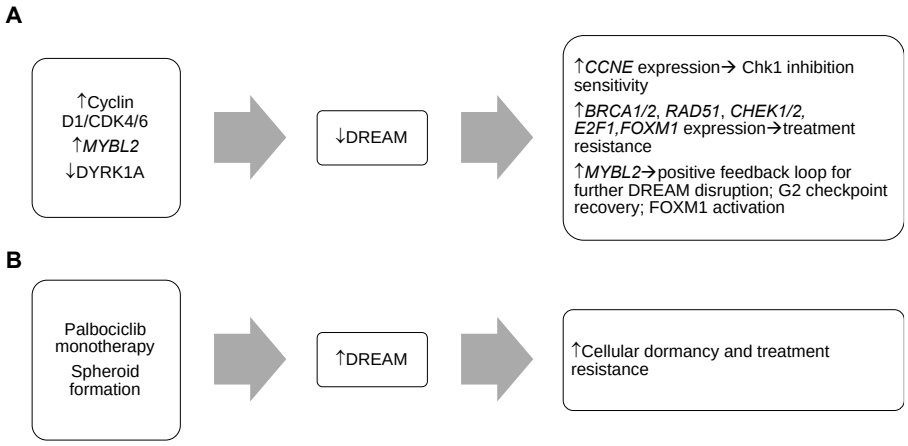


**Figure 34. Factors contributing to and effects of DREAM assembly (A) and disassembly (B).** Both DREAM formation and disruption have potentially unwanted effects depending on the state of HGSOC. Specific regulation of subsets of DREAM target genes may be a mechanism to circumvent the negative effects of global DREAM modulation.

To best utilize these cell cycle regulatory agents, it is important to first understand the cell cycle regulatory properties of the specific tumor, such as DREAM status. DREAM status may provide insights into treatment susceptibility. For example, if DREAM is disrupted, DNA damage response and repair pathways will be upregulated, contributing to possible resistance. On the other hand, if DREAM is assembled, then the cancer cells could enter a dormant state for spheroid formation and escape DNA-damaging therapy (69). **Figure 34** highlights some potential mechanisms by which DREAM formation may be increased or decreased. It is important to note that both of these conditions (global DREAM formation and DREAM disruption) carry pros and cons to HGSOC therapy. This further argues that specific modulation of DREAM, such as with LIN54-CHR inhibitor, is

likely needed to obtain desired therapeutic effects. Given that there are no reliable predictive biomarkers for HGSOC, DREAM status might be one indicator for guiding treatment methodology. DREAM formation could be assayed by using expression of DREAM target genes as a functional readout for its assembly. One such potential clinical approach is described in **Figure 35.**

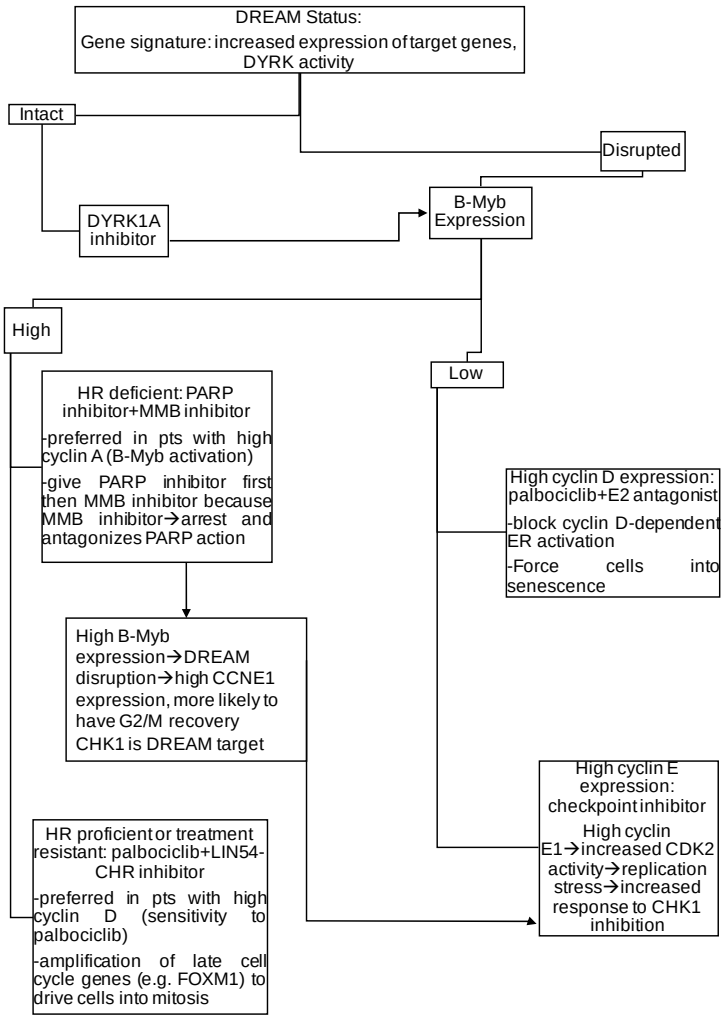


**Figure 35. Potential clinical algorithm for treating HGSOC with a combination of DNA damaging agents and cell cycle modulators.** Treatment could be personally tailored to individual patients based on the pattern of expression of cell cycle regulatory components.

Another important consideration in treatment selection is HGSOC transcriptional subtype. The Cancer Genome Atlas Research Network reported four transcriptional subtypes of ovarian cancer based on mRNA expression patterns: immunoreactive, differentiated, proliferative, and mesenchymal (23). Recent studies have assigned histological classifications to these transcriptional profiles and are characterizing them clinically (115). The proliferative subtype is genetically defined by high expression of proliferation markers, *MCM2* and *PCNA* (23). Interestingly, both of these markers are DREAM target genes (43). Their high expression, and co-expression with other DREAM targets (*MYBL2*, *CCNB2*, and *FOXM1*) is consistent with a phenotype of DREAM disruption. Additionally, another DREAM target, $p15^{PAF}$ (KIAA0101), was shown to be highly expressed in several cancers and a possible contributor to poor prognosis (117). This PCNA-associated factor competes with p21-PCNA binding to promote cell cycle progression and was recently suggested as a transcriptional target upregulation by FoxM1 in HGSOC (114). Together, these points propose that the proliferative subtype might be the subtype with the most prominent DREAM disruption and, in turn, several mechanisms for perpetuating cellular proliferation. It would be clinically valuable to further describe treatment responses in this subtype, especially since the DREAM complex has been implicated in recurrence (69).

Overall, much work remains to develop and test novel treatments for HGSOC. Further studies of the DREAM and MMB-mediated cell cycle regulation will inform specific treatments. Importantly, the impact of these signaling mechanisms on cell cycle control must be validated and related to clinical outcomes to provide sound rationale for targeted

therapy. Although several studies have focused on DNA damage response and repair, more are needed to further exploit the cell cycle for effective HGSOC treatment.

# Chapter 5: Materials and Methods

## Cells

T98G and SKOV3 cell lines were purchased from ATCC and used at low passage (<10) with routine mycoplasma testing. T98G cells stably expressing V5-tagged LIN52 or LIN52-S28A and BJ-hTERT cells were previously described (13, 90). T98G and BJ-hTERT cells were infected with a HA-FLAG-B-Myb (WT) or MuvB-binding deficient mutant B-Myb (Q674A/M677A) retroviruses produced using pMSCV-Puro vector, and selected on 1 μg/ml puromycin (13, 90). T98G DYRK1A KO cells were established using GeneArt CRISPR nuclease vector with OFP reporter (Life Technologies) harboring a DYRK1A-specific guiding RNA sequence (**Fig. 36**). For cell proliferation assay, 3,000 cells were plated per well of a 96-well plate, and luminescence was measured using ATPLite kit (PerkinElmer) at days 3 and 5. Invitrogen RNAiMAX$^{TM}$ was used for transfections of Ambion® Silencer® Select MYBL2 (s9117 and s9118), DYRK1A (s4399) and Negative Control No. 1 (4390843) siRNA oligonucleotides. Transfections of plasmid DNA were performed using polyethylenimine (153).

| Primers | Sequences (5'-3') |
|---|---|
| DYRK1A gRNA top strand | TCAGCAACCTCTAACTAACC |
| DYRK1A gRNA bottom strand | GGTTAGTTAGAGGTTGCTGA |
| Genomic PCR primers nested set #1 | Forward: AAACCTGGCAGCAGGTGC<br>Reverse: CTCATCACACATCAAATATCCG |
| Genomic PCR primers nested set #2 | Forward: AAACCTGGCAGCAGGTGC<br>Reverse: ACTTTCACACAACTACAGC |

**Figure 36. DNA oligos used to create and characterize T98G-DYRK1A KO cells.**

## Immunoprecipitations and Western blots

Antibodies for MuvB complex components LIN9, LIN37, LIN52 and pS28-LIN52 were previously described (13, 90). Commercially available antibodies are listed in **Figure**

**37**. For IP/WB assays using rabbit antibodies, Reliablot® Western blot kit (Bethyl Inc.) was used for detection. Protein band densities were quantified using ImageJ software and statistically analyzed by Student's two-tailed t-test to compare means of 3 biological repeats (154).

For immunoblotting, cells were lysed in EBC or RIPA buffers for 10 min at 4 °C and then centrifuged at 14,000g for 15 min at 4 °C. Protein concentrations were determined by DC protein assay (BioRad). Protein samples were resolved using polyacrylamide gels (BioRad), transferred to nitrocellulose membrane (GE Healthcare) and probed by specific antibodies. For immunoprecipitation, cell extracts were incubated with appropriate antibodies (1 µg/ml) and Protein A Sepharose beads (GE Healthcare) overnight at 4 °C, washed five times with lysis buffer and re-suspended in Laemmli sample buffer (BioRad). Antibodies against LIN52 and phospho-S28-LIN52 were described in (90).

| Protein | Vendor (Catalog #) |
|---|---|
| Tubulin | Sigma (SAB1411818) |
| β-actin | Cell Signaling (4970S) |
| Vinculin | Sigma (V9131) |
| GFP | Santa Cruz (sc-9996) |
| p130 | BD Biosciences (610262) |
| B-Myb | Santa Cruz (SC-724)<br>Millipore (MABE886) |
| DYRK1A | Cell Signaling (3965) |
| V5 | Bio-Rad (clone SV5-Pk1) |
| HA | Cell Signaling (3724) |

**Figure 37. Commercially available antibodies**

**Drugs**

The following chemicals were obtained from Sigma-Aldrich: Cycloheximide (3-[2-(3,5-Dimethyl-2-oxocyclohexyl)-2-hydroxyethyl]glutarimide, C7698), MG132 (Z-Leu-Leu-

Leu-al, C2211), Harmine (7-Methoxy-1-methyl-9H-pyrido[3,4-b]indole, 286044), Palbociclib (PD0332991 isethionate, PZ0199).

**Quantitative PCR**

RNA was isolated using TRIzol reagent (Invitrogen) and used to synthesize cDNA using SensiFAST$^{TM}$ kit (Bioline). qPCR with Maxima SYBR Green/ROX master mix (ThermoFisher) and gene specific primers (**Fig. 38**) was performed using Applied Biosystems 7900HT. Fold changes in mRNA expression relative to controls were calculated using the 2ΔΔCt methodology.

| Primers | Sequences (5'-3') |
|---|---|
| LIN52 3' UTR 1 | Forward: TCCGAAACCAAGCTCCCTTC<br>Reverse: TCCTGGAGGTACACCCTCTG |
| LIN52 3' UTR 2 | Forward: ACAATGCACACCTCACTGCT<br>Reverse: CAGACGTGTAGAGTGCCAGG |
| LIN52 ORF | Forward: TCACGTGACATGGGTTGGAA<br>Reverse: TCCAGATCTGTCCCGTCTGT |
| 18S rRNA | Forward: AACCCGTTGAACCCCATT<br>Reverse: CCATCCAATCGGTAGTAGCG |
| FOXM1 | Forward: GTCTGGAGGGTCCACACTTG<br>Reverse: CGACGGGGGCTAGTTTTCAT |
| MYBL2 | Forward: CATTGTGGATGAGGATGTGAAGC<br>Reverse: TGGTTGAGCAAGCTGTTGTCTTC |
| CCNB2 | Forward: GCTCCAAAGGGTCCTTCTCC<br>Reverse: TGCAGAGCAAGGCATCAGAA |
| AURKA | Forward: TGGCAAATGCCCTGTCTTACTGTCA<br>Reverse: GGGGGCAGGTAGTCCAGGGT |
| LIN9 | Forward: ATTCGGCGGCTTATGGGAAA<br>Reverse: AGAGCCTTATTTTCTGCCGT |
| KIF23 | Forward: TGCTGCCATGAAGTCAGCGAGAG<br>Reverse: CCAGTGGGCGCACCCTACAG |
| E2F1 | Forward: GCCACTGACTCTGCCACCATAG<br>Reverse: CTGCCCATCCGGGACAAC |

**Figure 38. qPCR primers.**

***In vitro* kinase assay**

Cell extracts from control and DYRK1A-KO T98G cells, or BJ-hTERT cell lines (3 mg/ml) were prepared using EDTA-free EBC buffer (13, 90) supplemented with

phosphatase inhibitors, 2 mM DTT, 10 mM MgCl2, 10 mM MnCl2 and 200 μM ATP, and incubated at 30°C with 6 ng GST-LIN52 in a 100 μl reaction volume. Reactions were terminated by adding SDS-PAGE loading buffer and heating at 95°C for 10 min, and analyzed by WB.

**Biostatistics**

Differential gene expression: To calculate statistical significance, data from at least 3 biological replicates was analyzed using two-tailed Student's t-test. Open access TCGA gene expression data for breast and ovarian cancers (summarized as RSEM values) were obtained using the TCGA2STAT R package v. 1.2. Data for each cancer were obtained separately and log2-transformed. Analysis of significantly upregulated genes in TCGA breast (107) and ovarian (23) cancer samples with *MYBL2* gene copy number gains was performed using cBio.org resource (http://www.cbioportal.org/). Gene set enrichment analysis was performed using MSigDB software (http://software.broadinstitute.org/gsea/msigdb/) (108). For differential expression analysis, samples in the selected cancer cohort were sorted by expression of *MYBL2*. Differentially expressed genes were detected between samples in the upper 75 and lower 25 percentiles of the expression gradient using the limma R package v. 3.32.6. P-values were corrected for multiple testing using False Discovery Rate (FDR) method. Genes differentially expressed at FDR <0.01 were selected for Metascape (http://metascape.org/) functional enrichment analysis using the latest 03-16-2017 database version (155). Top 50 genes up- and downregulated in the selected cancer were also overlapped with DREAM and MMB targets (13, 20, 43).

Survival Analysis: Level 3 gene expression data summarized as RSEM values was obtained using the TCGA2STAT R package v 1.2, along with the corresponding clinical annotations. Data for each of the 34 cancers was obtained separately. The data was log2-transformed and analyzed using Kaplan-Meier curves and Cox proportional hazard model. Each gene of interest was analyzed for its effect on survival by separating patients into high/low expression subgroups. A modified approach from (156) was used to estimate the best gene expression cutoff that separates high/low expression subgroups with differential survival. We took the advantage of the availability of clinical annotations. To identify if expression of a gene of interest affects survival in any specific clinical subgroup, subsets of patients annotated with specific clinical annotations were selected (e.g., “males” or “females” in the “gender” clinical annotation). Subgroups with <40 patients were not considered.

## References

1. DeCaprio JA, Duensing A. The DREAM complex in antitumor activity of imatinib mesylate in gastrointestinal stromal tumors. Current opinion in oncology. 2014;26(4):415-21.
2. Sadasivam S, DeCaprio JA. The DREAM complex: master coordinator of cell cycle-dependent gene expression. Nat Rev Cancer. 2013;13(8):585-95.
3. Iltzsche F, Simon K, Stopp S, Pattschull G, Francke S, Wolter P, et al. An important role for Myb-MuvB and its target gene KIF23 in a mouse model of lung adenocarcinoma. Oncogene. 2017;36(1):110-21.
4. Becker W. A wake-up call to quiescent cancer cells - potential use of DYRK1B inhibitors in cancer therapy. FEBS J. 2017.
5. Dedic Plavetic N, Jakic-Razumovic J, Kulic A, Vrbanec D. Prognostic value of proliferation markers expression in breast cancer. Medical oncology. 2013;30(2):523.
6. Musa J, Aynaud MM, Mirabeau O, Delattre O, Grunewald TG. MYBL2 (B-Myb): a central regulator of cell proliferation, cell survival and differentiation involved in tumorigenesis. Cell death & disease. 2017;8(6):e2895.
7. Boichuk S, Parry JA, Makielski KR, Litovchick L, Baron JL, Zewe JP, et al. The DREAM complex mediates GIST cell quiescence and is a novel therapeutic target to enhance imatinib-induced apoptosis. Cancer research. 2013;73(16):5120-9.
8. Dannenberg JH, van Rossum A, Schuijff L, te Riele H. Ablation of the retinoblastoma gene family deregulates G(1) control causing immortalization and increased cell turnover under growth-restricting conditions. Genes & development. 2000;14(23):3051-64.
9. Zalvide J, DeCaprio JA. Role of pRb-related proteins in simian virus 40 large-T-antigen-mediated transformation. Molecular and cellular biology. 1995;15(10):5800-10.
10. Cobrinik D. Pocket proteins and cell cycle control. Oncogene. 2005;24(17):2796-809.
11. Harrison MM, Ceol CJ, Lu X, Horvitz HR. Some C. elegans class B synthetic multivulva proteins encode a conserved LIN-35 Rb-containing complex distinct from a NuRD-like complex. Proceedings of the National Academy of Sciences of the United States of America. 2006;103(45):16782-7.
12. Korenjak M, Taylor-Harding B, Binne UK, Satterlee JS, Stevaux O, Aasland R, et al. Native E2F/RBF complexes contain Myb-interacting proteins and repress transcription of developmentally controlled E2F target genes. Cell. 2004;119(2):181-93.
13. Litovchick L, Sadasivam S, Florens L, Zhu X, Swanson SK, Velmurugan S, et al. Evolutionarily conserved multisubunit RBL2/p130 and E2F4 protein complex represses human cell cycle-dependent genes in quiescence. Mol Cell. 2007;26(4):539-51.
14. Schmit F, Korenjak M, Mannefeld M, Schmitt K, Franke C, von Eyss B, et al. LINC, a human complex that is related to pRB-containing complexes in invertebrates regulates the expression of G2/M genes. Cell cycle. 2007;6(15):1903-13.
15. Litovchick L, Florens LA, Swanson SK, Washburn MP, DeCaprio JA. DYRK1A protein kinase promotes quiescence and senescence through DREAM complex assembly. Genes & development. 2011;25(8):801-13.

16. Guiley KZ, Liban TJ, Felthousen JG, Ramanan P, Litovchick L, Rubin SM. Structural mechanisms of DREAM complex assembly and regulation. Genes & development. 2015;29(9):961-74.
17. Odajima J, Saini S, Jung P, Ndassa-Colday Y, Ficaro S, Geng Y, et al. Proteomic Landscape of Tissue-Specific Cyclin E Functions in Vivo. PLoS genetics. 2016;12(11):e1006429.
18. Pilkinton M, Sandoval R, Colamonici OR. Mammalian Mip/LIN-9 interacts with either the p107, p130/E2F4 repressor complex or B-Myb in a cell cycle-phase-dependent context distinct from the Drosophila dREAM complex. Oncogene. 2007;26(54):7535-43.
19. Osterloh L, von Eyss B, Schmit F, Rein L, Hubner D, Samans B, et al. The human synMuv-like protein LIN-9 is required for transcription of G2/M genes and for entry into mitosis. The EMBO journal. 2007;26(1):144-57.
20. Sadasivam S, Duan S, DeCaprio JA. The MuvB complex sequentially recruits B-Myb and FoxM1 to promote mitotic gene expression. Genes & development. 2012;26(5):474-89.
21. Muller GA, Wintsche A, Stangner K, Prohaska SJ, Stadler PF, Engeland K. The CHR site: definition and genome-wide identification of a cell cycle transcriptional element. Nucleic acids research. 2014;42(16):10331-50.
22. Muller GA, Stangner K, Schmitt T, Wintsche A, Engeland K. Timing of transcription during the cell cycle: Protein complexes binding to E2F, E2F/CLE, CDE/CHR, or CHR promoter elements define early and late cell cycle gene expression. Oncotarget. 2017;8(58):97736-48.
23. Cancer Genome Atlas Research N. Integrated genomic analyses of ovarian carcinoma. Nature. 2011;474(7353):609-15.
24. Cinti C, Leoncini L, Nyongo A, Ferrari F, Lazzi S, Bellan C, et al. Genetic Alterations of the Retinoblastoma-Related Gene RB2/p130 Identify Different Pathogenetic Mechanisms in and among Burkitt's Lymphoma Subtypes. The American Journal of Pathology. 2000;156(3):751-60.
25. Claudio PP, Howard CM, Pacilio C, Cinti C, Romano G, Minimo C, et al. Mutations in the retinoblastoma-related gene RB2/p130 in lung tumors and suppression of tumor growth in vivo by retrovirus-mediated gene transfer. Cancer Res. 2000;60(2):372-82.
26. Helin K, Holm K, Niebuhr A, Eiberg H, Tommerup N, Hougaard S, et al. Loss of the retinoblastoma protein-related p130 protein in small cell lung carcinoma. Proceedings of the National Academy of Sciences of the United States of America. 1997;94(13):6933-8.
27. Cerami E, Gao J, Dogrusoz U, Gross BE, Sumer SO, Aksoy BA, et al. The cBio cancer genomics portal: an open platform for exploring multidimensional cancer genomics data. Cancer Discov. 2012;2(5):401-4.
28. Fischer M, Muller GA. Cell cycle transcription control: DREAM/MuvB and RB-E2F complexes. Crit Rev Biochem Mol Biol. 2017:1-25.
29. Zhang Y, Ng HH, Erdjument-Bromage H, Tempst P, Bird A, Reinberg D. Analysis of the NuRD subunits reveals a histone deacetylase core complex and a connection with DNA methylation. Genes & development. 1999;13(15):1924-35.
30. Wolffe AP, Urnov FD, Guschin D. Co-repressor complexes and remodelling chromatin for repression. Biochemical Society transactions. 2000;28(4):379-86.

31. Loyola A, Almouzni G. Histone chaperones, a supporting role in the limelight. Biochimica et biophysica acta. 2004;1677(1-3):3-11.
32. Mages CF, Wintsche A, Bernhart SH, Muller GA. The DREAM complex through its subunit Lin37 cooperates with Rb to initiate quiescence. Elife. 2017;6.
33. Pilkinton M, Sandoval R, Barrett K, Tian X, Colamonici OR. Mip/LIN-9 can inhibit cell proliferation independent of the pocket proteins. Blood cells, molecules & diseases. 2007;39(3):272-7.
34. Pilkinton M, Sandoval R, Song J, Ness SA, Colamonici OR. Mip/LIN-9 regulates the expression of B-Myb and the induction of cyclin A, cyclin B, and CDK1. The Journal of biological chemistry. 2007;282(1):168-75.
35. Reichert N, Wurster S, Ulrich T, Schmitt K, Hauser S, Probst L, et al. Lin9, a subunit of the mammalian DREAM complex, is essential for embryonic development, for survival of adult mice, and for tumor suppression. Molecular and cellular biology. 2010;30(12):2896-908.
36. Wiseman EF, Chen X, Han N, Webber A, Ji Z, Sharrocks AD, et al. Deregulation of the FOXM1 target gene network and its coregulatory partners in oesophageal adenocarcinoma. Molecular cancer. 2015;14:69.
37. Schmit F, Cremer S, Gaubatz S. LIN54 is an essential core subunit of the DREAM/LINC complex that binds to the cdc2 promoter in a sequence-specific manner. The FEBS journal. 2009;276(19):5703-16.
38. Marceau AH, Felthousen JG, Goetsch PD, Iness AN, Lee H-W, Tripathi SM, et al. Structural basis for LIN54 recognition of CHR elements in cell cycle-regulated promoters. Nature Communications. 2016;7.
39. Matsuo T, Kuramoto H, Kumazaki T, Mitsui Y, Takahashi T. LIN54 harboring a mutation in CHC domain is localized to the cytoplasm and inhibits cell cycle progression. Cell cycle. 2012;11(17):3227-36.
40. Muller GA, Quaas M, Schumann M, Krause E, Padi M, Fischer M, et al. The CHR promoter element controls cell cycle-dependent gene transcription and binds the DREAM and MMB complexes. Nucleic acids research. 2012;40(4):1561-78.
41. Forristal C, Henley SA, MacDonald JI, Bush JR, Ort C, Passos DT, et al. Loss of the mammalian DREAM complex deregulates chondrocyte proliferation. Molecular and cellular biology. 2014;34(12):2221-34.
42. Classon M, Salama S, Gorka C, Mulloy R, Braun P, Harlow E. Combinatorial roles for pRB, p107, and p130 in E2F-mediated cell cycle control. Proceedings of the National Academy of Sciences of the United States of America. 2000;97(20):10820-5.
43. Fischer M, Grossmann P, Padi M, DeCaprio JA. Integration of TP53, DREAM, MMB-FOXM1 and RB-E2F target gene analyses identifies cell cycle gene regulatory networks. Nucleic acids research. 2016;44(13):6070-86.
44. Fischer M, Grundke I, Sohr S, Quaas M, Hoffmann S, Knorck A, et al. p53 and cell cycle dependent transcription of kinesin family member 23 (KIF23) is controlled via a CHR promoter element bound by DREAM and MMB complexes. PloS one. 2013;8(5):e63187.
45. Quaas M, Muller GA, Engeland K. p53 can repress transcription of cell cycle genes through a p21(WAF1/CIP1)-dependent switch from MMB to DREAM protein complex binding at CHR promoter elements. Cell cycle. 2012;11(24):4661-72.
46. Altieri DC. Survivin - The inconvenient IAP. Seminars in cell & developmental biology. 2015;39(1096-3634 (Electronic)):91-6.

47. Fischer M, Quaas M, Nickel A, Engeland K. Indirect p53-dependent transcriptional repression of Survivin, CDC25C, and PLK1 genes requires the cyclin-dependent kinase inhibitor p21/CDKN1A and CDE/CHR promoter sites binding the DREAM complex. Oncotarget. 2015;6(39):41402-17.
48. Mannefeld M, Klassen E, Gaubatz S. B-MYB is required for recovery from the DNA damage-induced G2 checkpoint in p53 mutant cells. Cancer Res. 2009;69(9):4073-80.
49. Calvisi DF, Simile MM, Ladu S, Frau M, Evert M, Tomasi ML, et al. Activation of v-Myb avian myeloblastosis viral oncogene homolog-like2 (MYBL2)-LIN9 complex contributes to human hepatocarcinogenesis and identifies a subset of hepatocellular carcinoma with mutant p53. Hepatology. 2011;53(4):1226-36.
50. Munger K. The role of human papillomaviruses in human cancers. Frontiers in bioscience : a journal and virtual library. 2002;7:d641-9.
51. DeCaprio JA. How the Rb tumor suppressor structure and function was revealed by the study of Adenovirus and SV40. Virology. 2009;384(2):274-84.
52. DeCaprio JA. Human papillomavirus type 16 E7 perturbs DREAM to promote cellular proliferation and mitotic gene expression. Oncogene. 2014;33(31):4036-8.
53. Nor Rashid N, Yusof R, Watson RJ. Disruption of repressive p130-DREAM complexes by human papillomavirus 16 E6/E7 oncoproteins is required for cell-cycle progression in cervical cancer cells. The Journal of general virology. 2011;92(Pt 11):2620-7.
54. Rashid NN, Yusof R, Watson RJ. A B-myb--DREAM complex is not critical to regulate the G2/M genes in HPV-transformed cell lines. Anticancer research. 2014;34(11):6557-63.
55. Fischer M, Uxa S, Stanko C, Magin TM, Engeland K. Human papilloma virus E7 oncoprotein abrogates the p53-p21-DREAM pathway. Scientific reports. 2017;7(1):2603.
56. Fischer M, Uxa S, Stanko C, Magin TM, Engeland K. Human papilloma virus E7 oncoprotein abrogates the p53-p21-DREAM pathway. Scientific Reports. 2017;7(1):2603.
57. Fischer M, Quaas M, Steiner L, Engeland K. The p53-p21-DREAM-CDE/CHR pathway regulates G2/M cell cycle genes. Nucleic acids research. 2016;44(1):164-74.
58. Tanner MM, Grenman S, Koul A, Johannsson O, Meltzer P, Pejovic T, et al. Frequent amplification of chromosomal region 20q12-q13 in ovarian cancer. Clinical cancer research : an official journal of the American Association for Cancer Research. 2000;6(5):1833-9.
59. Thorner AR, Hoadley KA, Parker JS, Winkel S, Millikan RC, Perou CM. In vitro and in vivo analysis of B-Myb in basal-like breast cancer. Oncogene. 2009;28(5):742-51.
60. Guan Z, Cheng W, Huang D, Wei A. High MYBL2 expression and transcription regulatory activity is associated with poor overall survival in patients with hepatocellular carcinoma. Curr Res Transl Med. 2017.
61. Wolter P, Hanselmann S, Pattschull G, Schruf E, Gaubatz S. Central spindle proteins and mitotic kinesins are direct transcriptional targets of MuvB, B-MYB and FOXM1 in breast cancer cell lines and are potential targets for therapy. Oncotarget. 2017;8(7):11160-72.
62. Carter SL, Eklund AC, Kohane IS, Harris LN, Szallasi Z. A signature of chromosomal instability inferred from gene expression profiles predicts clinical outcome in multiple human cancers. Nature genetics. 2006;38(9):1043-8.

63. Chibon F, Lagarde P, Salas S, Pérot G, Brouste V, Tirode F, et al. Validated prediction of clinical outcome in sarcomas and multiple types of cancer on the basis of a gene expression signature related to genome complexity. Nature medicine. 2010;16(7):781-7.
64. Bowtell DD. The genesis and evolution of high-grade serous ovarian cancer. Nature reviews Cancer. 2010;10(11):803-8.
65. Lowe KA, Chia VM, Taylor A, O'Malley C, Kelsh M, Mohamed M, et al. An international assessment of ovarian cancer incidence and mortality. Gynecol Oncol. 2013;130(1):107-14.
66. National Cancer I. Cancer Stat Facts: Ovarian Cancer. 2014.
67. Slaughter K, Holman LL, Thomas EL, Gunderson CC, Lauer JK, Ding K, et al. Primary and acquired platinum-resistance among women with high grade serous ovarian cancer. Gynecol Oncol. 2016;142(2):225-30.
68. Christie EL, Bowtell DDL. Acquired chemotherapy resistance in ovarian cancer. Annals of oncology : official journal of the European Society for Medical Oncology. 2017;28(suppl_8):viii13-viii5.
69. MacDonald J, Ramos-Valdes Y, Perampalam P, Litovchick L, DiMattia GE, Dick FA. A Systematic Analysis of Negative Growth Control Implicates the DREAM Complex in Cancer Cell Dormancy. Molecular cancer research : MCR. 2017;15(4):371-81.
70. Ogawa Y, Nonaka Y, Goto T, Ohnishi E, Hiramatsu T, Kii I, et al. Development of a novel selective inhibitor of the Down syndrome-related kinase Dyrk1A. Nat Commun. 2010;1:86.
71. Abbassi R, Johns TG, Kassiou M, Munoz L. DYRK1A in neurodegeneration and cancer: Molecular basis and clinical implications. Pharmacology & therapeutics. 2015;151:87-98.
72. Duchon A, Herault Y. DYRK1A, a Dosage-Sensitive Gene Involved in Neurodevelopmental Disorders, Is a Target for Drug Development in Down Syndrome. Frontiers in behavioral neuroscience. 2016;10:104.
73. Adayev T, Wegiel J, Hwang YW. Harmine is an ATP-competitive inhibitor for dual-specificity tyrosine phosphorylation-regulated kinase 1A (Dyrk1A). Archives of biochemistry and biophysics. 2011;507(2):212-8.
74. Kim H, Lee KS, Kim AK, Choi M, Choi K, Kang M, et al. A chemical with proven clinical safety rescues Down-syndrome-related phenotypes in through DYRK1A inhibition. Disease models & mechanisms. 2016;9(8):839-48.
75. Leder S, Weber Y, Altafaj X, Estivill X, Joost HG, Becker W. Cloning and characterization of DYRK1B, a novel member of the DYRK family of protein kinases. Biochemical and biophysical research communications. 1999;254(2):474-9.
76. Ewton DZ, Hu J, Vilenchik M, Deng X, Luk KC, Polonskaia A, et al. Inactivation of mirk/dyrk1b kinase targets quiescent pancreatic cancer cells. Molecular cancer therapeutics. 2011;10(11):2104-14.
77. Friedman E. The Kinase Mirk/dyrk1B: A Possible Therapeutic Target in Pancreatic Cancer. Cancers. 2010;2(3):1492-512.
78. Friedman E. Mirk/dyrk1B Kinase in Ovarian Cancer. International journal of molecular sciences. 2013;14(3):5560-75.
79. Hu J, Deng H, Friedman EA. Ovarian cancer cells, not normal cells, are damaged by Mirk/Dyrk1B kinase inhibition. Int J Cancer. 2013;132(10):2258-69.

80. Gao J, Aksoy BA, Dogrusoz U, Dresdner G, Gross B, Sumer SO, et al. Integrative analysis of complex cancer genomics and clinical profiles using the cBioPortal. Sci Signal. 2013;6(269):pl1.
81. Ashford AL, Oxley D, Kettle J, Hudson K, Guichard S, Cook SJ, et al. A novel DYRK1B inhibitor AZ191 demonstrates that DYRK1B acts independently of GSK3beta to phosphorylate cyclin D1 at Thr(286), not Thr(288). The Biochemical journal. 2014;457(1):43-56.
82. Nomura N, Takahashi M, Matsui M, Ishii S, Date T, Sasamoto S, et al. Isolation of human cDNA clones of myb-related genes, A-myb and B-myb. Nucleic acids research. 1988;16(23):11075-89.
83. Solin LJ, Gray R, Baehner FL, Butler SM, Hughes LL, Yoshizawa C, et al. A multigene expression assay to predict local recurrence risk for ductal carcinoma in situ of the breast. Journal of the National Cancer Institute. 2013;105(10):701-10.
84. Allegra CJ, Aberle DR, Ganschow P, Hahn SM, Lee CN, Millon-Underwood S, et al. National Institutes of Health State-of-the-Science Conference statement: Diagnosis and Management of Ductal Carcinoma In Situ September 22-24, 2009. Journal of the National Cancer Institute. 2010;102(3):161-9.
85. Ness SA. Myb protein specificity: evidence of a context-specific transcription factor code. Blood cells, molecules & diseases. 2003;31(2):192-200.
86. Tanaka Y, Patestos NP, Maekawa T, Ishii S. B-myb is required for inner cell mass formation at an early stage of development. The Journal of biological chemistry. 1999;274(40):28067-70.
87. Sala A. B-MYB, a transcription factor implicated in regulating cell cycle, apoptosis and cancer. European journal of cancer. 2005;41(16):2479-84.
88. Lewis PW, Beall EL, Fleischer TC, Georlette D, Link AJ, Botchan MR. Identification of a Drosophila Myb-E2F2/RBF transcriptional repressor complex. Genes & development. 2004;18(23):2929-40.
89. Korenjak M, Brehm A. E2F-Rb complexes regulating transcription of genes important for differentiation and development. Curr Opin Genet Dev. 2005;15(5):520-7.
90. Litovchick L, Florens L, Swanson SK, Washburn MP, DeCaprio JA. DYRK1A protein kinase promotes quiescence and senescence through DREAM complex assembly. Genes & development. 2011;25:801 - 13.
91. Chen X, Muller GA, Quaas M, Fischer M, Han N, Stutchbury B, et al. The forkhead transcription factor FOXM1 controls cell cycle-dependent gene expression through an atypical chromatin binding mechanism. Mol Cell Biol. 2012;33(2):227-36.
92. Sala A, Casella I, Bellon T, Calabretta B, Watson RJ, Peschle C. B-myb promotes S phase and is a downstream target of the negative regulator p107 in human cells. The Journal of biological chemistry. 1996;271(16):9363-7.
93. Sala A, Kundu M, Casella I, Engelhard A, Calabretta B, Grasso L, et al. Activation of human B-MYB by cyclins. Proceedings of the National Academy of Sciences of the United States of America. 1997;94(2):532-6.
94. Hahn WC, Counter CM, Lundberg AS, Beijersbergen RL, Brooks MW, Weinberg RA. Creation of human tumour cells with defined genetic elements. Nature. 1999;400(6743):464-8.
95. Lundin A, Hasenson M, Persson J, Pousette A. Estimation of biomass in growing cell lines by adenosine triphosphate assay. Methods in enzymology. 1986;133:27-42.

96. Guiley KZ IA, Saini S, Tripathi S, Lipsick JS, Litovchick L, Rubin SM. . Structural mechanism of Myb-MuvB assembly. . Proc Natl Acad Sci USA. 2018.
97. Stein GH. T98G: an anchorage-independent human tumor cell line that exhibits stationary phase G1 arrest in vitro. Journal of cellular physiology. 1979;99(1):43-54.
98. Ran FA, Hsu PD, Wright J, Agarwala V, Scott DA, Zhang F. Genome engineering using the CRISPR-Cas9 system. Nature protocols. 2013;8(11):2281-308.
99. Becker W, Sippl W. Activation, regulation, and inhibition of DYRK1A. The FEBS journal. 2011;278(2):246-56.
100. Iwahori S, Kalejta RF. Phosphorylation of transcriptional regulators in the retinoblastoma protein pathway by UL97, the viral cyclin-dependent kinase encoded by human cytomegalovirus. Virology. 2017;512:95-103.
101. Barretina J, Caponigro G, Stransky N, Venkatesan K, Margolin AA, Kim S, et al. The Cancer Cell Line Encyclopedia enables predictive modelling of anticancer drug sensitivity. Nature. 2012;483(7391):603-7.
102. Bodurka DC, Deavers Mt Fau - Tian C, Tian C Fau - Sun CC, Sun Cc Fau - Malpica A, Malpica A Fau - Coleman RL, Coleman Rl Fau - Lu KH, et al. Reclassification of serous ovarian carcinoma by a 2-tier system: a Gynecologic Oncology Group Study. (1097-0142 (Electronic)).
103. Miller DS, Blessing Ja Fau - Drake RD, Drake Rd Fau - Higgins R, Higgins R Fau - McMeekin DS, McMeekin Ds Fau - Puneky LV, Puneky Lv Fau - Krasner CN, et al. A phase II evaluation of pemetrexed (Alimta, LY231514, IND #40061) in the treatment of recurrent or persistent endometrial carcinoma: a phase II study of the Gynecologic Oncology. (1095-6859 (Electronic)).
104. Soletormos G, Duffy Mj Fau - Othman Abu Hassan S, Othman Abu Hassan S Fau - Verheijen RHM, Verheijen Rh Fau - Tholander B, Tholander B Fau - Bast RC, Jr., Bast Rc Jr Fau - Gaarenstroom KN, et al. Clinical Use of Cancer Biomarkers in Epithelial Ovarian Cancer: Updated Guidelines From the European Group on Tumor Markers. (1525-1438 (Electronic)).
105. Inoue K, Fry EA. Novel Molecular Markers for Breast Cancer. Biomarkers in cancer. 2016;8:25-42.
106. Sotiriou C, Neo SY, McShane LM, Korn EL, Long PM, Jazaeri A, et al. Breast cancer classification and prognosis based on gene expression profiles from a population-based study. Proceedings of the National Academy of Sciences of the United States of America. 2003;100(18):10393-8.
107. Ciriello G, Gatza ML, Beck AH, Wilkerson MD, Rhie SK, Pastore A, et al. Comprehensive Molecular Portraits of Invasive Lobular Breast Cancer. Cell. 2015;163(2):506-19.
108. Liberzon A, Subramanian A, Pinchback R, Thorvaldsdottir H, Tamayo P, Mesirov JP. Molecular signatures database (MSigDB) 3.0. Bioinformatics. 2011;27(12):1739-40.
109. Subramanian A, Tamayo P, Mootha VK, Mukherjee S, Ebert BL, Gillette MA, et al. Gene set enrichment analysis: a knowledge-based approach for interpreting genome-wide expression profiles. Proceedings of the National Academy of Sciences of the United States of America. 2005;102(43):15545-50.
110. Zhang S, Royer R Fau - Li S, Li S Fau - McLaughlin JR, McLaughlin Jr Fau - Rosen B, Rosen B Fau - Risch HA, Risch Ha Fau - Fan I, et al. Frequencies of BRCA1 and

BRCA2 mutations among 1,342 unselected patients with invasive ovarian cancer. (1095-6859 (Electronic)).
111. Li YL, Ye F Fau - Hu Y, Hu Y Fau - Lu W-G, Lu Wg Fau - Xie X, Xie X. Identification of suitable reference genes for gene expression studies of human serous ovarian cancer by real-time polymerase chain reaction. (1096-0309 (Electronic)).
112. Barger CJ, Zhang W, Hillman J, Stablewski AB, Higgins MJ, Vanderhyden BC, et al. Genetic determinants of FOXM1 overexpression in epithelial ovarian cancer and functional contribution to cell cycle progression. (1949-2553 (Electronic)).
113. Chen X, Muller GA, Quaas M, Fischer M, Han N, Stutchbury B, et al. The forkhead transcription factor FOXM1 controls cell cycle-dependent gene expression through an atypical chromatin binding mechanism. Molecular and cellular biology. 2013;33(2):227-36.
114. Jin C, Liu ZA-Ohoo, Li Y, Bu H, Wang Y, Xu Y, et al. PCNA-associated factor P15(PAF) , targeted by FOXM1, predicts poor prognosis in high-grade serous ovarian cancer patients. LID - 10.1002/ijc.31800 [doi]. (1097-0215 (Electronic)).
115. Murakami R, Matsumura N, Mandai M, Yoshihara K, Tanabe H, Nakai H, et al. Establishment of a Novel Histopathological Classification of High-Grade Serous Ovarian Carcinoma Correlated with Prognostically Distinct Gene Expression Subtypes. (1525-2191 (Electronic)).
116. Kommoss S, Winterhoff B, Oberg AL, Konecny GE, Wang C, Riska SM, et al. Bevacizumab May Differentially Improve Ovarian Cancer Outcome in Patients with Proliferative and Mesenchymal Molecular Subtypes. (1078-0432 (Print)).
117. Yu P, Huang B Fau - Shen M, Shen M Fau - Lau C, Lau C Fau - Chan E, Chan E Fau - Michel J, Michel J Fau - Xiong Y, et al. p15(PAF), a novel PCNA associated factor with increased expression in tumor tissues. (0950-9232 (Print)).
118. Chang CN, Feng Mj Fau - Chen Y-L, Chen Yl Fau - Yuan R-H, Yuan Rh Fau - Jeng Y-M, Jeng YM. p15(PAF) is an Rb/E2F-regulated S-phase protein essential for DNA synthesis and cell cycle progression. (1932-6203 (Electronic)).
119. Fang P, Madden JA, Neums LA-Ohoo, Moulder RK, Forrest MLA-Ohoo, Chien J. Olaparib-induced Adaptive Response Is Disrupted by FOXM1 Targeting that Enhances Sensitivity to PARP Inhibition. (1557-3125 (Electronic)).
120. Westhoff GL, Chen Y Fau - Teng NNH, Teng NNH. Targeting FOXM1 Improves Cytotoxicity of Paclitaxel and Cisplatinum in Platinum-Resistant Ovarian Cancer. (1525-1438 (Electronic)).
121. Charrasse S, Carena I Fau - Brondani V, Brondani V Fau - Klempnauer KH, Klempnauer Kh Fau - Ferrari S, Ferrari S. Degradation of B-Myb by ubiquitin-mediated proteolysis: involvement of the Cdc34-SCF(p45Skp2) pathway. (0950-9232 (Print)).
122. Arend RC, Londono AI, Montgomery AM, Smith HJ, Dobbin ZC, Katre AA, et al. Molecular Response to Neoadjuvant Chemotherapy in High-Grade Serous Ovarian Carcinoma. (1557-3125 (Electronic)).
123. Iness AN, Litovchick L. MuvB: A Key to Cell Cycle Control in Ovarian Cancer. (2234-943X (Print)).
124. Iness AN, Felthousen J, Ananthapadmanabhan V, Sesay F, Saini S, Guiley KZ, et al. The cell cycle regulatory DREAM complex is disrupted by high expression of oncogenic B-Myb. LID - 10.1038/s41388-018-0490-y [doi]. (1476-5594 (Electronic)).

125. Visconti R, Della Monica R, Grieco D. Cell cycle checkpoint in cancer: a therapeutically targetable double-edged sword. (1756-9966 (Electronic)).
126. Lin AB, McNeely SC, Beckmann RP. Achieving Precision Death with Cell-Cycle Inhibitors that Target DNA Replication and Repair. (1078-0432 (Print)).
127. Konstantinopoulos PA, Ceccaldi R, Shapiro GI, D'Andrea AD. Homologous Recombination Deficiency: Exploiting the Fundamental Vulnerability of Ovarian Cancer. (2159-8290 (Electronic)).
128. Sakurikar N, Eastman A. Will targeting Chk1 have a role in the future of cancer therapy? (1527-7755 (Electronic)).
129. Lee JM, Nair J, Zimmer A, Lipkowitz S, Annunziata CM, Merino MJ, et al. Prexasertib, a cell cycle checkpoint kinase 1 and 2 inhibitor, in BRCA wild-type recurrent high-grade serous ovarian cancer: a first-in-class proof-of-concept phase 2 study. (1474-5488 (Electronic)).
130. Lukin DJ, Carvajal LA, Liu WJ, Resnick-Silverman L, Manfredi JJ. p53 Promotes cell survival due to the reversibility of its cell-cycle checkpoints. (1557-3125 (Electronic)).
131. Patch AM, Christie EL, Etemadmoghadam D, Garsed DW, George J, Fereday S, et al. Whole-genome characterization of chemoresistant ovarian cancer. (1476-4687 (Electronic)).
132. Masselink H, Vastenhouw N Fau - Bernards R, Bernards R. B-myb rescues ras-induced premature senescence, which requires its transactivation domain. (0304-3835 (Print)).
133. Garcia P, Frampton J. The transcription factor B-Myb is essential for S-phase progression and genomic stability in diploid and polyploid megakaryocytes. (0021-9533 (Print)).
134. Guiley KZ, Iness AN, Saini S, Tripathi S, Lipsick JS, Litovchick L, et al. Structural mechanism of Myb–MuvB assembly. Proceedings of the National Academy of Sciences. 2018.
135. Tsibulak I, Wieser V, Degasper C, Shivalingaiah G, Wenzel S, Sprung S, et al. BRCA1 and BRCA2 mRNA-expression prove to be of clinical impact in ovarian cancer. (1532-1827 (Electronic)).
136. Cojocaru E, Parkinson CA, Brenton JD. Personalising Treatment for High-Grade Serous Ovarian Carcinoma. (1433-2981 (Electronic)).
137. Shen YTA-Ohoo, Evans JC, Zafarana G, Allen CA-Ohoo, Piquette-Miller M. BRCA Status Does Not Predict Synergism of a Carboplatin and Olaparib Combination in High-Grade Serous Ovarian Cancer Cell Lines. (1543-8392 (Electronic)).
138. Dziadkowiec KN, Gasiorowska E, Nowak-Markwitz E, Jankowska A. PARP inhibitors: review of mechanisms of action and BRCA1/2 mutation targeting. (1643-8876 (Print)).
139. Quinn JE, James Cr Fau - Stewart GE, Stewart Ge Fau - Mulligan JM, Mulligan Jm Fau - White P, White P Fau - Chang GKF, Chang Gk Fau - Mullan PB, et al. BRCA1 mRNA expression levels predict for overall survival in ovarian cancer after chemotherapy. (1078-0432 (Print)).
140. Scott LJ. Niraparib: First Global Approval. (1179-1950 (Electronic)).
141. Lee JM, Peer CJ, Yu M, Amable L, Gordon N, Annunziata CM, et al. Sequence-Specific Pharmacokinetic and Pharmacodynamic Phase I/Ib Study of Olaparib Tablets and Carboplatin in Women's Cancer. (1078-0432 (Print)).

142. Konecny GE, Wahner Hendrickson AE, Jatoi A, Burton JK, Paroly J, Glaspy JA, et al. A multicenter open-label phase II study of the efficacy and safety of palbociclib a cyclin-dependent kinases 4 and 6 inhibitor in patients with recurrent ovarian cancer. Journal of Clinical Oncology. 2016;34(15_suppl):5557-.
143. Owonikoko TK. Palbociclib With Cisplatin or Carboplatin in Advanced Solid Tumors. ClinicalTrialsgov. 2018.
144. Zwijsen RM, Wientjens E Fau - Klompmaker R, Klompmaker R Fau - van der Sman J, van der Sman J Fau - Bernards R, Bernards R Fau - Michalides RJ, Michalides RJ. CDK-independent activation of estrogen receptor by cyclin D1. (0092-8674 (Print)).
145. Chen S, Dai X, Gao Y, Shen F, Ding J, Chen Q. The positivity of estrogen receptor and progesterone receptor may not be associated with metastasis and recurrence in epithelial ovarian cancer. (2045-2322 (Electronic)).
146. Voutsadakis IA. Hormone Receptors in Serous Ovarian Carcinoma: Prognosis, Pathogenesis, and Treatment Considerations. (1179-5549 (Print)).
147. Hatch KD, Beecham Jb Fau - Blessing JA, Blessing Ja Fau - Creasman WT, Creasman WT. Responsiveness of patients with advanced ovarian carcinoma to tamoxifen. A Gynecologic Oncology Group study of second-line therapy in 105 patients. (0008-543X (Print)).
148. Bowman A, Gabra H Fau - Langdon SP, Langdon Sp Fau - Lessells A, Lessells A Fau - Stewart M, Stewart M Fau - Young A, Young A Fau - Smyth JF, et al. CA125 response is associated with estrogen receptor expression in a phase II trial of letrozole in ovarian cancer: identification of an endocrine-sensitive subgroup. (1078-0432 (Print)).
149. George A, McLachlan J, Tunariu N, Della Pepa C, Migali C, Gore M, et al. The role of hormonal therapy in patients with relapsed high-grade ovarian carcinoma: a retrospective series of tamoxifen and letrozole. BMC cancer. 2017;17(1):456-.
150. Halasi M, Gartel AL. Suppression of FOXM1 sensitizes human cancer cells to cell death induced by DNA-damage. (1932-6203 (Electronic)).
151. Zona S, Bella L, Burton MJ, Nestal de Moraes G, Lam EW. FOXM1: an emerging master regulator of DNA damage response and genotoxic agent resistance. (0006-3002 (Print)).
152. Parikh N, Hilsenbeck S Fau - Creighton CJ, Creighton Cj Fau - Dayaram T, Dayaram T Fau - Shuck R, Shuck R Fau - Shinbrot E, Shinbrot E Fau - Xi L, et al. Effects of TP53 mutational status on gene expression patterns across 10 human cancer types. (1096-9896 (Electronic)).
153. Longo PA, Kavran JM, Kim MS, Leahy DJ. Transient mammalian cell transfection with polyethylenimine (PEI). Methods in enzymology. 2013;529:227-40.
154. Schneider CA, Rasband WS, Eliceiri KW. NIH Image to ImageJ: 25 years of image analysis. Nature methods. 2012;9(7):671-5.
155. Tripathi S, Pohl MO, Zhou Y, Rodriguez-Frandsen A, Wang G, Stein DA, et al. Meta- and Orthogonal Integration of Influenza "OMICs" Data Defines a Role for UBR4 in Virus Budding. Cell Host Microbe. 2015;18(6):723-35.
156. Mihaly Z, Kormos M Fau - Lanczky A, Lanczky A Fau - Dank M, Dank M Fau - Budczies J, Budczies J Fau - Szasz MA, Szasz Ma Fau - Gyorffy B, et al. A meta-analysis of gene expression-based biomarkers predicting outcome after tamoxifen treatment in breast cancer. (1573-7217 (Electronic)).